TECHNISCHE UNIVERSITÄT MÜNCHEN

Lehrstuhl für Ernährungsphysiologie

Role of adipokines in the regulation of intestinal GLP-1 secretion

Ramona Nisha Pais

Vollständiger Abdruck der von der Fakultät Wissenschaftszentrum Weihenstephan für Ernährung, Landnutzung und Umwelt der Technischen Universität München zur Erlangung des akademischen Grades eines

Doktors der Naturwissenschaften

genehmigten Dissertation.

Vorsitzender: Univ.-Prof. Dr. M. Klingenspor

Prüfer der Dissertation:

1. Univ.-Prof. Dr. H. Daniel
2. Univ.-Prof. Dr. J. J. Hauner

Die Dissertation wurde am 19.04.2012 bei der Technischen Universität München eingereicht und durch die Fakultät Wissenschaftszentrum Weihenstephan für Ernährung, Landnutzung und Umwelt am 04.06.2012 angenommen.

.

An investment in knowledge pays the best interest.

-Benjamin Franklin

ACKNOWLEDGEMENT

This is perhaps the easiest and hardest chapter that I had to write. Looking back, I am most grateful for all I have received, the last three and a half years. It has given me much and shaped me into the stronger person that I am today. It will be simple to name all the people that helped to get this done, but it will be tough to thank them enough. I will nonetheless try.

In the first place, I would like to express my gratitude to my mentor and guide, Prof. Dr. Hannelore Daniel for her supervision, advice, and guidance right from the nascent stage of this research till its completion. She provided me unflinching encouragement and support in various ways. Her passion towards science, her scientific intuition and foresight made her a constant oasis of ideas which enriched my growth as a student, a researcher and a scientist. Her strong belief in the concept of "try, try and try again and you will succeed" exceptionally inspired me during my failures and persuaded me to strive for success. I am truly indebted to her.

I gratefully acknowledge my supervisor, Dr. Thomas Skurk for his advice and crucial contribution, which made him a backbone of this research and so to this thesis. His involvement, with his originality has triggered and nourished my intellectual maturity that I will benefit from, for a long time to come. Throughout my thesis-writing period, he provided encouragement, good teaching, good company, and lots of good ideas. I thank him for his detailed review and constructive criticism during the preparation of this thesis.

I have also benefited from the advice and guidance of Prof. Dr. Hans Hauner which was rewarding in shaping up my ideas and research.

Very special thanks to my erstwhile colleague and good friend Dr. Laure Fourchaud for introducing me to the subject and for her invaluable help during the initial period of my PhD studies. Special thanks to Dr. Tamara Zietek and Kerstin Geillinger for insightful discussions and invaluable help, collective and individual acknowledgements are also owed to my colleagues at the institute, Pieter Giesbertz, Mena Marth, Anja Höfle, Manuela Sailer, Christina Schulze, Vernonika Müller, Simone Matthae, Tobias Ludwig and Tilo Wünch who created a pleasant work atmosphere and provided constant support. I greatly appreciate the help from Dominika Kolodziejczak, Sebastian Dreyer and Pia Röder during

my big ‘mice experiments’. Thank you guys for the fun times spent inside and outside the lab.

Words cannot express how much gratitude I hold towards the technical assistants “my foster moms” in the lab, Margot Siebler, Beate Rauscher and Helene Prunkl for their unconditional love and support. Many thanks to Beate for her excellent technical help with the calcium imaging experiments. I am also grateful to Manuela Hubersberger, Elisabeth Hofmair and Ronny Scheundel for their excellent technical support.

I will forever remain indebted to Dorothea Woerner for assisting me in so many different ways. She deserves special mention for helping me deal with bureaucratic matters during my stay in Freising. Without her, I would have been lost. Thanks to all the secretaries, Brigette Asafu, Cordula Hertwig and Sylvia Heinrich for taking care of travel funds and other administrative procedures.

I was extraordinarily fortunate in having Drs Shobha and Ullas Kamath as my professors and mentors during my master’s course in Manipal, India. They instilled in me deep love and passion for the subject biochemistry. I could never have embarked and started all of this without the prior teachings of my high school science teachers at St Joseph’s School, Abu Dhabi, late Mrs. Saro George, Mrs. Mercy John and Mrs. Susan .Thank you.

My first teachers, my parents Meena and Robin Pais who taught me the most important lessons of life, that honesty and hard work are the keys to success. Thank you for believing in me. The knowledge that they will always be there to pick up the pieces is what allows me to repeatedly risk getting shattered. To them I dedicate this thesis. My sister Renita, though much younger than me in earthly years, much wiser, for her support and for listening to my complaints and constantly encouraging me. I am also thankful to my in-laws Fredrick and Cecilia Menezes for their unconditional love and support. Also, I acknowledge the rest of family members for their assurance and good-will in every way.

Last but not the least, immense gratitude to my husband, Prashanth. He was my pillar of strength and support throughout and without him; I would never have achieved this. Thank you for taking the load off my shoulders.

Above all, I thank God for giving me the strength and courage to do this and for reasons too numerous to mention. They would be too many to recount.

CONTENTS

ABSTRACT

Obesity is characterized by an increased production and secretion of pro-inflammatory factors such as acute phase proteins, cytokines and chemokines. The constitutively increased circulating levels of these factors are considered to contribute to a low grade inflammatory condition which may promote the co-morbidities of obesity like atherosclerosis or diabetes mellitus type 2. GLP-1 is a peptide hormone secreted from intestinal L-cells upon nutrient ingestion. It not only promotes insulin secretion from ß-cells but also appears to protect from ß-cell loss. GLP-1 secretory responses are impaired in obese and diabetic humans. In search of the underlying causes, we screened a panel of adipokines that have been associated with, and predict the risk for diabetes and identified RANTES and Angiotensin II as possible causal factors. RANTES (Regulated upon Activation, Normal T cell Expressed, and Secreted), circulates in increased concentrations in subjects with type 2 diabetes and its levels in serum and gene expression in white adipose tissue is higher in obese than in lean individuals. Plasma renin activity, angiotensinogen, and angiotensin II levels are also significantly increase during obesity.

The aims of the present thesis were, (1) to determine the presence of RANTES and Angiotensin II receptors, in the intestinal epithelium and on NCI-H716 cells, (2) to test the effects of recombinant RANTES and Angiotensin II on glucose stimulated GLP-1 secretion *in vitro*, and (3) to confirm the effects on glucose-dependent GLP-1 secretion in an *in vivo* model employing C57BL/6 mice. We demonstrated that RANTES reduces glucose stimulated GLP-1 secretion from *in vitro* cultures of human enteroendocrine cells and Met-RANTES (RANTES receptor antagonist) blocking this effect. Moreover, administration of RANTES in mice revealed reduced plasma GLP-1 and GLP-2 levels after an oral glucose load as well as impaired insulin secretion. In addition, Angiotensin II also lowered GLP-1 secretion from enteroendocrine cells and blockage of its receptor with Candesartan improved secretion. Administration of Angiotensin II to mice lowered plasma GLP-1 levels, although not as potently as RANTES.

This thesis describes a cross talk between the intestine and adipose tissue with the novel finding that elevated RANTES and Angiotensin-II blood levels as found in obese individuals may cause the altered GLP-1 secretory response and identifies their receptors as potential targets in diabetes therapy.

ZUSAMMENFASSUNG

Adipositas ist durch eine vermehrte Produktion und Sekretion vo pro-inflammatorischen Faktoren, wie Akute-Phase Proteinen, Zytokinen und Chemokinen gekennzeichnet. Es wird angenommen, dass diese konstitutiv erhöht zirkulierenden Faktoren zu einem niedrig-gradigen Entzündungszustand beitragen, der Folgeerkrankungen der Adipositas, wie z. B. Arteriosklerose oder Typ 2 Diabetes mellitus fördert. GLP-1 ist ein Peptidhormon, welches von intestinalen L-Zellen nach Nahrungsaufnahme sezerniert wird. Es stimuliert nicht nur die Insulinsekretion der ß-Zellen sondern schützt auch vor dem ß-Zelltod. Die GLP-1 Antwort nach Nahrungsstimulation ist bei Adipösen und Patienten mit Typ 2 Diabetes mellitus gestört. Auf der Suche nach den zu Grunde liegenden Ursachen untersuchten wir eine Reihe von Adipokinen, welche mit dem Auftreten von Diabetes assoziiert sind. Wir identifizierten RANTES (regulated upon activation normal T cell expressed and secreted) und Angiotensin II als mögliche kausale Faktoren dieses Geschehens. RANTES zirkuliert mit erhöhten Serumspiegeln bei Patienten mit Typ 2 Diabetes. Seine Genexpression ist im weißen Fettgewebe bei Adipösen höher als bei Schlanken. Weiterhin sind die Plasma-Renin-Aktivität, Angiotensinogen und Angiotensin II-Spiegel bei Adipositas signifikant erhöht.

Die Ziele der vorliegenden Arbeit waren: (1) die Rezeptoren für RANTES und Angiotensin II auf intestinalen Epithelzellen und in NCI-H716 Zellen nachzuweisen, (2) den Einfluss von rekombinantem RANTES und Angiotensin II auf die Glukose-stimulierte GLP-1 Sekretion *in vivo* zu untersuchen und (3) die Effekte auf die Glukose-abhängige GLP-1 Sekretion bei C57 BL/6 Mäusen zu bestätigen. An Hand dieser Studien gelang es uns nachzuweisen, dass RANTES die Glukose-stimulierte GLP-1 Sekretion in Zellkulturen von menschlichen enteroendokrinen Zellen in einer Dosis-abhängigen Weise vermindert und Met-RANTES (einem RANTES-Rezeptorantagonisten) diesen Effekt blockieren kann. Weiterhin konnten wir zeigen, dass die Verabreichung von RANTES im Mausmodel die Plasmaspiegel von GLP-1 und GLP-2 nach einem oralen Glukosetoleranztest reduziert und die Insulinspiegel vermindert. Darüber hinaus verminderte Angiotensin II die GLP-1 Sekretion enteroendokrinen Zellen. Dieser Effekt war mit einem spezifischen AT-1 Rezeptorantagonisten Candesarten aufgehoben. Auch Angiotensin II verminderte die GLP-1 Spiegel im Mausmodell, auch wenn der Effekt nicht so stark wie mit RANTES war.

Die Arbeit beschreibt das Zusammenspiel zwischen dem Magen-Darm-Trakt und dem Fettgewebe mit neuen Ergebnissen bezüglich RANTES und Angiotensin II. Beide Adipokine sind bei Adipösen erhöht und spielen somit möglicherweise eine wichtige Rolle beider veränderte Dynamik der GLP-1 Sekretion. Der Nachweis der jeweiligen Rezeptoren belegt dazu die Spezifität der Ergebnisse und legt möglicherweise den Grundstein für weitere Therapieoptionen bei Typ 2 Diabetes mellitus.

1 INTRODUCTION

1.1 Adipose tissue as an endocrine organ

Adipose tissue (AT) is a specialized connective tissue that functions as the major storage site of fat in the form of triglycerides. AT is found in mammals in two different forms: white adipose tissue (WAT) and brown adipose tissue (BAT). The presence and distribution of each varies depending upon the species. In humans, WAT is dispersed throughout the body with major intra-abdominal depots around the omentum, intestines, and perirenal areas, as well as in subcutaneous depots in the buttocks, thighs, and abdomen. It is now being realized that the AT is more than just a passive energy storing organ. It is multifunctional, with complex, essential, and highly active metabolic and endocrine functions (1).

1.1.1 Adipose tissue development and expansion

The major bulk of the AT is an association of lipid-filled cells called adipocytes, which are held in a framework of collagen fibres. In addition to adipocytes, adipose tissue contains stromal–vascular cells including fibroblastic connective tissue, leucocytes, macrophages and pre-adipocytes (not yet filled with lipid), which contribute to structural integrity. WAT serves three functions; heat insulation, mechanical cushioning and most importantly, a source of energy.

Adipocytes arise from mesenchymal/mesodermal stem cells by a sequential pathway of differentiation. When triggered by appropriate developmental cues, mesenchymal stem cells (MSCs) become committed to the adipocyte lineage. This differentiation pathway presumably involves a common preadipocyte or adipoblast, which has the capacity to differentiate into white or brown preadipocytes (2).

AT grows by two mechanisms, hyperplasia (cell number increase) and hypertrophy (cell size increase). Genetics and diet affect the relative contribution of these two mechanisms to the growth of AT (3-5).

1.1.2 Inflammation of the adipose tissue in obesity and adipokines

Obesity is defined as excessive accumulation of AT in the human body to an extent that it begins to negatively affect the quality of life. In obesity, there is an enlargement of the AT

to store excess energy. Hypertrophy and hyperplasia are the two growth mechanisms (3, 6). Hyperplastic growth appears only at early stages in adipose tissue development (7, 8). Hypertrophy occurs prior to hyperplasia to meet the need for additional fat storage capacity in the progression of obesity (9). It is now known that in obesity, the AT is in a state of inflammation due to the infiltration of immune cells such as macrophages and T cells. Some of the consequences of hypertrophy of AT include fatty acid flux, decreased vascularisation, hypoxia and ultimately adipocyte cell death. These adipocyte related consequences of AT expansion are potential contributors to the initiation of macrophage recruitment since they are recruited to phagocytose dead or dying adipocytes in the expanding AT depot (Figure 1).

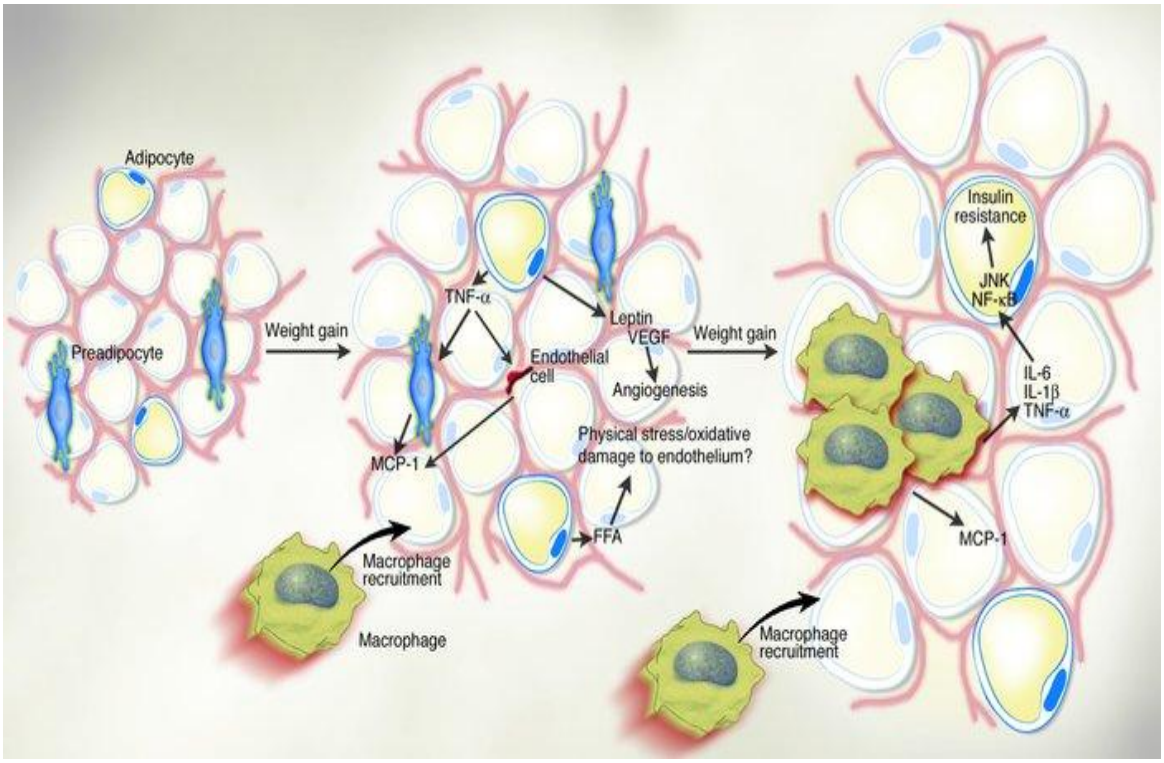

Figure 1: Initiation and recruitment of macrophages in adipose tissue with progressive weight gain. Obese adipose tissue is characterized by inflammation and progressive infiltration by macrophages as obesity develops. In obesity, adipocytes begin to secrete low levels of TNF-α, which can stimulate preadipocytes to produce monocyte chemoattractant protein-1 (MCP-1). Increased secretion of leptin (and/or decreased production of adiponectin) by adipocytes may also contribute to macrophage accumulation. Whatever the initial stimulus to recruit macrophages into adipose tissue is, once these cells are present and activated, they, along with adipocytes and other cell types, could perpetuate a vicious cycle of macrophage recruitment, production of inflammatory cytokines, and impairment of adipocyte function. Scheme adapted from Kathryn E. Wellen, Gökhan S. Hotamisligil; Obesity-induced inflammatory changes in adipose tissue, Journal of Clinical investigation, 2003

The presence of macrophages in AT was first reported more than 10 years ago (10). Subsequent studies showed that macrophage infiltration in white AT is increased in obesity (11). Also, immunohistochemical analysis of perigonadal, perirenal, mesenteric, and subcutaneous adipose tissue in mice revealed that the percentage of cells expressing the macrophage marker F4/80 (F4/80+) was significantly and positively correlated with both adipocyte size and body (fat) mass. Similar relationships were found in human subcutaneous adipose tissue stained for the macrophage antigen CD68 (12).

With the discovery of TNF-α in 1993 (13) and leptin (14, 15) in 1994 from the AT, the endocrine role of the AT was recognized the first time. Since then a diverse range of other protein factors have been discovered and characterized (16). These various protein signals have been given the collective name 'adipocytokines' or 'adipokines'. However, since most are neither 'cytokines' nor 'cytokine-like', it is recommended that the term 'adipokine' be universally adopted to describe a protein that is secreted from (and synthesized by) adipocytes. Data demonstrate that adipokines like interleukin (IL)-6, tumor necrosis factor (TNF)-α, C-reactive protein and other various factors circulate in increased concentrations in obese individuals (17-21).

1.1.3 Obesity and insulin resistance/type 2 diabetes

The World Health Organization has termed the increased prevalence of obesity and diabetes as a 21st century epidemic. Obesity is the most frequently encountered metabolic disease worldwide. Being overweight constitutes a health risk as it is associated with several co-morbidities including type 2 diabetes mellitus (T2DM), cardiovascular diseases, hypertension, dyslipidemia, hyperuricemia, respiratory diseases, osteo-arthritis and depression (22, 23). According to Ford *et al*, for every kilogram of weight gain, the risk of diabetes increases between 4.5 and 9% (24).

The relationship between obesity and diabetes is of such interdependence that the term 'diabesity' was coined by Zimmet *et al* to illustrate the interdependence between these two diseases (25). The passage from obesity to diabetes is made by a progressive defect in insulin secretion coupled with a progressive rise in insulin resistance. Both, insulin resistance and defective insulin secretion appear very prematurely in obese patients and both worsen similarly towards diabetes. Inflammatory mediators are found to be elevated in patients suffering from many co-morbidities of obesity independent of body weight, including atherosclerosis, diabetes and steatohepatitis (18, 26).

1.1.4 Adipokines and insulin resistance

Recent data have revealed that the plasma concentrations of inflammatory mediators, such as tumor necrosis factor-alpha (TNF-α) and interleukin-6 (IL-6), are increased in the insulin resistant states of obesity and type 2 diabetes, raising questions about the mechanisms underlying inflammation in these two conditions. The expanding volume of adipose tissue during obesity raises circulating levels of these inflammatory markers and is therefore, thought to cause insulin resistance, thereby leading to the development of T2DM. More than 100 factors secreted by adipocytes have been identified over the past years, and it seems likely that this number will increase further due to the progress in analytical chemistry.

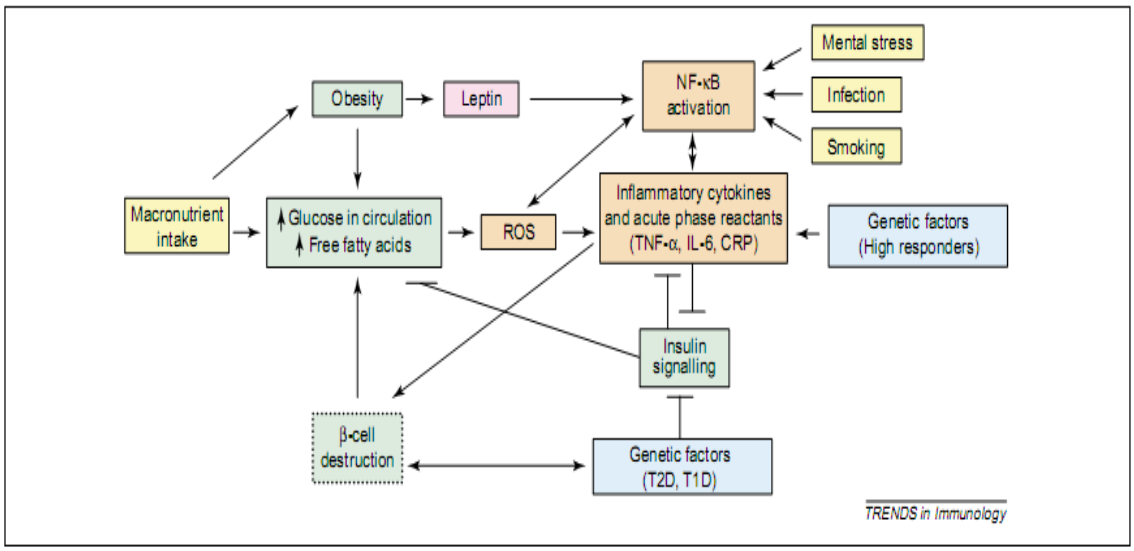

Figure 2: The induction of reactive oxygen species (ROS) generation and inflammation (NF-κB activation) by macronutrient intake, obesity, free fatty acids, leptin and genetic factors. Interference with insulin signaling (insulin resistance) leads to hyperglycemia and proinflammatory changes. Proinflammatory changes (increased TNF-α and IL-6) also lead to the inhibition of insulin signaling and insulin resistance. Inflammation in β cells leads to β-cell dysfunction, which in combination with insulin resistance leads to type 2 diabetes. Adapted from Dandona P, Aljada A, Bandyopadhyay A; Inflammation: the link between insulin resistance, obesity and diabetes; Trends in Immunology, 2004.

Two mechanisms might be involved in the pathogenesis of inflammation. Firstly, glucose and macronutrient intake causes oxidative stress and inflammatory changes. Chronic overnutrition (obesity) might thus be a proinflammatory state with oxidative stress. Secondly, increased concentrations of TNF-α and IL-6, associated with obesity and type 2

diabetes, might interfere with insulin action by suppressing insulin signal transduction. This might interfere with the anti-inflammatory effect of insulin, which in turn might promote inflammation (Figure 2).

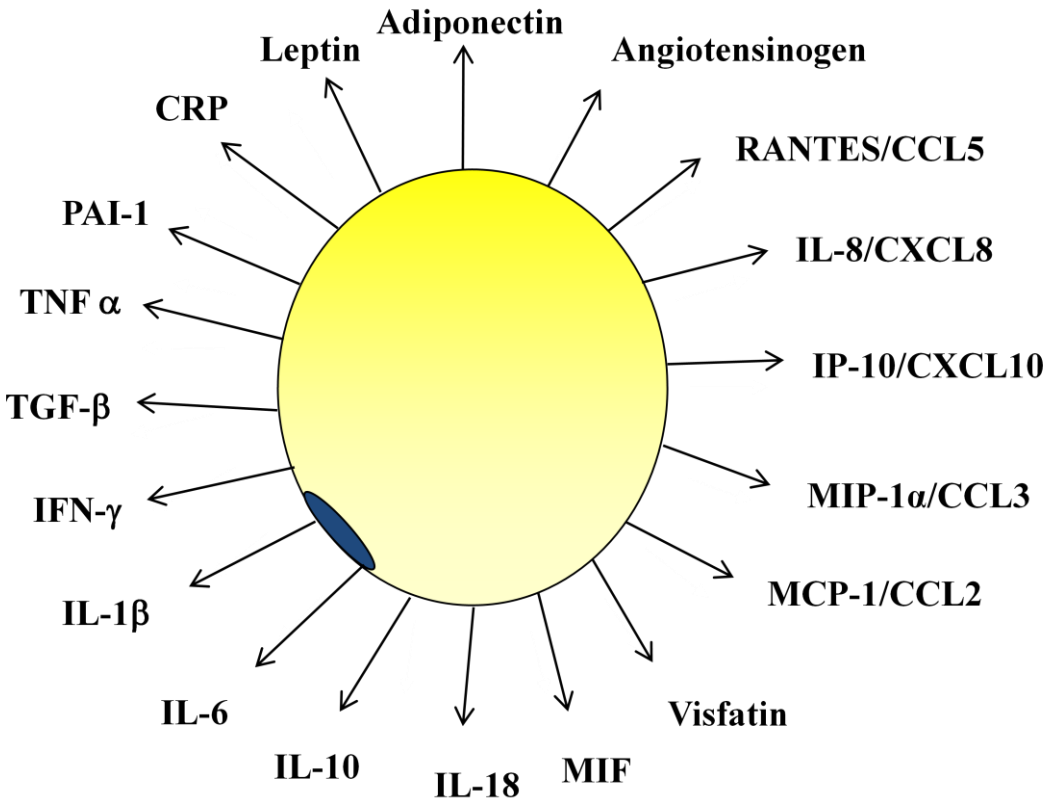

Figure 3: Endocrine function of the adipose tissue. The adipose tissue secretes a variety of proteins such as acute phase proteins, cytokines and chemokines and, in obesity; the secretory pattern becomes dysregulated with elevated levels of secretion.

TNF-α

TNF-*α* is a pluripotent cytokine primarily produced from macrophages. Its expression was shown to be elevated in different mouse and rat models of obesity and diabetes (13). It was also shown that TNF-*α* induces insulin resistance, at least in part, through its ability to inhibit intracellular signalling from the insulin receptor (27). Moreover, addition of TNF-α to leukemic cells *in vivo* increased the intracellular concentration of ceramides (28). Ceramides can directly induce DNA fragmentation and apoptosis. In skeletal muscle, diacylglycerols and ceramides operate as lipotoxic mediators engaging serine kinases that disrupt the insulin signalling cascade and deteriorate insulin sensitivity. Further, it was discussed that ceramides are able to induce lipoapoptosis in *β*-cells (29). In addition, TNF-

α was described to induce the formation of reactive oxygen species (ROS) (30). Production of ROS increased selectively in adipose tissue of obese mice, causing dysregulated production of adipokines, including adiponectin, plasminogen activator inhibitor-1, interleukin-6, and monocyte chemotactic protein-1 (31).

MCP-1

The proinflammatory chemokine monocyte chemotactic protein-1 (MCP-1) attracts leukocytes to inflamed sites and is regulated by NF-κB (32). Insulin was found to induce expression and secretion of MCP-1 substantially both *in vitro* in insulin-resistant adipocytes and *in vivo* in insulin-resistant obese mice (*ob/ob*). It was suggested that elevated MCP-1 levels may induce adipocyte dedifferentiation and contribute to pathologic states associated with hyperinsulinemia and obesity, including type 2 diabetes (33). Expression and plasma concentration of MCP-1, however, were shown to be increased both in genetically obese diabetic (*db/db*) mice and in wild type mice with high-fat diet-induced obesity, leading to the assumption that increased MCP-1 expression contributes to macrophage infiltration into adipose tissue and finally to the development of insulin resistance (34).

IL-6

The role of the cytokine interleukin-6 (IL-6) in the regulation of lipid metabolism is controversially discussed (35). If produced in large amounts by adipose tissue, IL-6 causes insulin resistance in adipocytes and skeletal muscle (36). Contrary to the expectations, IL-6 deficient mice develop obesity. However, the body weight deviation was only reported in very mature animals (37). Interestingly, chronic exposure of IL-6 produces insulin resistance in skeletal muscle, whereas short-term exposure as consequence of exercise has beneficial effects on insulin sensitivity (37). Thus, despite the evidence of IL-6 as a major player in the regulation of metabolism, the role of this cytokine in the pathogenesis of insulin resistance and diabetes remains not completely understood.

Leptin

Leptin is predominantly secreted from white adipose tissue and exerts its main function by repressing food intake and promoting energy expenditure (38). The leptin receptor is expressed in the arcuate, ventromedial, dorsomedial, and lateral hypothalamic nuclei, which are known to regulate food intake (39). Mutations of both the leptin gene (*ob*) as

well as the leptin receptor gene (*db*) leads to severe obesity, hyperphagia and insulin resistance in mice (40). Expression and secretion of leptin is correlated with the amount of body fat and adipocyte size. Humans with mutations in both alleles of either leptin or the leptin receptor are obese, but these homozygous mutations are extremely rare (40). To the contrary, the vast majority of obese individuals display high plasma leptin levels. Leptin improves insulin sensitivity by several mechanisms. In the liver and in skeletal muscle, leptin enhances glucose homeostasis by decreasing intracellular lipid accumulation (41) and, in skeletal muscle, by direct activation of AMP-activated protein kinase (AMPK) (42).

RANTES

RANTES is a small protein of 68 amino acids belonging to the C-C subfamily of chemokines. It plays a primary role in the inflammatory immune response via its ability to chemoattract leukocytes and modulates their function. It promotes the recruitment and activation of inflammatory cells such as monocytes (43), lymphocytes (44), mast cells (45), and eosinophils (46) and exerts its biological effects by binding to specific receptors in the seven-transmembrane G-protein-coupled receptor (GCPR) family, namely CCR1 (47), CCR3 (48), and CCR5 (47). RANTES is secreted from platelets, macrophages, eosinophils, fibroblasts and was only very recently described as an adipokine (49). Its secretion positively correlates with adipocyte size (50) and is gender specific (51) and its levels in serum and gene expression in white adipose tissue is higher in obese than in lean (52). Murine diet induced obesity is associated with elevated levels of RANTES and its receptor CCR5 in adipose tissue, together with enhanced local T cell accumulation (51). RANTES circulates in increased concentrations in subjects with impaired glucose tolerance and type 2 diabetes (53).

Angiotensin II

Angiotensin II is an octapeptide and an important regulator of blood pressure and salt and water balance. It is the main active component of the renin-angiotensin system (RAS); the other components include the precursors, angiotensinogen and angiotensin I, the cleavage enzymes renin and angiotensin converting enzyme (ACE) and its receptors. Local RAS is present in vascular smooth muscle cells, the heart, kidneys, adrenals, liver (54), adipose tissue (55) and the gastrointestinal tract (56, 57). The effects of angiotensin II on peripheral tissues are mediated by two receptors, the more prevalent AT_1 and the AT_2

receptor. Plasma renin activity, angiotensinogen, and angiotensin II levels significantly increase during obesity. This may be responsible in part for the metabolic and inflammatory disorders associated with obesity like type 2 diabetes (58). Blockage of the type 1 receptor improves β cell function and glucose tolerance in mice models of diabetes (59).

1.2 Gastro-intestinal hormones

The gastro-intestinal (GI) hormones are so called because they are secreted from different parts of the gastro-intestinal tract. The GI hormones are secreted by special epithelial cells called enteroendocrine cells (EEC), lining the lumen of the stomach, small and large intestine. These hormone-secreting cells enteroendocrine cells are interspersed among a much larger number of epithelial cells accounting to only ≤ 1% of the total cell population. GI hormones are secreted into blood, and hence circulate systemically, where they affect functions of other parts of the digestive system, liver, pancreas, brain and a variety of other targets. Selected peptide hormones of the gut along with their functions have been listed in the table below.

Table 1: Gastro-intestinal hormones along with their functions.

Hormone	Produced by	Major function (s)
Gastrin	Stomach antrum (60) and G-cells of duodenum	• Stimulates gastric secretion • Lowers esophageal sphincter pressure and gastric emptying (61)
Cholecystokinin (CCK)	I-cells of the duodenum and proximal jejunum (62)	• stimulates gall bladder contraction and emptying (63) • stimulates pancreatic secretion • appetite regulation, reduces feeding and signals satiety (64, 65)
Ghrelin	A-cells of the stomach (66)	• stimulates appetite (67) • promotes release of growth hormone (66) • promotes gastric motility
Leptin	Fundic glands of stomach (68)	• reduces food intake and body weight (68)
Secretin	S-cells of the duodenum (69)	• stimulates secretion of water and bicarbonates from the pancreas and bile ducts
GIP	K-cells of duodenum and jejunum (70)	• stimulates insulin secretion from pancreas (71) • protective function on β-cells of

		pancreas (72-74)
PYY	L-cells of ileum, colon and rectum (75)	• contributes to ileal brake, reduces further food intake (76, 77)
GLP-1	L-cells of ileum, colon and rectum (78)	• stimulation of glucose-dependent insulin secretion (79, 80) • insulin biosynthesis (79, 80) • inhibition of glucagon secretion and gastric emptying, and inhibition of food intake (79, 80)
GLP-2	L-cells of ileum, colon and rectum (78)	• stimulates mucosal growth in small and large intestine, inhibits enterocyte and crypt cell apoptosis (81) • increases nutrient absorption, stimulates enterocyte glucose transport and GLUT-2 expression (82) • reduces intestinal permeability • inhibits gastric emptying and gastric acid secretion (83)

1.2.1 Incretin hormones and their functions

Incretin hormones are a class of gastro-intestinal hormones, which are secreted in response to the presence of nutrients in the intestinal lumen, and which act to potentiate glucose induced insulin secretion. The incretin effect is defined as the amplification of glucose induced insulin secretion upon oral vs. intravenous glucose administration. It was first described in 1964 by McIntyre *et al* (84), who also suggested it to be mediated by gut-derived factors. The incretin effect is mediated almost equally by the two incretin hormones; glucose-dependent insulinotropic polypeptide (GIP) and glucagon-like peptide (GLP)-1 (85). Both hormones powerfully enhance insulin secretion to an extent that can fully account for the incretin effect (86).

GIP

Gastric inhibitory polypeptide, also known as glucose-dependent insulinotropic polypeptide (GIP), is a 42 amino acid peptide, synthesized in, and secreted by enteroendocrine K-cells which are found in highest numbers in the duodenal and proximal jejunal epithelia (87). GIP is rapidly degraded, with a half-life of 7 minutes, by the enzyme dipeptidyl peptidase- 4 (DPP-4) (88) and its secretion is primarily regulated by nutrients, especially fats and glucose (89, 90) with plasma levels rising by 10-20 fold and reaching a

peak 15-30 minutes after meal ingestion. The primary action of GIP is the stimulation of glucose-dependent insulin secretion, GIP exhibits potent incretin activity in rodents and human subjects (91). GIP has also been shown to stimulate β-cell proliferation and exert anti-apoptotic actions *in vitro* (92-94). Furthermore, GIP was found to be involved in brain cell proliferation (95) and in bone formation (96). In addition, inhibition of the GIP signalling ameliorates obesity, obesity-related hyperglycemia and dyslipidemia in rodents, indicating that GIP can play a role in obesity and obesity-related diseases (97). Expression of the GIP receptor has been detected on rat (98) and human adipocytes (99), and it has been found that GIP promotes triglyceride incorporation into adipose tissue (100, 101), although in human volunteers this was only observed under conditions of hyperglycemia and did not significantly alter the concentration of circulating triglycerides (100). Additional evidence demonstrated that GIP can also increase glucose transport and promote fatty acid synthesis in isolated adipocytes (102). In healthy humans, GIP infusion did not affect glucose and insulin at normoglycemia (5 mM glucose), but GIP co-administered with the sulfonyl urea glibenclamide increased plasma insulin levels (103). The mechanisms underlying this intriguing observation remain unclear. Whether an enhancement of GIP receptor signalling is a viable strategy for the treatment of type 2 diabetes remains to be determined. Human data demonstrating the efficacy of GIP agonists in type 2 diabetes are quite limited.

GLP-1

Glucagon-like peptide-1 (GLP-1) is synthesized in and secreted from intestinal endocrine L-cells of distal small intestine and large intestine in response to nutrient ingestion, and similar to GIP acts as an incretin hormone (86). GLP-1 is also expressed in neurons within the NTS of the brainstem. GLP-1 is released 5-30 min after food ingestion in proportion to the energy content. Maximum circulating GLP-1 levels are usually reached after 40 minutes. Fatty acids and proteins have been shown to be the most potent effectors for GLP-1 secretion *in vivo* (104, 105). The biological activities of GLP-1 include stimulation of glucose-dependent insulin secretion, increased insulin sensitivity in peripheral tissues, inhibition of glucagon secretion and delay in gastric emptying and reduced food intake (106). GLP-1 receptors are found in all brain regions involved in food intake regulation including the nucleus arcuatus (ARC) regions within the hypothalamus and the NTS of the brainstem and in addition, in various peripheral tissues (107, 108). Central and peripheral administration of GLP-1 to rats inhibits food intake (109, 110). Peripheral administration

to humans also inhibits food intake (110) and increases postprandial satiety and delayed gastric emptying both in lean and obese humans (111). Some of the other functions of GLP-1 are shown in Figure 4.

One barrier to the use of native GLP-1 in a clinical setting is its short half-life. GLP-1 is rapidly cleaved in plasma into the inactive forms GLP-1 (9-37) and (9-36) by the enzyme DPP-4 within minutes. To overcome this obstacle GLP-1 analogs with a significantly greater plasma half-life such as exendin-4 (half-life around 30 min) have been developed which are meanwhile used in the treatment of type 2 diabetes (112).

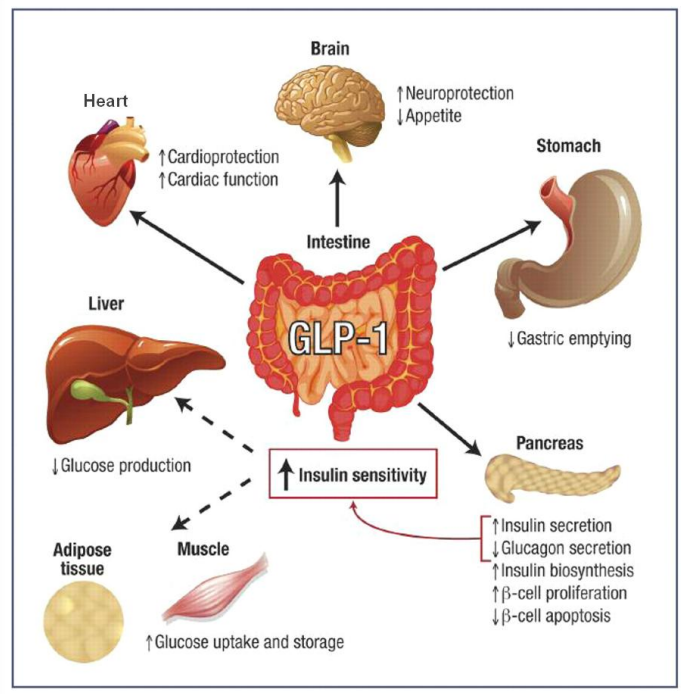

Figure 4: GLP-1 actions on peripheral tissues. GLP-1 (7-36) amide, which is known to regulate pancreatic functions, also exerts actions in heart, stomach, brain, liver and muscle. GLP-1 affects liver and muscle via direct and indirect mechanisms through its metabolite GLP-1 (9-36) amide (113). Picture courtesy, Baggio and Drucker (114).

1.2.2 Disturbances in GLP-1 secretion in obesity and type 2 diabetes

In type 2 diabetes

In patients with type 2 diabetes, a reduced or absent incretin effect has been described (115). It is now clear that, diabetes affects the two incretin hormones differently in several aspects. With respect to GIP, there is almost a complete loss of its insulinotropic effect, whereas the secretion seems only slightly decreased (116, 117).

In a study in patients with type 2 diabetes covering a wide clinical spectrum of the disease, Toft-Nielsen *et al*. (116), using a highly specific COOH-terminal GIP assay, found near-normal fasting levels and meal responses with no correlations between metabolic parameters and GIP responses. In the same study, a very significant impairment of GLP-1 secretion was observed.

In contrast, both GLP-1 potency and GLP-1 secretion in relation to a meal is substantially reduced (116, 118). In a previous study in a small group of identical twins discordant for type 2 diabetes, the GLP-1 response was lower in the diabetic twin (119), whereas in first-degree relatives of diabetic individuals, the 24-hour GLP-1 profiles were normal (120), probably indicating that impaired secretion is a consequence rather than a cause of diabetes. GLP-1 is metabolized extremely rapidly by the ubiquitous enzyme DPP-4, which cleaves off two amino acid residues from the NH_2-terminus and renders the metabolite (designated GLP-1 (9-36) amide) inactive. In agreement with this, the circulating concentrations of the intact hormone are much lower than those of the metabolite, but in patients with type 2 diabetes during meal intake, intact hormone concentrations are lower than in control subjects (121). Differences in elimination cannot explain this (122), which must therefore be due to decreased secretion.

In obesity

In a study conducted with obese women, L R Ranganath *et al* observed a pronounced impairment of plasma GLP-1 secretion to oral carbohydrates in obese compared to lean subjects but no such difference in response to oral fat feeding (123). There were no differences in the plasma GIP responses to carbohydrate or fat feeding. Subsequent studies conducted in obese subjects to undergo gastric banding and Roux-en-Y gastric bypass (RYGB) also demonstrated lower plasma GLP-1 levels in comparison to lean subjects after an isocaloric test meal (124, 125). Although the cause of this attenuation of GLP-1 secretion is still not clear, recently the role of pro-inflammatory cytokines which circulate in higher levels in obesity, have been demonstrated to play a role.

Further, plasma DPP-4 activity has previously been reported to be elevated in obese subjects compared with normal-weight subjects (126, 127), but the impact of this on the clearance of the incretin hormones is unknown. High circulating levels of the enzyme could indicate that, the incretins might be degraded more rapidly in obese than in lean subjects, and it could, therefore, be speculated that increased rates of metabolism of the

incretin hormones in obesity may contribute to changes in postprandial incretin and islet hormone secretion.

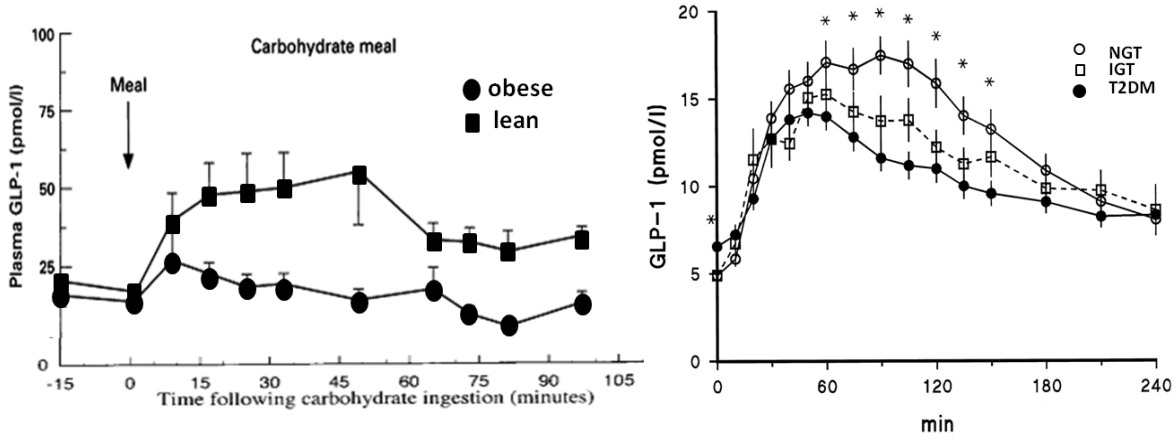

Figure 5: Reduced plasma GLP-1 secretion following a meal in obese (128) and in impaired glucose tolerant (IGT) and type 2 diabetic subjects (T2DM) (116).

1.3 Nutrient sensing by intestinal endocrine cells

GIP secreting K-cells and GLP-1 secreting L-cells are "open-type" cells. They exhibit a polarized morphology, with an apical surface in close contact with the gut lumen and a basolateral membrane in close proximity to the circulatory system. This so called open-type morphology enables them to sense dietary nutrients and non-nutrient substances, present in the intestinal lumen. There are, however, some differences between GIP and GLP-1 secretory responses to nutrient ingestion and it has been proposed that GIP secretion requires nutrient absorption (129, 130), while the mere presence of nutrients in the lumen is sufficient to trigger GLP-1 secretion.

Further, due to the different distribution of K- and L-cells along the length of the gut, any intervention that partially interferes with nutrient absorption causing more nutrients to enter the distal parts of the small intestine where most L-cells are found, results in increased GLP-1 release.

In live preparations, enteroendocrine cells are not easily distinguished from surrounding enterocytes and thus for many years, attempts to study their stimulus sensing pathways were restricted to the use of perfused intestinal preparations and intestinal model cell lines such as GLUTag, STC-1 and NCI-H716. The recent development of transgenic mice in

which GLP-1 or GIP producing cells are labelled with a fluorescent marker has enabled the identification of adult murine L- or K-cell populations in culture, and subsequently the use of single cell recording techniques for the characterization of nutrient sensing mechanisms in these cell types (87, 131). Both primary L-cells and the model GLP-1 secreting cell line GLUTag are electrically active and nutrient responsive (132-135). Consistent with findings from other endocrine cell types, alterations in membrane potential are coupled via voltage gated Ca^{2+} entry to the release of secretory vesicles. All enteroendocrine cell types studied to date are also responsive to signals that activate G-protein coupled receptors.

1.3.1 Carbohydrates

It has been shown in many studies that glucose is the most potent secretagogue for both GIP and GLP-1. Oral glucose stimulates GLP-1 secretion more effectively than other monosaccharides such as fructose, although both have been reported to affect appetite similarly. Similarly, higher levels of GIP were elicited following consumption of glucose than equivalent portions of complex carbohydrates in the form of barley or brown rice (136). Further elevated blood glucose does not stimulate incretin secretion, suggesting that there must be a mechanism for sensing luminal glucose.

Mechanisms involving metabolism and K_{ATP} channel modulation

Patch clamp studies that were conducted in the model cell line GLUTag revealed that glucose reduced membrane conductance, depolarized the cell membrane, and triggered action potentials which led to an increase in intracellular ATP and calcium and the release of GLP-1. Together, with the finding that the electric activity could be abolished by addition of diazoxide, the opener of K_{ATP} channel, these results suggested an involvement of K_{ATP} channels in the stimulatory effects of glucose in the GLUTag cells (132, 135). Further, the K_{ATP} channel subunits, Kir6.2 and SUR1 (sulphonylurea receptor), and the rate limiting glycolytic glucokinase, have been detected in GLUTag (132) cells and primary K- and L-cells from mouse (131) and human (137). However, there have been contradictory studies showing that mice lacking the Kir6.2 subunit of the K_{ATP} channels exhibited increased rather than reduced levels of GIP secretion in response to an oral glucose load.

Metabolism independent mechanisms

Non-metabolisable sugars like alpha-methyl-glucopyranoside and 3-O-methylglucose have been reported to stimulate GIP and GLP-1 secretion both *in vitro* and *in vivo* (131, 138, 139), hence suggesting that K_{ATP} closure in response to increased metabolism cannot be exclusively responsible for glucose sensing by K- and L- cells.

Sweet taste receptor(s): Other groups have postulated that glucose sensing in the intestine is similar to sweet taste perception in the tongue and involves two G protein coupled receptors, known as Tas1R2 and Tas1R3, which form a heterodimeric sweet taste receptor recognizing glucose and other natural and synthetic sweeteners. Upon ligand activation, a pathway involving α-gustducin is stimulated, resulting in stored calcium release and subsequent activation of the transient receptor potential channel, TRPM5 (140, 141). Expression of the sweet taste receptor, together with key elements of the signalling pathway such as α-gustducin, PLCβ2 and TRPM5, have been reported in human and mouse small intestine and colon (142, 143), and colocalisation of α-gustducin with the peptides GLP-1 and PYY has been demonstrated immunohistochemically in human L-cells (143, 144). In contrast to experiments in cell lines, studies in healthy humans have shown a lack of effect of sucralose on GLP-1 and GIP secretion (145).

Sodium/glucose co–transporter1 (SGLT1): The non metabolisable sugar like α-MDG that triggers incretin hormone secretion are substrates for SGLT1, which is responsible for the active uptake of a variety of sugars across the small intestinal brush border membrane. SGLT1 transports glucose along with two sodium ions, this causes membrane depolarization and triggers action potentials causing opening of voltage gated calcium channels and calcium influx. Further, the SGLT1 inhibitor phlorizin reduced glucose triggered incretin secretion both *in vitro* and *in vivo* (146, 147). Further proof for the importance of SGLT1 driven glucose uptake for incretin secretion was recently demonstrated in SGLT1 knock-out mice, where there was no GIP and GLP-1 response to an oral glucose challenge (148).

1.3.2 Lipids

Fat is a well known stimulant for both GIP and GLP-1 secretion. Secretion of these two hormones depends on meal size and on the degree of fatty acid saturation, since secretion of GLP-1 was shown to be preferentially triggered by long chain monounsaturated fatty acids compared to their saturated equivalents (149). Long-chain unsaturated fatty acids

(LCFA) are ligands for the Gq-protein coupled receptors GPR40 (150) and GPR120 (151). Messenger RNAs for both of these receptors have been detected by quantitative RT-PCR in L- and K-cells (152). Knock-down of GPR120, but not GPR40, interfered with CCK-release from STC-1 cells (151) and selective GPR120 agonists, were shown to elicit a GLP-1 secretion from this cell line (151, 153).

Short chain fatty acids such as acetic acid, propionic acid and butyric acid are products of bacterial fermentation in the colon and have been shown to stimulate the related G-protein coupled receptors GPR41 and GPR43, which have been localized immunohistochemically on L-cells in rats and humans (154, 155). Activation of GPR43 resulted in acute Ca^{2+} responses in primary L-cells, whereas short chain fatty acid dependent GLP-1 secretion was abolished in GPR43 knock-out mice (134)

Other lipid compounds that are found in the gut lumen after a lipid rich meal, such as lysophosphatidylcholine, oleoylethanolamide or bile acids, have been shown to stimulate the Gs-protein coupled receptors GPR119 (156) and TGR5 (157), respectively. GPR119 agonists stimulate GIP and GLP-1 secretion *in vivo* (156, 158), while TGR5 activation has been shown to stimulate GLP-1 secretion *in vitro* and *in vivo* (157, 159). GPR119 knock-out animals showed an attenuated postprandial GLP-1 secretion, but did not reveal significantly altered glucose homeostasis (160).

1.3.3 Proteins

The role played by protein or individual amino acids in triggering incretin secretion remains an area of controversy. In humans, for example, protein-rich meals were ineffective in altering post-prandial GIP levels (136) whereas intraduodenal infusion of mixed amino acids (161, 162) or oral consumption of the amino acid glutamine (163) was found to increase GIP release.

The primary mechanisms underlying detection of amino acids or small peptides in enteroendocrine cells remain uncertain, as a range of potential signalling pathways have been postulated. Activation of the ERK1/2 MAPK and p38 MAPK pathway has been observed in NCI-H716 cells treated with meat hydrolysate or mixtures of essential amino acids (164), and may provide a link to GLP-1 release. Glutamine promotes the secretion of GLP-1 from rodent primary cultures and GLUTag cells via two pathways. Electrogenic Na^+ coupled amino acid uptake appears responsible for initiating membrane depolarization and voltage gated Ca^{2+} entry, while a second pathway involves elevation of intracellular

cAMP levels (135). Synergy between these Ca^{2+} and cAMP signalling pathways seems a particularly potent stimulus of GLP-1 release *in vitro*. The diversity of electrogenic uptake mechanisms for amino acids and dipeptides across the intestinal epithelium, together with the range of G-protein coupled receptors now believed to respond to specific groups of amino acids or small peptides, may provide enteroendocrine cells with a broad repertoire of potential sensors of digested protein.

PEPT1, which is predominantly expressed in the apical membrane of intestinal epithelial cells, is a proton/oligopeptide cotransporter that selectively takes up di- and tripeptides. It has been shown *in vitro* that peptide-induced proton influx through PEPT1 triggers a membrane depolarization followed by Ca^{2+} influx through voltage dependent calcium channels (VDCCs), which in turn induces hormone secretion from STC-1 cells when cells were transfected with PEPT1 (165). Normal STC-1 cells however do not express PEPT1. Darcel *et al*. showed in rats that, protein digests which activate vagal afferents known to induce satiety may depend on PEPT1 (166).

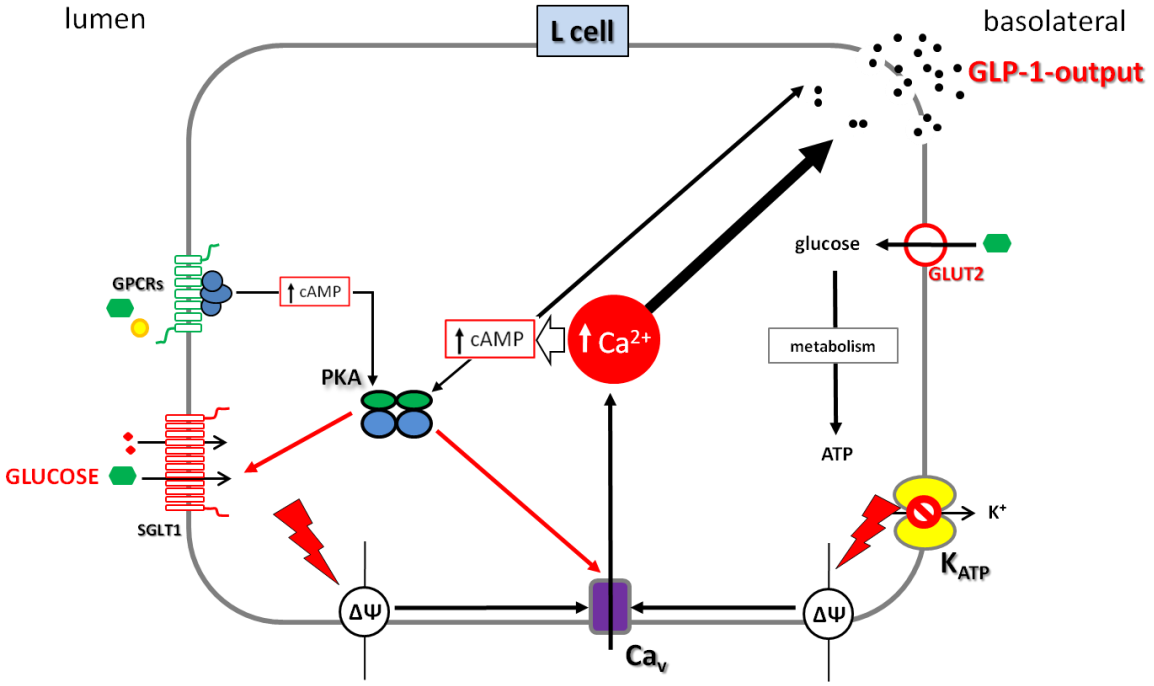

Figure 6: Nutrient sensing by L-cells. Dietary components passing in the intestinal lumen are detected by the L-cells. Potential nutrient sensing pathways include electrogenic uptake pathways, such as SGLT1, metabolic closure of K_{ATP} channels and activation of G protein-coupled receptors (GPCRs). Downstream signaling pathways include elevated intracellular cAMP and [Ca^{2+}], which stimulate vesicle fusion and the consequent release of GLP-1.

2 MATERIALS & METHODS

2.1 Materials

2.1.1 Chemicals

2-desoxy-D-glucose	Roth GmbH &Co KG, Karlsruhe, Germany
Acetic Acid	Roth GmbH &Co KG, Karlsruhe, Germany
Acrylamide- Solution Rotiphorese 30	Roth GmbH &Co KG, Karlsruhe, Germany
Agarose GTQ	Roth GmbH &Co KG, Karlsruhe, Germany
Ammoniumpersulfate (APS)	Roth GmbH &Co KG, Karlsruhe, Germany
Bovine serum albumin (BSA)	Sigma Aldrich, Hamburg, Germany
Calcium Chloride dihydrate	Roth GmbH &Co KG, Karlsruhe, Germany
Chloroform	Merck, Germany
Coomassie Brilliant Blue (R-250)	Roth GmbH &Co KG, Karlsruhe, Germany
Dimethylsulfoxide (DMSO)	Serva Heidelberg, Germany
Dithiothreitol (DTT)	Roth GmbH &Co KG, Karlsruhe, Germany
Ethyldiaminetetraacetate (EDTA)	Roth GmbH &Co KG, Karlsruhe, Germany
EGTA	Sigma Aldrich, Hamburg, Germany
Ethanol (99%)	Serva Heidelberg, Germany
Ethidiumbromide	Roth GmbH &Co KG, Karlsruhe, Germany
Formaldehyde	Roth GmbH &Co KG, Karlsruhe, Germany
Glucose monohydrate	Roth GmbH &Co KG, Karlsruhe, Germany
Glycin	Serva Heidelberg, Germany
Glycylglycine	Bachem, Bubendorf, Switzerland
Glycylsarcosine	Sigma Aldrich, Hamburg, Germany
[Glycine-1-14C] glycylsarcosine	Amersham Biosciences
HEPES	Roth GmbH &Co KG, Karlsruhe, Germany
Hydrochloric Acid	Roth GmbH &Co KG, Karlsruhe, Germany
Ionomycin	Sigma Aldrich, Hamburg, Germany
Magnesium Sulphate Heptahydrate	Roth GmbH &Co KG, Karlsruhe, Germany
Mannitol	Roth GmbH &Co KG, Karlsruhe, Germany
2-Mercaptoethanol	Roth GmbH &Co KG, Karlsruhe, Germany
Methanol	Roth GmbH &Co KG, Karlsruhe, Germany
Methyl-α-D-gluco-pyranoside [glucose-14C (U)]	American Radiolabeled Chemical, Inc
Milk powder	Granovita, GmbH, Heimertingen, Germany
Nitrogen (liquid)	Linde, Pullach, Germany
Paraplast X-TRA	Sigma Aldrich, Hamburg, Germany
Phlorizin dihydrate	Sigma Aldrich, Hamburg, Germany
Phenylmethylsulfonyfluoride (PMSF)	Roth GmbH &Co KG, Karlsruhe, Germany
Phorbol Myristate Acetate (PMA)	Sigma Aldrich, Hamburg, Germany
Potassium Chloride	Roth GmbH &Co KG, Karlsruhe, Germany
Potassium Dihydrogenphosphate	Roth GmbH &Co KG, Karlsruhe, Germany
Potassium Hydroxide	Roth GmbH &Co KG, Karlsruhe, Germany
Sodium Dodecyl sulphate (SDS)	Roth GmbH &Co KG, Karlsruhe, Germany
Sodium Chloride	Roth GmbH &Co KG, Karlsruhe, Germany
Sodium Hydrogencarbonate	Roth GmbH &Co KG, Karlsruhe, Germany

Sodium Hydroxide	Roth GmbH &Co KG, Karlsruhe, Germany
Tetramethylethylendiamine (TEMED)	Roth GmbH &Co KG, Karlsruhe, Germany
Trishydroxymethylaminomethane (TRIS)	Merck, Darmstadt, Germany
Tris-Hydrochloride (TRIS-HCl)	Roth GmbH &Co KG, Karlsruhe, Germany
Triton-X	Applichem GmbH, Darmstadt, Germany
Tween 20	Sigma Aldrich, Hamburg, Germany
Xylene	Roth GmbH &Co KG, Karlsruhe, Germany

2.1.2 Cell culture media and supplements

All culture media and supplements were purchased from PAA laboratories Gmbh, Pasching, Austria, unless otherwise stated.

RPMI 1640 with L-glutamine	
MEM with Earles's salt with L-glutamine	
MEM:F12 (1:1)	
Hanks Balanced Salt Solution (HBSS), 1X	Gibco™, Invitrogen, Karlsruhe, Germany
Penicillin/Streptomycin, 100X	Gibco™, Invitrogen, Karlsruhe, Germany
Hepes buffer solution, 1M	
Sodium Pyruvate	
Non essential amino acids, 100X	
Gentamycin, 50 mg/ml	

2.1.3 Cytokines and antagonists

Lyophilized cytokines and antagonists were reconstituted in PBS, 0.01% BSA to make desired stock concentrations which were then made into aliquots and stored at -80^{o}C.

rh Leptin	PeproTech Gmbh & Immunotools, Germany
rh TNF-α	Immunotools, Germany
rh RANTES	PeproTech Gmbh, Hamburg Germany
rh MCP-1	Immunotools, Germany
rh IL-6	Immunotools, Germany
Angiotensin-II	Sigma Aldrich, Hamburg, Germany
rm RANTES	PeproTech Gmbh, Hamburg Germany
Candesartan	Sigma Aldrich, Hamburg, Germany
rh Met-RANTES	R&D Systems, Germany / P.J. Nelson (LMU, Munich)

2.1.4. Buffers and solutions

Krebs Ringer Phosphate (KRP 0%) buffer:

KRP buffer was always freshly made and pH adjusted to 7.4 with NaOH adding slowly to avoid $CaCl_2$ precipitation.

NaCl	154 mM
KCl	154 mM
$CaCl_2$	110 mM
$MgSO_4$	154 mM
NaH_2PO_4	100 mM

Krebs Buffer (KB)

Krebs buffer was always made fresh before use; pH was set to either 7.4 or 6.4 depending on the nature of the experiment with, 1M HEPES and 20 mM MES respectively. Before use, the buffer was gassed for a minimum of 1 hour with 95% O_2 and 5% CO_2.

NaCl	119 mM
KCl	24.7 mM
$CaCl_2.2H_2O$	2.5 mM
$MgSO_4.7H_2O$	1.2 mM
KH_2PO_4	1.2 mM
$NaHCO_3$	25 mM

Citrate buffer

Citrate buffer was made fresh and pH set to 6.0 with NaOH.

Citric acid	2.3 mM
Tri sodium citrate dihydrate	12 mM

TAE Buffer, pH 8-8.2

Glacial acetic acid	5.14% v/v
TRIS	24.2% w/v
EDTA	0.5 M

M300 Buffer, pH 7.4

Mannitol	300 mM
HEPES	20 mM

1 tablet of anti-protease (Sigma P8340) was added to 1L of M300 buffer just before use.

2.1.5 Antibodies

Primary antibodies that were used are listed in the table below

Antibody	Target species	Provider	Application	Dilution
Goat anti-GLP-1	Mu, Rat, Hu	Santa Cruz Biotechnology, Inc ,USA	IF	1:50
Rabbit anti-GLP-1	Mu, Rat, Hu	Epitomics, USA	IF	1:100
Rabbit anti-PEPT1	Mu, Rat	Pineda antikörper service, Germany	IF,WB	1:1,500, 1:2,500
Rabbit anti-SGLT1	Mu	Kindly provided by Hermann Koepsell	IF,WB	1:2,000
Rabbit anti-SGLT1	Hu, Mu	Millipore, Germany	IF,WB	1:500
Rabbit anti-RANTES	Hu	Abcam , Cambridge, UK	neutralization	7µg/ml
Rabbit anti-AT_1	Mu, Rat, Hu	Santa Cruz Biotechnology, Inc ,USA	IF,WB	1:50, 1:200
Goat anti- AT_2	Mu, Rat, Hu	Santa Cruz Biotechnology, Inc ,USA	IF,WB	1:50, 1:200
Rabbit anti-CCR1	Mu, Rat, Hu	Santa Cruz Biotechnology, Inc ,USA	IF,WB	1:50, 1:200
Mouse anti-CCR5	Mu, Rat, Hu	Santa Cruz Biotechnology, Inc, USA	IF,WB	1:50, 1:200
Rat anti-F4/80-Alexa Flou 488	Mu	AbD Serotec, Oxford, UK	IF	1:100
Goat anti-Villin	Mu, Rat, Hu	Santa Cruz Biotechnology, Inc, USA	IF,WB	1:50, 1:200

Secondary antibodies used are listed in the table below

Antibody	Provider	Fluorescent dye	Dilution
Donkey anti-goat	Jackson ImmunoResearch, UK	Cy5	1:400
Donkey anti-goat	Santa Cruz Biotechnology, Inc, USA	FITC	1:150
Donkey anti-goat	Jackson ImmunoResearch, UK	Dy Light 649	1:250
Donkey anti-rabbit	Jackson ImmunoResearch, UK	Dy Light 549	1:250
Donkey anti-rabbit	Santa Cruz Biotechnology, Inc, USA	FITC	1:150
Donkey anti-mouse	Santa Cruz Biotechnology, Inc, USA	Cy5	1:150
Donkey anti-goat	Bio-Rad Laboratories, Germany	IRDye 800	1:20,000
Donkey anti-rabbit	Bio-Rad Laboratories, Germany	IRDye 680	1:20,000

2.1.6 Nuclear stains

Dye	Provider	Dilution
DAPI	Sigma Aldrich, Germany	1:500
Propidium Iodide	Molecular Probes, CA, USA	1:150
Draq-5	Cell Signaling Technology, Inc, USA	1:150

2.2 Methods

2.2.1 *In vitro* methods

2.2.1.1 Isolation and primary culture of mature human adipocyte

Isolation of adipocytes from human adipose tissue

Subcutaneous adipose tissue samples were obtained from subjects undergoing elective plastic surgery. Patient consent was obtained beforehand. Tissue samples were transported in DMEM: F12 medium containing 1% Pen/Strep. Blood vessels and connective tissue were removed and tissue was minced carefully under a sterile hood and tissue pieces were added into a 50 ml falcon tube up to the 10-13 ml marking. The volume was made up to 45 ml with 4% BSA, KRP buffer containing 100 U/ml collagenase. The tubes were sealed with parafilm and placed in a shaking water bath (60-80 beats/minute) maintained at 37^{o}C for 60-90 minutes. After digestion, the material was filtered with an autoclaved nylon mesh of 2,000 um pore size to remove undigested material and connective tissue. A second filtration step was done with the filtrate using a nylon mesh of 250 µm pore size. Next, three washing steps were performed with wash buffer. The adipocytes were left in the wash buffer for a few minutes so that they could float to the top.

Preparation of pre-conditioned adipocyte medium (PAM)

1ml floating adipocytes was seeded with 4 ml of DMEM: F12 containing 1% Pen/Strep. After 30 minutes, media was replaced with fresh media and cells were cultured in a humidified chamber maintained at 37^{o}C. After 16 hours, pre conditioned media was collected, made into aliquots, snap frozen and stored at -80^{o}C until further use

Figure 7: Isolation of mature adipocytes from human adipose tissue. Adipose tissue was obtained from human subjects undergoing elective plastic surgery. The tissue was minced and digested with collagenase. After a series of filtration steps, mature adipocytes were obtained and cultured in DEME:F12.

2.2.1.2 Intestinal epithelial and endocrine cell culture conditions

Cells were grown and maintained in a humidified atmosphere at 37^{o}C and 5% CO_2.

NCI-H716 cells

Human enteroendocrine NCI-H716 cells (ATCC, CCL-251) were obtained from the American Type Culture Collection. The cells were grown in suspension in RPMI 1640 medium supplemented with 10% FBS, 2 mM L-glutamine, 100 IU/ml penicillin, 100 µg/ml streptomycin, 2.5 g/l glucose, 10 mM HEPES, 1 mM Na-pyruvate. Fresh media was added to the cells twice a week. Cells were counted in a Neubauer's chamber after staining with Trypan blue (1:5 dilution). Cells were split by mixing the cells thoroughly and gently with a pipette and then taking desired volume of cell suspension and growth media in a new flask. Cells were usually split when they reached 1 million/ml.

Caco-2 cells

Caco-2 is a colonic tumor cell line which, when cultured, spontaneously exhibits enterocyte-like characteristics. Caco-2 cells were obtained by ATCC and cultured in a culture medium consisting of MEM with Earle's salts with L-glutamine, 2% non essential amino acids, 10% FCS, 100 µg/ml gentamycin. Cells were used between passages 30 and 60. Cells were split when they reached about 80% confluency by adding trypsin (concentration, 0.5 ml for a 5ml culture flask) to detach the adherent cells. Cells were incubated with trypsin for 5 minutes at 37^{o}C and then growth media was added to neutralize the trypsin. This was followed by mixing the cell suspension, centrifugation, dissolution of the cell pellet in fresh growth media and finally seeding desired volume of cell suspension with fresh growth media in a new culture flask.

2.2.2 *Ex vivo* models

Mouse intestinal rings

The method of Jang *et al* was adapted for this (144). Mice were anesthetized with isoflurane (Baxter GmbH, Germany) and sacrificed by cervical dislocation. The abdominal wall was opened by midline laparotomy and the whole small intestine was removed carefully by making one cut below the stomach and another before the caecum. Care was taken to remove mesenteric fat sticking to the walls of the intestine. The intestine was flushed carefully with ice cold Krebs buffer saturated with 95% O_2/ 5% CO_2. The cleaned intestine was everted using a custom made metal rode and laid on a glass plate kept on ice. The everted intestine was then sliced into 0.5 cm wide ring pieces.

2.2.3 GLP-1 secretion assay

2.2.3.1 NCI-H716 cells

For GLP-1 secretion experiments, NCI-H716 cells were plated at a density of 4.10^5 (1ml/well) on 24-well cell culture plates pre-coated with Matrigel™ basement membrane matrix (BD Biosciences) diluted (1:100) in DMEM high glucose (4g/L) medium. Medium was changed every day until the experiment. Cells were cultured until they reached 80% confluency and then growth medium was removed and the cells were washed twice with warm Hank's Balanced Salt Solution without calcium and magnesium (HBSS, Invitrogen). Compounds to test were made in PBS buffer supplemented with 1 mM $CaCl_2$. DPP-4

inhibitor was added to the effector solutions (20 µl/ml), pH adjusted to 7.2 , pre-warmed to 37^{o}C and incubated on the cells (0.5ml/well) for 1 hour at 37^{o}C in a humidified incubator at 5% CO_2. At the end of 1 hour, the plate was immediately placed on ice to stop further secretion; medium was collected and centrifuged at 4^{o}C for 10 minutes at 3,000 rpm to remove cell debris. Supernatant was collected and stored at -80^{o}C until GLP-1 determination. Effectors were always tested in duplicate. Cells were homogenized with 0.1 M NaOH and protein concentration per well was measured by Bradford assay (Bio-Rad, Munich, Germany). GLP-1 (active) was assayed using an ELISA (Millipore) specific for GLP-1 (7-36) amide and GLP-1 (7- 37) amide and normalized to protein content.

To study the effect of cytokines on nutrient stimulated GLP-1 secretion, cells were washed and pre-incubated with test cytokines supplemented in growth medium for defined time periods at 37^{o}C in a humidified incubator at 5% $CO_{2.}$ After the incubation period, media was removed and cells were incubated with effector solution for 1 hour.

2.2.3.2 Everted mouse intestinal rings

After isolation of intact whole small intestine from the mouse, the intestine was cut into two halves, proximal and distal small intestine. The distal half was used for GLP-1 secretion. It was everted with a custom made metal rod of narrow bore and rinsed in Krebs buffer, pH 7.4 containing 500 µM DTT. Everted intestine was sliced into roughly 0.5 cm wide rings and placed in ice cold KRB + 500 µM DTT in a 96-well plate. Once all the rings were prepared, they were blotted on a paper towel and then transferred into pre-warmed (37^{o}C) effector solutions in 96-well plate and incubated for 45 minutes. Effectors were made in Krebs buffer, pH 7.4 without DTT. DPP-4 inhibitor (20 µl/ml was added to the effector solution. After the incubation period, intestinal rings along with effector solution were collected in microcentrifuge tubes and centrifuged at 4^{o}C for 10 minutes at 10,000 rpm. Supernatants were collected and stored at -80^{o}C. Rings were digested in 1 M NaOH and protein concentration was measured by Bradford assay (Bio-Rad, Munich, Germany). GLP-1 (active) was assayed using an ELISA (Millipore) specific for GLP-1 (7-36) amide and GLP-1 (7- 37) amide and normalized to protein content.

2.2.4 Immuno staining and confocal microscopy

2.2.4.1 Cells

NCI-H716 and Caco-2 cells were grown on Matrigel coated sterile glass cover slips until confluency. Growth medium was removed; cells were washed twice with PBS and fixed with 4% formalin in PBS, pH 7.4 for 15 minutes at room temperature. After fixation, cells were washed twice and permeabilised for 10 minutes with 0.25% Triton X-100 in PBS. Cells were washed again with PBS and incubated in blocking solution (5% milk in PBS) for 30 minutes at room temperature. This was followed by overnight incubation at 4^{o}C with primary antibodies prepared in PBS containing 0.05% Tween 20 (PBS-T) in a humidified chamber. Cells were washed twice with PBS and incubated with appropriate secondary antibodies conjugated with a fluorescent dye for 1 hour at room temperature in the dark. Secondary antibodies were also diluted in PBS-T. Cells were washed twice with PBS and mounted on glass slides using fluorescent mounting medium (DAKO North America Inc.; Carpenteria, USA) and allowed to air dry in the dark. Cells were visualized with a laser scanning spectral confocal microscope (Leica TCS SP2, spectral confocal and multiphoton system).

2.2.4.2 Tissue

Tissue processing

Mouse tissue was excised after midline laparotomy and gently flushed with Krebs buffer to remove faecal debris. Small pieces of the intestine (approximately 2 mm) were cut and fixed in 4% formalin in PBS, pH 7.4 for 6-8 hours at room temperature. After fixation, tissue pieces were dehydrated in graded concentrations of ethanol, 70% and 80% for 30 min, 2 × 95% for 45 min, 3 × 100% 45 min and 2 × 100% xylene for 45 min at 40^{o}C, and then embedded in paraffin with the help of an embedding machine (Microm, Walldorf, Germany). Paraffin embedded tissue was sectioned into 7 µm thick sections with a microtome (Thermo Scientific Microm, Walldorf, Germany) and dried overnight at room temperature on Superfrost Plus micro slides (Menzel GmbH, Braunschweig, Germany) which were then stored at 4^{o}C until further use.

Immunofluorescent staining

For staining, tissue sections were first dewaxed in xylene (2 × 5 minutes), rehydrated in descending concentrations of ethanol (2 × 100% for 5 minutes, 1 × 100% for 2 minutes, 2 × 96% for 2 minutes and, 1 × 80% for 2 minutes) and finally rinsed under running tap water for 3 minutes. For antigen retrieval, the slides were boiled in 10 mM citrate-buffer in a pressure cooker for 20 minutes in a microwave oven. The slides were then left to cool in citrate buffer for 7 minutes. Slides were incubated for 1 hour in blocking solution of 5% milk (Frema Reform Instant-Magermilchpulver; GRANOVITA GmbH; Heimertingen, Germany) in PBS to block unspecific binding sites. After blocking, slides were washed 3 times with PBS. Primary antibodies were made in PBS-T (PBS containing 0.05% Tween 20) and applied on the slides and incubated overnight in a humidified chamber at 4^{o}C. Slides were washed twice with PBS, and incubated for 1 hour in the dark with appropriate fluorescent labelled secondary antibodies made in PBS-T. For nuclei staining, sections were counterstained with DAPI or propidium iodide or Draq5 along with the secondary antibody mix. After washing 3× with PBS, slides were mounted with a drop of fluorescent mounting medium (DAKO North America Inc.; Carpenteria, USA) and sealed with a cover slip (Carl Roth GmbH & Co KG: Karlsruhe, Germany) and allowed to air dry. Slides were stored at 4^{o}C and protected from light. Stained tissue was observed by using a confocal microscope (Leica TCS SP2, spectral confocal and multiphoton system, Wetzlar, Germany).

H&E staining

Some of the tissue section slides were control-stained with hemalum and eosin. Hemalum is a complex of hematoxylin and aluminum ions that stains the nucleus of the cell dark violet color, whilst eosin stains the cytosol and other eosinophilic structures red-pink shade.

The dried slides were rehydrated by several incubation steps at room temperature:

100% Xylol	3 min
100% Xylol	3 min
100% Ethanol	2 min
96% Ethanol	2 min
80% Ethanol	1 min
deionised water	1 min
Meyer’s Hemalum	4 min
tap water	2 min

96% Ethanol	0.5 min
Eosin	2 min
70% Ethanol	1 min
96% Ethanol	1 min
100% Ethanol	1 min
100% Ethanol	1.5 min
100% Xylol	1.5 min

One drop of mounting medium (DAKO fluorescent mounting medium S3023, Dako, Carpinteria, CA, USA) was put on each slide and a cover slip was put on them. They were dried completely under the hood in the dark for a few hours before being examined under a light microscope (Leica Microsystems, Wetzlar, Germany).

2.2.5 Molecular biology

2.2.5.1 RNA isolation from cells and intestinal mucosal tissue

Cells

Cells (NCI-H716 cells and Caco-2) were grown in 6-well culture plates till they reached a confluent state. Cells were washed once with ice cold PBS and total RNA was extracted by using TRIzol® (Invitrogen) according to the manufacturer's instructions. RNA was dissolved in Diethylpyrocarbonate (DEPC)-treated water (0.01% v/v). RNA concentration was estimated with Nanodrop 1000 spectrophotometer (Thermo Fischer Scientific).

Tissue

Mouse intestine was everted and mucosal tissue was scraped using a glass slide. Tissues were transferred to a 2 ml vial and snap frozen immediately. For isolation of RNA, 1 ml/tube TRIzol® was added to the mucosa before it thawed completely and homogenized using Ultraturrax (Polytron Pt1600E, Kinematic AG, Lucerne, Switzerland). Rest of the steps were performed as per manufacturer's instructions (Invitrogen). RNA purification was done using RNeasy® columns (RNeasy mini kit, Qiagen). RNA was dissolved in Diethylpyrocarbonate (DEPC)-treated water (0.01% v/v). RNA concentration was estimated with Nanodrop 1000 spectrophotometer (Thermo Fischer Scientific).

Quality control for RNA isolated

The absorbance ratios of RNA (at λ=260 nm) and protein (at λ=280 nm) and phenol/ethanol (at λ=230 nm) obtained with the Nanodrop revealed the purity of the obtained RNA. The 260/280 nm absorbance ratio should be 1.7-2.0, the 260/230 ratio should be > 1.5. Intact RNA was confirmed by running the isolated RNA on an agarose gel.

Composition and preparation of the RNA gel

0.8 g agarose was dissolved in 65 ml DEPC water and was heated in a microwave oven for 1.5 minutes to form a homogenous mixture. The mixture was allowed to cool at room temperature for 5 minutes and 6.6 ml of 37% formaldehyde and 8 ml of 10X MOPS buffer was added to it. The entire mix was gently poured in the electrophoresis tray and allowed to polymerize for 1-2 hours.

One the gel polymerized, it was placed in the electrophoresis chamber containing 500 ml of 1X MOPS. RNA sample (2 µg of RNA + 3- fold the volume of loading dye (Promega) made up to a volume of 10 µl with DEPC water) was heated at 75^{o}C for 5 minutes and immediately placed on ice until it was loaded in the well on the gel. The gel was run at 80 V for 1.5–2 h. After completion of the run, a picture was made. 2 crisp bands corresponding to 28 S and 18 S in the ratio of 2:1 denote intact RNA.

2.2.5.2 Synthesis of cDNA and real time RT-PCR

cDNA was synthesized from 5µg of RNA using commercially available kits from Ambion, Applied Biosystems and Promega. Quantitative real-time PCR (qPCR) was performed in a Lightcyler (Roche, Germany) with 12.5 ng of cDNA per PCR reaction with the FastStart SYBR Green kit (Roche, Germany). Cycle parameters were annealing at x^{o}C (depending on primer pair used) for 10 seconds, elongation at 72^{o}C for 20 s and melting at 95^{o}C for 15 seconds. PCR was usually done for 35 cycles.

The primer sequences and annealing temperature for primers used are given in the table below.

Product size, bp	Upstream sequence (sense)	Downstream sequence (antisense)	Ann. T (^{o}C)	Gene	Species
296	TGG AAA CTC CAA ACA CCA CAG	CCC AGT CAT CCT TCA ACT TG	60	CCR1(167)	human

539	TGA CAA CCT CAC TAG ATA CAG TTG	CTC TTC AAA CAA CAA CTC TTC AGT CTC	58	CCR3(167)	human
280	AAT AAT TGC AGT AGC TCT AAC AGG	TTG AGT CCG TGT TCA CAA GCC C	58	CCR5(167)	human
255	GAT GAT TGT CCC AAA GCT GG	TAG GTA ATT GCC AAA GGG CC	60	AT_1	human
293	AGT AAG CAC AGA ATT CAA AG	AGT AAA GAA TAG GAA TTG CAT	57	AT_2	human
215	CATCGCTCAGAC ACCA	AGCTTCCCGTTCTC AG	60	GAPDH	human
298	TTT GCC TAC CTC TCC CTA GAG CTG	ATG CCG ATT TTC CCA GGA CC	60	RANTES	murine
239	TGA CTA CAG CAA GTA TCT GG	CAA CAA TGG CGA CCT C	60	Proglucagon	human
303	ATC TAC GCC AAG GTC C	CCC GGT TCC ATA AGC A	60	SGLT1	human
100	TTA GCT TCC ATG CCG GCC TTA TA	TCC ACT GCT TCA GGC TCT TGT	60	CCR1	murine
128	CAA GAC AAT CCT GAT CGT GCA A	TCC TAC TCC CAA GCT GCA TAG AA	60	CCR5	murine
63	CCA TTG TCC ACC CGA TGA AG	TGC AGG TGA CTT TGG CCA C	60	AT-1	murine
80	CAG CAG CCG TCC TTT TGA TAA	TTA TCT GAT GGT TT TGT GAG CAA	60	AT-2	murine
75	GAG GCA AAT CTG AGC AAC ATT G	GAG TTC GAG GAG GAT GCT ATT GA	60	Angiotensin-ogen	murine
198	ATCCCAGAGCTG AACG	GAAGTCGCAGGAG ACA	60	GAPDH	murine

The reaction mix for one reaction is given in the table

Components	**Volume [µl] per reaction**
cDNA (25 ng/µl)	1
H_2O	6.4
$MgCl_2$ (25 mM)	1.2
Forward primer (20 µM)	0.2
Reverse primer (20 µM)	0.2
LC-SYBR-Green Enzyme mix (10X)	1
Total volume per reaction	10

DNA products were run on an agarose gel to confirm product size obtained with the predicted size. 2% agarose gel was made in TAE Buffer. 1 µl 10X blue DNA loading dye (Promega Madison, WI USA) was added to each sample and spun down. 10 µl sample mix

was loaded into the well pocket. The gel was run at 135 V for 45 min. For product size estimation, 5 µl of a 100 bp ladder (Promega, Madison, WI USA) was used.

2.2.5.3 siRNA transfection of NCI-H716 cells

Pre-designed siRNA (*Silencer*® Select siRNA) targeting human CCR1 and CCR5 were purchased from Ambion (Applied Biosystems). These RNA oligonucleotides were re-suspended in nuclease-free water to obtain a final concentration of 10 µM. NCI-H716 cells were seeded at a density of 50,000/well in a 24-well plate format in normal growth medium without antibiotics. The next day, subconfluent differentiated NCI-H716 cells were transiently transfected with siRNAs, using Lipofectamine 2000 according to the manufacturer's protocol (Life Technologies, Carlsbad, CA). Briefly, a mixture of siRNA and Opti-MEM® I reduced serum medium 1X (Gibco) was made. Another mixture of Lipofectamine 2000 and Opti-MEM® I reduced serum medium 1X was made. The two mixtures were combined and the complex incubated for 20 minutes at room temperature following which 100 µl of the complex was added to the wells containing cells and 400 µl growth medium, without antibiotics resulting in a final concentration of 5 nM for the siRNAs. The plate was gently rocked back and forth and incubated at 37^{o}C in a humidified incubator at 5% CO_2. Cells were examined 24, 48 and 72 hours after transfection by performing a western blot. Cells were also transfected with negative control siRNA.

2.2.5.6 SDS PAGE and Western blot

10% running gel

The ingredients for the preparation of 1 running gel for the separation of proteins with MW in the range between 20-70 kD are listed in the table below.

Component	Volume (ml)
30% Acrylamide/Bis-acrylamide	2
1.5 M Tris HCl, pH 8.8	1.5
10% SDS	0.06
H_2O	2.5
TEMED	0.002
10% (w/v) ammonium persulfate (APS)	0.062
Total volume	6

5% stacking gel

The ingredients for preparation of 1 stacking gel are listed in the table below

Components	Volume (ml)
Stacking gel	2
TEMED	0.002
10% (w/v) APS	0.015

Protein extraction

Protein extraction from NCI-H716 cells were done as follows. Growth media was removed. Cells were washed twice with in ice cold PBS and scraped off from the well of the cell culture plate with PBS supplemented with 1mM PMSF. Cell suspension was centrifuged at 3,000 rpm for 5 minutes at 4^{o}C. The supernatant was discarded and cell pellet re-suspended in PBS containing 1mM PMSF by passing seven times through a 24-gauge needle. Cell suspension was re-centrifuged at 3,000 rpm for 5 minutes at 4^{o}C. The resulting supernatant containing total protein was transferred into a pre-cooled microfuge tubes. Protein content was determined by a Bradford protein assay kit (Bio-Rad, Munich, Germany).

Western blot

10 µg of proteins was loaded into the well and subjected to electrophoresis on a 10% (w/v) polyacrylamide gel at 15 mA and 120 V for 1.5 hours. Semi-dry transfer of protein was done onto a nitrocellulose membrane (Whatman Optitran BA-S 85 Reinforced NC, 0.45 µM, Whatman GmbH, Germany). After transfer was complete, the membrane was incubated in blocking solution, 3% BSA (Fraction V, Sigma) in PBS (pH 7.4) for 1 hour at room temperature. The membranes were incubated with primary antibody in PBS with 0.1% (v/v) Tween 20 (PBT-T) overnight with gentle agitation at 4^{o}C. After three washes in PBS-T, the membranes were incubated with secondary antibodies labelled with IRDye infra red dyes, (LI-COR Biosciences) diluted in PBS-T (1:20,000) for 1 hour at room temperature with gentle agitation. At the end of the incubation, the membranes were visualized and analyzed by the ODYSSEY® Infrared Imaging System (LI-COR Bioscience).

2.2.6. Measurement of intracellular calcium

Live cell imaging of NCI-H716 cells

Levels of $[Ca^{2+}]_i$ was quantified by fluorescence imaging, using the calcium indicator dye Fura-2AM. Briefly, NCI-H716 cells were seeded on Matrigel® coated slides. On the day of the experiment, growth media was removed, cells were incubated for 5 minutes in PBS containing 1.8 mM $CaCl_2$ at 37°C in a humidified incubator at 5% CO_2. Then, cells were incubated for 30 minutes in dye solution containing 10 µM Fura-2AM (F1221, Molecular Probes, Karlsruhe, Germany) in pre-warmed oxygenated PBS buffer, pH 7.4 along with 4% Pluronic acid (Molecular probes) and 1.8 mM $CaCl_2$ at 37°C humidified incubator. This was followed by 2× washing steps for 5 minutes in the incubator with PBS, calcium free buffer. Slides were mounted on the stage of an inverted microscope (Leica, AF6000LX, Mannheim, Germany) fitted with an incubation chamber and equilibrated to 37°C. Cells were perfused with pre-warmed PBS, calcium free for few minutes to reach stable base line readings. Cells were then perfused with an effector solution at a rate of 30 ml/hour. Changes in $[Ca^{2+}]_i$ in the cells loaded with Fura-2 were measured ratiometrically using dual wavelength excitation, employing a designated Fura-2 filter cube and a fast external filter wheel (Leica, Mannheim, Germany). This setup allowed to record fluorescence at 510 nm with excitation at 380 nm or 340 nm. Pairs of images were obtained every 1.5 seconds and the image ratio from each pair was computed. In order to investigate the role of cytokines and phlorizin (inhibitor of SGLT1) on intracellular calcium, cells were first perfused with 1 ml of cytokine/inhibitor solution prior to effector + cytokine/inhibitor stimulation. Ionomycin [2 µM] was used as a positive control in all the experiments.

2.2.7 cAMP measurement

NCI-H716 cells were seeded at a density of 4^*10^5 cells/ml in 24-well plates. Media was removed and cells washed twice with HBSS containing 1 mM IBMX to inhibit phosphodiesterases and incubated in the last wash for 5 minutes at 37°C. Cells were incubated with 300 µl of effectors and RANTES diluted in HBSS for defined time periods ranging from 5 minutes to 1 hour. At the end of the incubation periods, supernatant was aspirated from the wells and 200 µl of 0.1M HCL was added and incubated at room temperature for 20 minutes. Cells were scraped off the surface with a cell scraper. Mixture

was dissociated by pipetting up and down until the suspension became homogenous and transferred into centrifuge tubes and centrifuged at 1000 rcf for 10 minutes. Supernatant was decanted into a clean tube and stored at -80^{o}C until analysis. cAMP was measured using a commercially available kit from Cayman Chemical Company. The assay is based on the competition between free cAMP and a cAMP-acetyl cholinesterase conjugate (tracer) for a limited number of cAMP- specific rabbit antibody binding sites. The rabbit antibody-cAMP (either free or tracer) complex binds to the mouse monoclonal anti-rabbit IgG that is previously attached to the well. The plate is developed with Ellman's Reagent which contains the substrate to acetyl cholinesterase. Intensity of the color formed is determined spectrophotometrically.

2.2.8 PKA assay

Mouse intestine was everted and 5 cm long segments were made and incubated for 30 min at 37^{o}C in an incubator in Krebs buffer containing 1 mM glucose in the absence (control) or presence of desired concentrations of cytokine. After the incubation time, mucosa from each segment was scraped and homogenised in 500 µl of cell lysis buffer (Cell Signalling) supplemented with 1 mM DTT, 1 mM PMSF and 10 µg/ml Aprotinin on ice using a polytron at setting of 10,000 rpm (2 × 10 sec bursts). Samples were kept on ice for 10 minutes followed by centrifugation at 150,000 rcf for 30 minutes at 4^{o}C. The clear supernatant was transferred to pre-chilled microcentrifuge tubes. This is the cytosolic fraction. An aliquot was taken for protein determination and samples stored at -80^{o}C. Protein kinase activity in each sample homogenate was detected and quantified using a commercially available kit (Enzo Life Sciences) according to manufacturer's instructions.
In the assay, the substrate, which is readily phosphorylated by PKA, is pre-coated on the wells of the provided PKA substrate microtiter plate. The samples to be assayed are added to the appropriate wells, followed by the addition of ATP to initiate the reaction. The kinase reaction is terminated and a phosphospecific substrate antibody is added to the wells which bind specifically to the phosphorylated peptide substrate. The phosphospecific antibody is subsequently bound by a peroxidase conjugated secondary antibody. The assay is developed with tetramethylbenzidine substrate (TMB) and the color develops in proportion to PKA phosphotransferase activity (Figure 8). The color development is stopped with acid stop solution and the intensity of the color is measured in a microplate reader at 450 nm. The relative kinase activity in the cell lysate was calculated by

subtracting the absorbance of each sample from the blank (without any kinase) and dividing it by the quantity of crude protein used per assay. Results were expressed as fold change of cytokine treated tissue by control treatment.

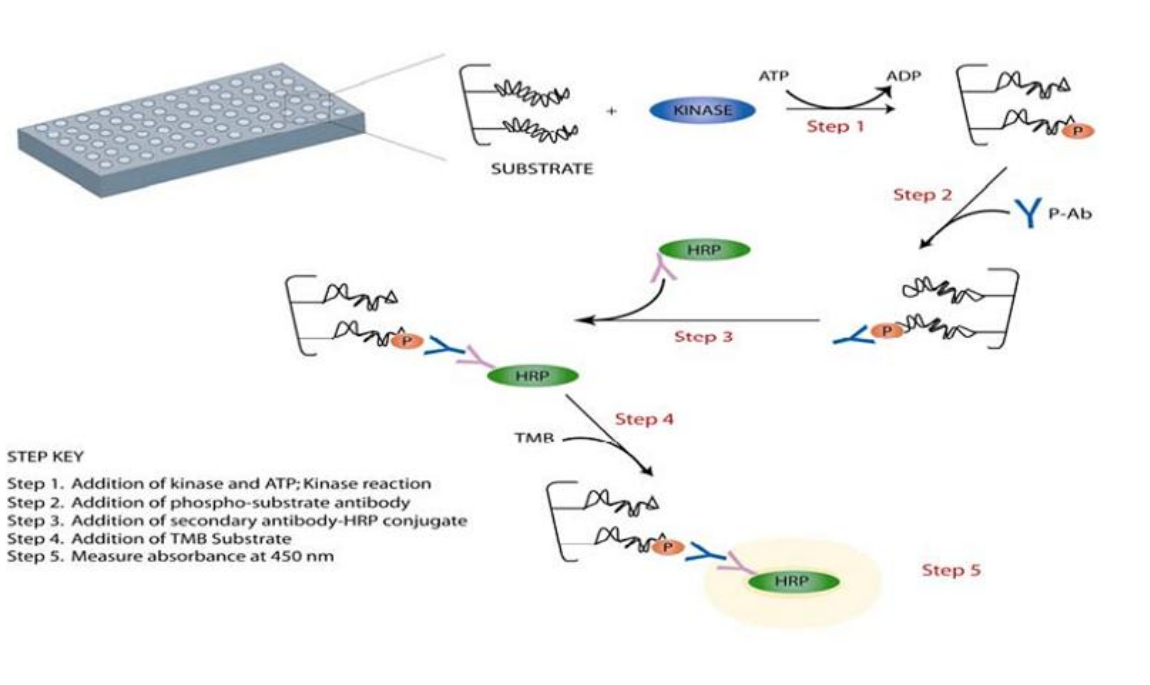

Figure 8: Principle of Protein kinase A activity assay. Scheme adapted from Enzo life sciences.

2.2.9. Isotope labelled substrate uptake by mouse intestinal rings

Everted mouse intestinal rings were prepared as previously described in section 2.2.2. Groups of four to six intestinal rings of 1 cm in length were incubated at 37°C for 3 minutes in Krebs buffer in the absence (control) and the presence of cytokines and the inhibitor of SGLT1, phlorizin [0.5mmol/l] as indicated. Then, the rings were incubated for 2 minutes in an uptake solution corresponding to Krebs buffer containing 1 mmol/l α-MDG and 1 µmol/l of the isotopic tracer d-[^{14}C] α-MDG for SGLT1 or 1mmol/l gly-sar and 10 µmol/l [^{14}C] gly-sar for PEPT1. For SGLT1 transport experiments, pH of the substrate solution was set at 7.4 and for PEPT1, it was set at 6.4. After the incubation period, the rings were washed twice in ice-cold Krebs buffer, pH 7.4. Rings were blotted on a tissue and put into counting vials (one per vial). Rings were digested in 200 µl of BIOSOL™, tissue solubilizer (National Diagnostics, Atlanta, U.S.A) overnight in a shaking incubator at 50°C. The next day, 20 µl of hydrogen peroxide was added in the vials to decolorize the samples and incubated at room temperature for 1 hour. Then, 3 ml of

BIOSCINT™ scintillation cocktail (National Diagnostica, Atlanta, U.S.A) was added to the vials and vortexed well. Radioactivity incorporated in the tissue was quantified by a liquid scintillation counter (Wallack, Germany). Results were expressed as picomoles α-MDG/gly-sar per cm of tissue per minute.

2.2.10 Brush border membrane preparation

Mucosa was scraped from the first 10 cm of mouse small intestine and snap frozen for brush border membrane (BBM) preparation for later use. 1 µl of 1M PMSF was added directly onto the mucosal tissue before it thawed. Frozen tissue was thrown into 20 ml of M300 buffer and homogenized for 10 seconds with an Ultraturax. To this mixture, 0.4 ml of 1M $MgCl_2$ and 0.22 ml of 0.416 M EGTA was added and centrifuged for 7 minutes at 3840 rcf at 4^{o}C. Supernatant was carefully transferred into another falcon; 0.4 ml of 1M $MgCl_2$ was added to it and incubated for 15 minutes on ice. Then the mixture was centrifuged for 15 minutes at 2750 rcf at 4^{o}C. The supernatant was poured into centrifuge tubes, weighed and centrifuged again at 32,500 rcf for 30 minutes at 4^{o}C. The supernatant was discarded and the pellet obtained, was resuspended first in 1 ml of M300 Buffer with a needle. 0.4 ml of $MgCl_2$ was added to it and volume made up to 20 ml with M300 buffer. The mixture was incubated for 15 minutes on ice followed by another centrifugation step for 15 minutes at 2750 rcf at 4^{o}C. The supernatant was poured into centrifuge tubes, weighed and centrifuged again at 32,500 rcf for 30 minutes at 4^{o}C. The supernatant was discarded and the pellet obtained was resuspended in 30-50 µl of M300 buffer. 1 µl of PMSF was added to it. The mixture was homogenized with a needle. Aliquots were made and snap frozen in liquid nitrogen.

2.2.11 *In vivo* mice experiments

2.2.11.1 Mouse husbandry

Mice were maintained at 22 ± 2^{o}C and a 12:12 hour light/dark cycle with access to water and a chemically defined diet (Ssniff GmbH, S5745-E702) *ad libitum* unless otherwise stated. All procedures applied during this study were conducted according to the German guidelines for animal care and approved by the state ethics committee under reference number 55.2-1-54-2532-67-11.

2.2.11.2 Intraperitoneal (IP) injection of adipokines

For acute experiments, the mice received only a single IP injection of the adipokine dissolved in 200 µl PBS while the control group received 200 µl PBS alone. For chronic experiments, they received 4 injections, a single injection on four consecutive days. Throughout this period, they had *ad libitum* access to food and water and mice were monitored for any adverse effects induced by the injections.

2.2.11.3 Oral glucose challenge

Mice were deprived of food for 6 hours usually from 7.30-13.30 with only *ad libitum* access to water. Mice were weighed. Fasting blood glucose was measured from the tail vein blood sample with a glucometer (FreeStyle Lite, Abbott). Mice were given orally with the help of a gavage feeding needle (Fine Science Tools), 6g/kg glucose immediately after the IP injection of adipokine/PBS. Control group received water. Another blood glucose measurement was done 10 minutes following glucose/water administration.

2.2.11.4 Blood, organ collection and storage

At the end of 10 minutes following the glucose/water administration, mice were anesthetized with isoflurane. Blood samples were obtained by puncturing the retro-orbital sinus with heparin coated capillaries (Neolab, Heidelberg, Germany) and collected into pre-cooled Na-EDTA coated tubes (Sarstedt, Nuembrecht, Germany). 20 µl/ml DPP-4 inhibitor (Millipore) was added to the blood within 30 seconds of collection and tubes were inverted gently to allow mixing of the blood with the inhibitor. Blood was kept back on ice and centrifuged at 4^{o}C at 3,200 rpm for 20 minutes. Plasma was collected, made into aliquots and stored at -80^{o}C. The plasma was used to measure active GLP-1 (Millipore, Germany), total GLP-1 (Yanaihara Institute, Japan), total GIP (Millipore, Germany) and Insulin (Crystal Chem, USA) by ELISAs.

The abdominal cavity of the mouse was cut open by midline incision, and pancrea, liver, epididymal adipose tissue were collected and snap frozen in liquid nitrogen. The whole small intestine was isolated; mucosa scraped off and snap frozen. Tissue samples were then stored at -80^{o}C. In another set of mice, rings were made from everted intestine and used for radiolabeled uptake experiments.

3 RESULTS

3.1 Proof of concept

3.1.1 Weight gain in C57BL/6 mice on a high fat diet

C57BL/6 mice were fed a high diet (Ssniff® EF, D12492 (II) mod.) for 12 weeks with 60% of the total energy coming from fat. Mice on normal rodent chow served as the control group. Body weight was measured throughout the feeding period. Mice on the high fat (HF) diet gained 16 ± 2g, while on the control diet (CD), 8 ± 2g over 12 weeks (Figure 9).

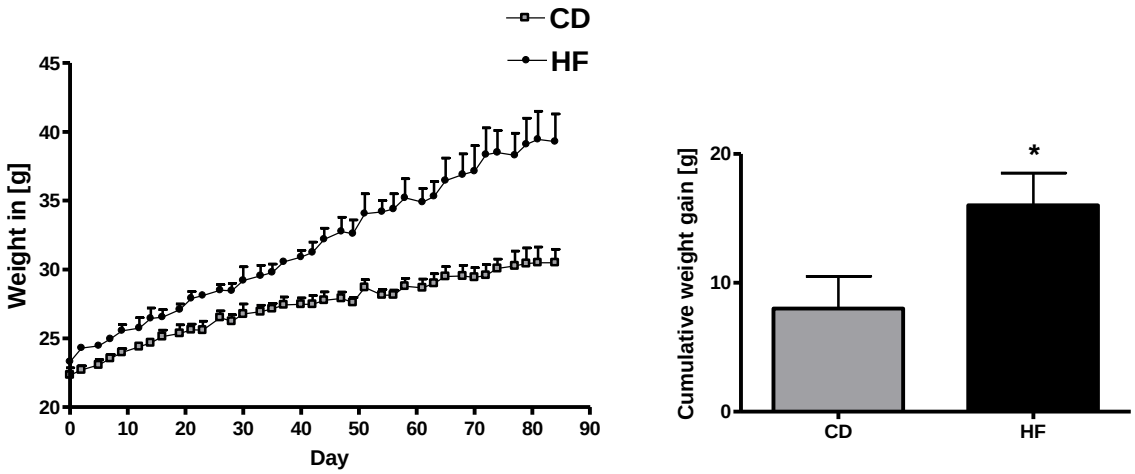

Figure 9: Weight gain on 60% high fat diet. Statistical significance determined by Student's t test, *$p < 0.05$, n = 6 mice per group.

3.1.2 Adipose tissue weight and morphology

Epididymal, subcutaneous and mesenteric adipose tissue were collected and weighed in both the groups, HF and CD. All the three fat depots were significantly increased in the mice on HF diet (Figure 10).

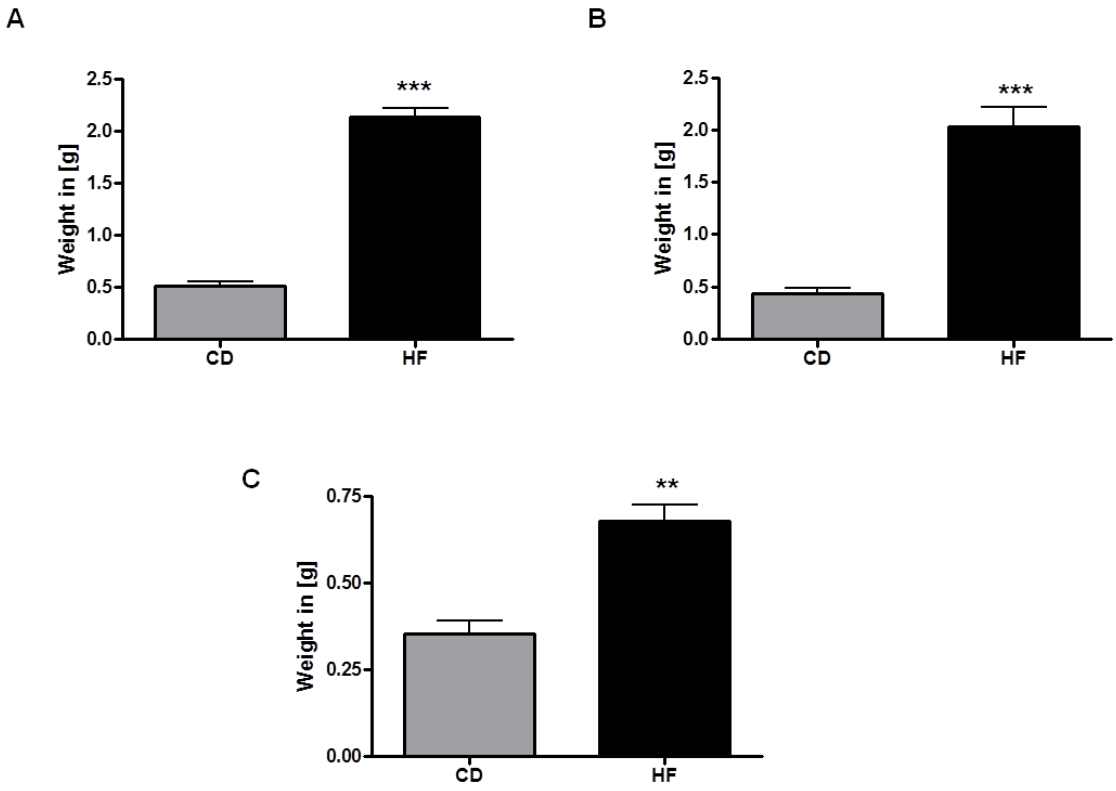

Figure 10: Weight of (A) epididymal adipose tissue, (B) subcutaneous adipose tissue and (C) mesenteric adipose tissue in mice on CD and HF diet. Statistical significance was determined by Student's t test, **p < 0.01, **p < 0.001, n = 6 mice per group.

Epididymal fat was sectioned and then stained with Hematoxylin and eosin (H&E) to observe the morphology of the adipocytes. Adipocytes were much larger in the obese animals (Figure 11) in accordance with literature suggesting hypertrophy and hyperplasia that occurs with progressive weight gain (6, 9).

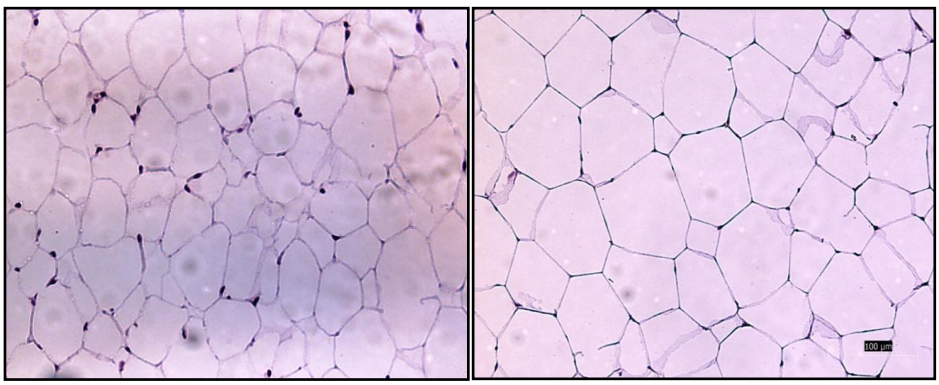

Figure 11: H&E staining of epididymal adipose tissue in lean (left) and obese (right) mice.

3.1.3 Macrophage infiltration in WAT in a mouse model of obesity and diabetes

Epididymal fat was collected from *db/db* (model of diabetes, obesity and dyslipidemia due to deficient leptin receptor activity) mice and subjected to H&E, and immunofluorescent staining with an antibody against F4/80 which is a transmembrane protein present on the cell-surface of mouse macrophages and is associated with mature macrophages. Macrophages were found to surround dying or necrosing adipocytes in a 'crown' like structure as can be seen in the figures below.

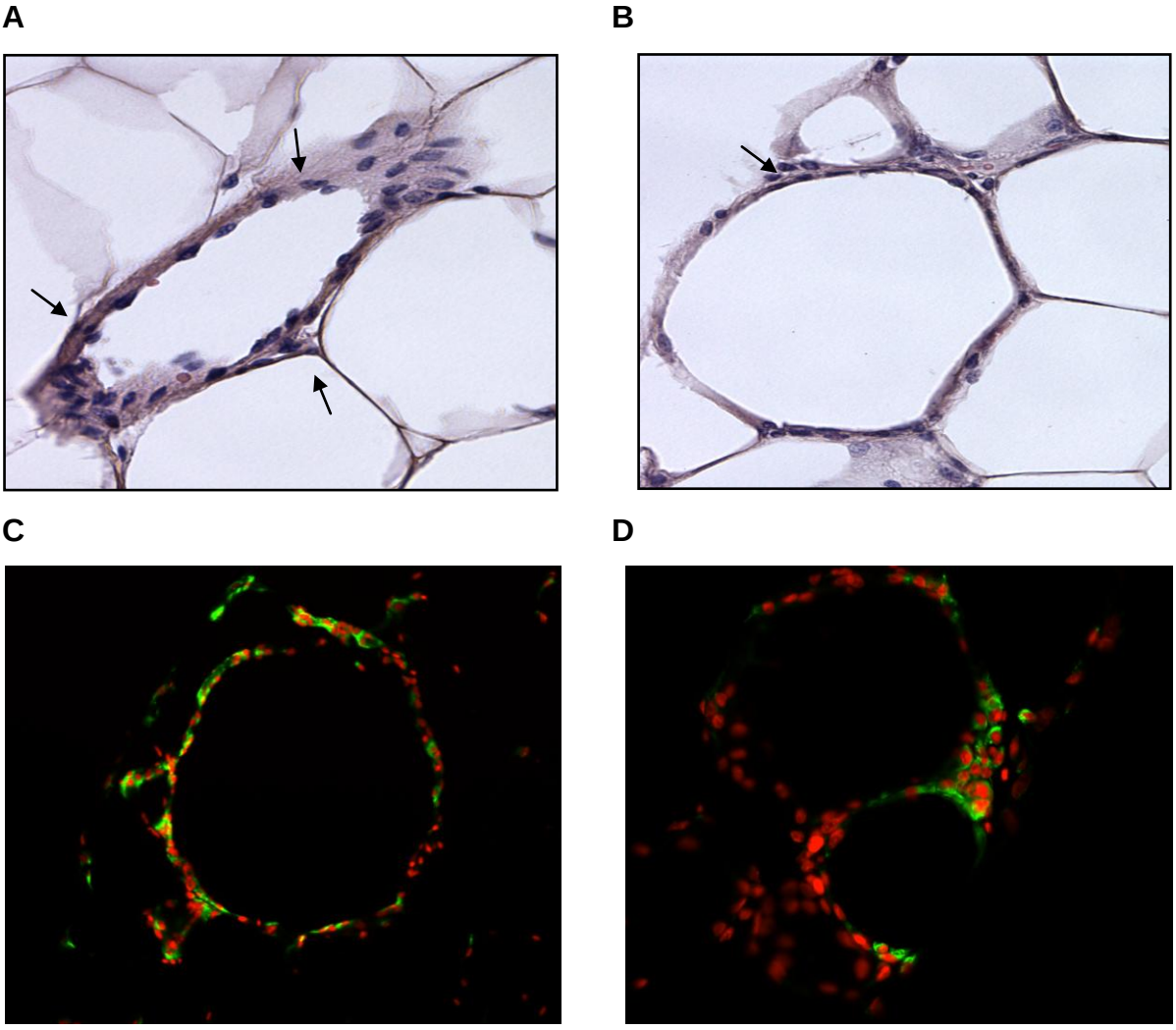

Figure 12: (A) and (B) H&E staining of epididymal adipose tissue from *db/db* mouse. (C) and (D) IF staining with anti-F4/80 (green) for macrophages and propidium iodide (red) for nuclei.

3.1.4 Elevated circulating plasma cytokines in obese mice

Adipokines were measured in plasma of lean and obese mice using a multiplex technology (MILLIPLEX™ MAP kit from Millipore). The kit is based on Luminex® technology which allows simultaneous quantification of multiple analytes in the same sample by using color-coded beads coated with a specific capture antibody. This allows the addition of multiple conjugated beads to each sample resulting in the ability to obtain multiple results from each sample. Leptin, MCP-1, IL-6, TNFα, tPAI-1 and resistin were measured.

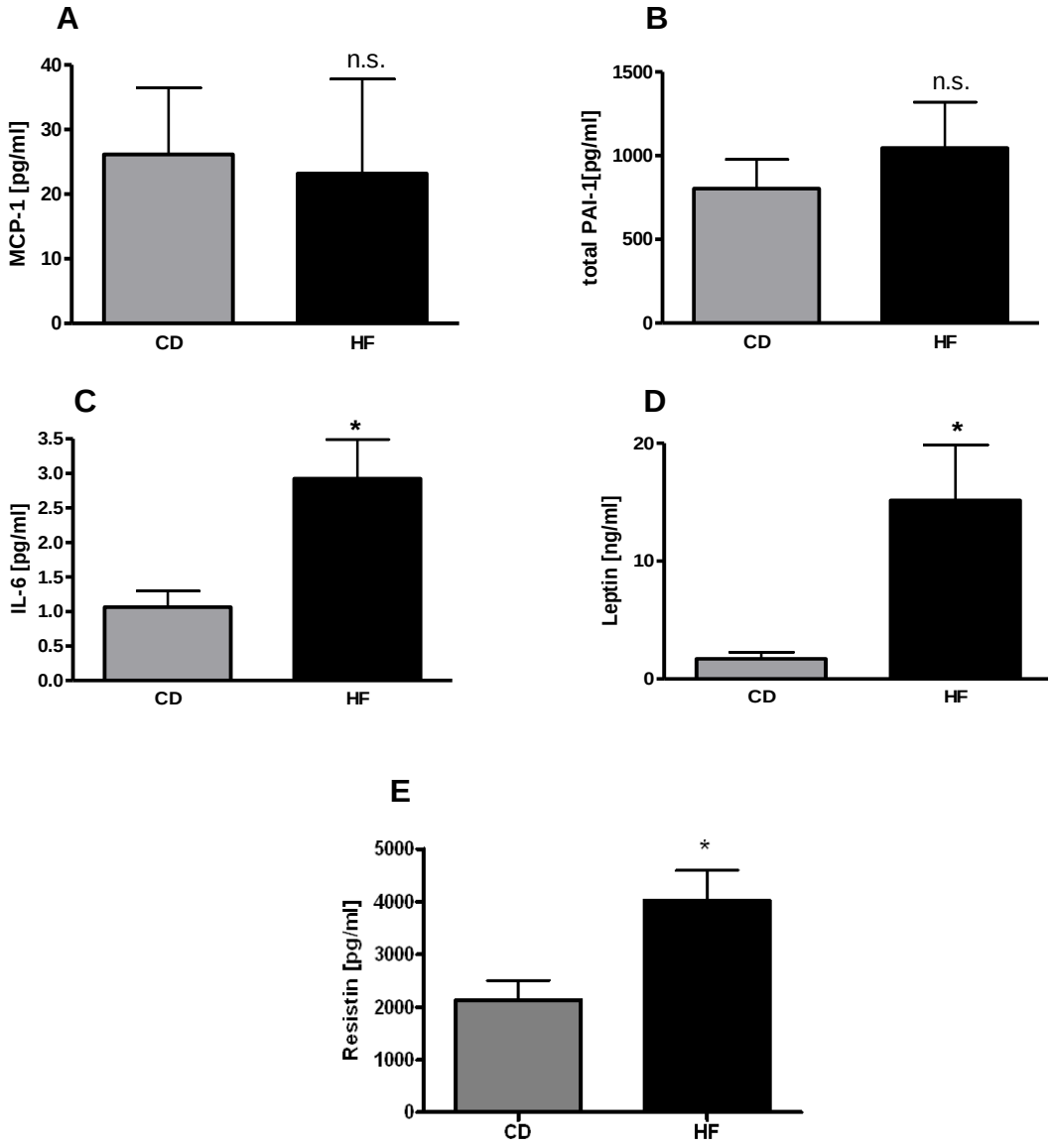

Figure 13: Plasma adipokine levels in obese and lean mice. Data are shown as mean ± SEM. Each group consisted of 6 mice. Statistical significance was determined by Student's t test, *p < 0.05., n.s. = non significant.

All the adipokines with the exception of MCP-1 (Figure 13A) showed a trend towards higher levels in the obese mice. IL-6 (Figure 13C), leptin (Figure 13D) and resistin (Figure 13E) were significantly increased in obese mice.

3.1.5 Reduced GLP-1 secretion in obese mice

Mice were put on a high fat diet with 48% of the total energy coming from plant based oils (S5745-E702, Ssniff GmbH, Germany). Mice on normal chow served as the control group. The study was conducted for a period of 12 weeks during which body weight was regularly monitored. Mice on the high fat diet showed significant increase in body weight in comparison to mice on rodent chow. After culling, small intestine was excised and stimulated for GLP-1 secretion. Since, GLP-1 secreting enteroendocrine cells (EEC) show their highest density of distribution in the ileal segment of the small intestine, therefore, the distal half of the small intestine was everted and sliced into approximately 0.5 cm long rings. Rings were then incubated in glucose [50 mM], glycyl-glycyl [20 mM] and buffer alone (control) for 45 minutes to allow for GLP-1 secretion.

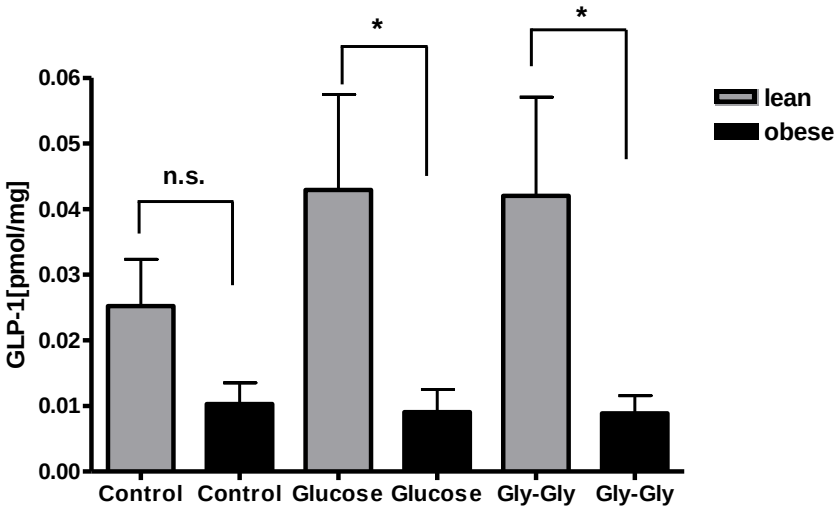

Figure 14: GLP-1 secretion in mouse intestinal rings in response to different nutrients. Data are shown as mean ± SEM. Each group consisted of 10 animals. Statistical significance was determined by two way ANOVA, *$p < 0.05$, n.s. = non significant.

It was observed that the basal secretion of GLP-1 in obese mice was 0.010 ± 0.003 pmol/mg while in the lean mice it was more than doubled with 0.025 ± 0.007 pmol/mg (Figure 14). Further, the increment in GLP-1 in the lean mice upon glucose stimulation (0.043 ± 0.015 pmol/mg) and glycyl-glycyl stimulation (0.042 ± 0.015 pmol/mg) was not

observed in the obese mice. In the obese group, GLP-1 secretion upon nutrient stimulation remained the same like with buffer alone.

3.1.6 Proglucagon gene expression in *db/db* mice

In order to investigate differences in the basal expression of GLP-1, the small intestine was excised from *db/db* mice which are a model of obese and diabetic mice and RNA was isolated from the distal half. cDNA was synthesized and qPCR performed for proglucagon (*gcg*), the gene that encodes GLP-1. There was an 89.6 ± 4.1% reduction in the expression of *gcg* in the *db/db* mice (0.00125 ± 0.00057) in comparison to control mice (0.00013 ± 0.00002).

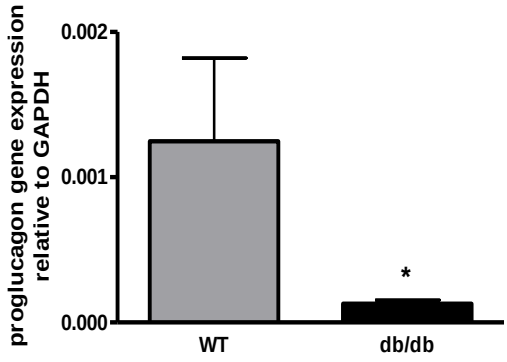

Figure 15: Proglucagon gene expression in *db/db* mice and control mice**.** Data are shown as mean ± SEM. Each group consisted of 5 animals. Statistical significance was determined by Student's t-test, *p < 0.05, n = 6.

3.2 Effect of preconditioned adipocyte media on GLP-1 secretion from NCI-H716 cells.

Isolated mature adipocytes form human subjects undergoing plastic surgery were incubated in culture medium (DMEM:F12) for 16 hours to allow fat cells to secrete adipokines into the medium. Pre-conditioned adipocyte media (PAM) were prepared from primary adipocytes of lean and obese subjects and assigned to 2 groups, a lean group with a BMI ≤ 25 kg/m^2 and an obese group with a BMI ≥ 25 kg/m^2. The human enteroendocrine cell line, NCI-H716 was exposed to these media or DMEM:F12 (control medium) for 2 hours followed by 1 hour stimulation with glucose which is a potent stimulant of GLP-1 secretion. The response of the NCI-H716 cells to glucose diminished following incubation with pre-conditioned media from both lean and obese subjects with a lowering effect of 32.2 ± 17.0% in media of lean and a statistically significant reduction of

56.7 ± 20.0% with media obtained from cells of obese individuals as compared to control culture medium. This finding demonstrated that adipocyte-derived factors adversely affect GLP-1 output from endocrine cells with a reduction of GLP-1 secretion in a donor BMI-dependent manner.

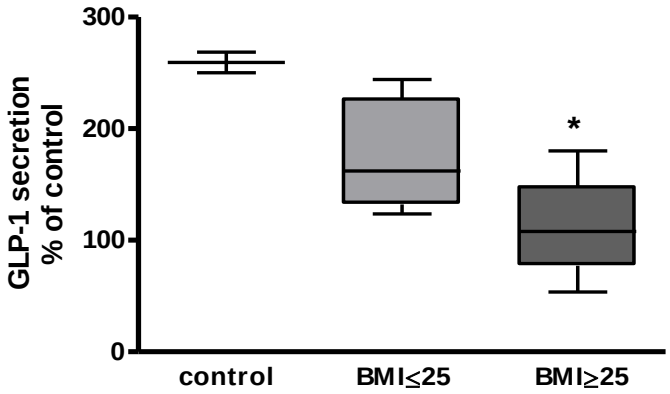

Figure 16: Glucose stimulation of NCI-H716 cells for GLP-1 secretion following two hours treatment with PAM**.** PAM prepared from adipocytes of obese and lean human subjects, or DMEM:F12 (adipocyte culture medium) was applied on NCI-H716 for 2 hours and then stimulated for 1 hour with 500 mM glucose for GLP-1 secretion. GLP-1 is expressed as a percent of control (basal secretion with buffer). Statistical significance was determined by one way ANOVA, followed by Bonferroni's post test, *$p < 0.05$. vs. control, n = 5-6 conditioned media per group.

3.3 Screening for potential adipokines with inhibitory roles on GLP-1 secretion

To identify which component/s of the pre-conditioned media could be responsible for the reduced response of the NCI-H716 cells to glucose, we screened few defined adipokines which have been shown to be predictive for the development of metabolic alterations. Leptin, MCP-1, IL-6, TNF-α, Angiotensin II and RANTES were individually applied on the NCI-H716 cells for defined time periods (2-24 hours) before stimulation with 10% glucose (1 hour). Supernatants were collected for GLP-1 determination by commercially available ELISA. The screening experiments revealed that RANTES (Figure 17D) and angiotensin II (Figure 17C) had the highest consistent and significant effects on the reduction of GLP-1 secretion in the NCI-H716 cells following stimulation with glucose. Leptin on the other hand had no effect on GLP-1 secretion (Figure 17A), while TNF-α (Figure 17B) showed a trend to reduce GLP-1 but was not significant.

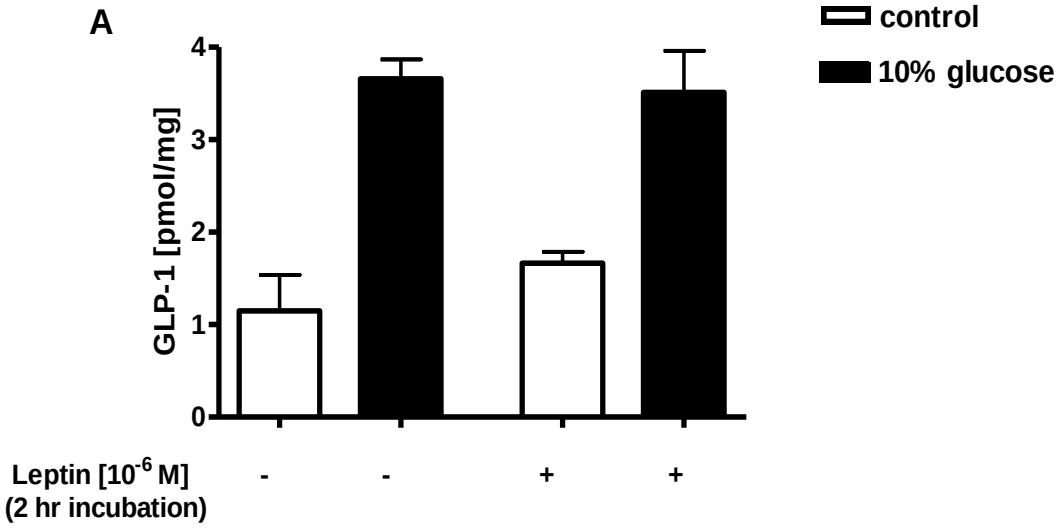

Figure 17A: Leptin [10^{-6}M] was incubated on the NCI-H716 cells for 2 hours in growth medium following which the cells were stimulated for 1 hour with 10% glucose made in PBS buffer, 1 mM $CaCl_2$. Basal secretion corresponds to GLP-1 secretion observed with buffer alone. Data are represented as mean ± SEM. Bars represent absolute values of GLP-1 in pmol/mg, n = 4.

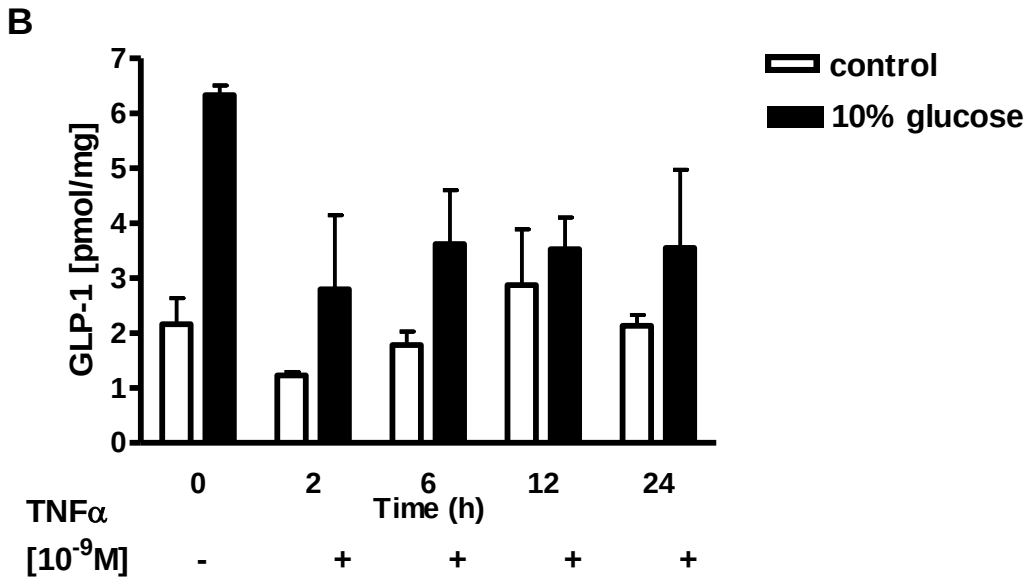

Figure 17B: TNF-α [10^{-9}M] was incubated on the NCI-H716 cells for 2, 6, 12 and 24 hours before stimulation with 10% glucose. Data are represented as mean ± SEM. Bars represent absolute values of GLP-1 in pmol/mg, n = 4.

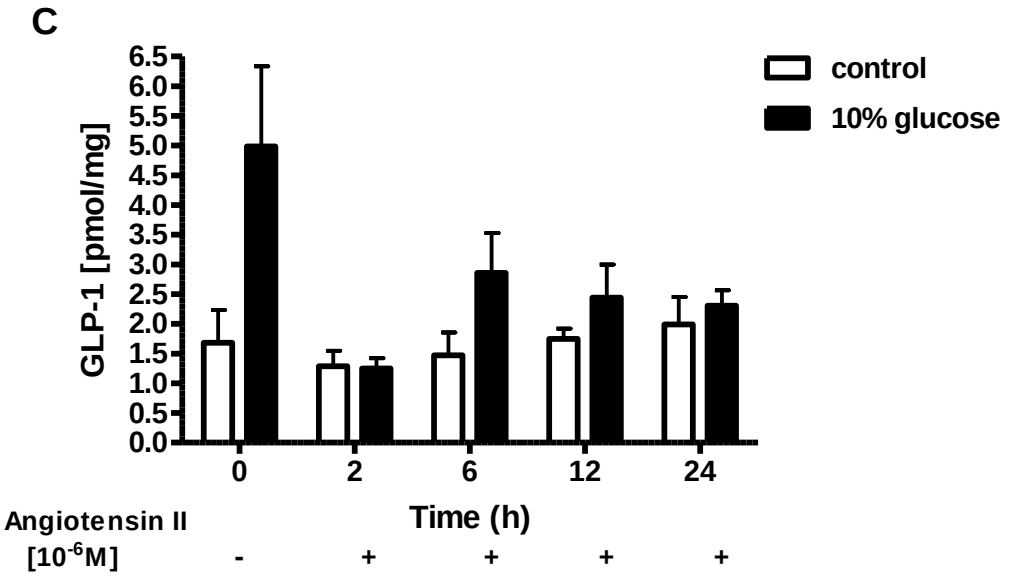

Figure 17C: Angiotensin II [10^{-6}M] was incubated on the NCI-H716 cells for 2, 6, 12 and 24 hours before stimulation with 10% glucose. Data are represented as mean ± SEM. Bars represent absolute values of GLP-1 in pmol/mg, n = 4.

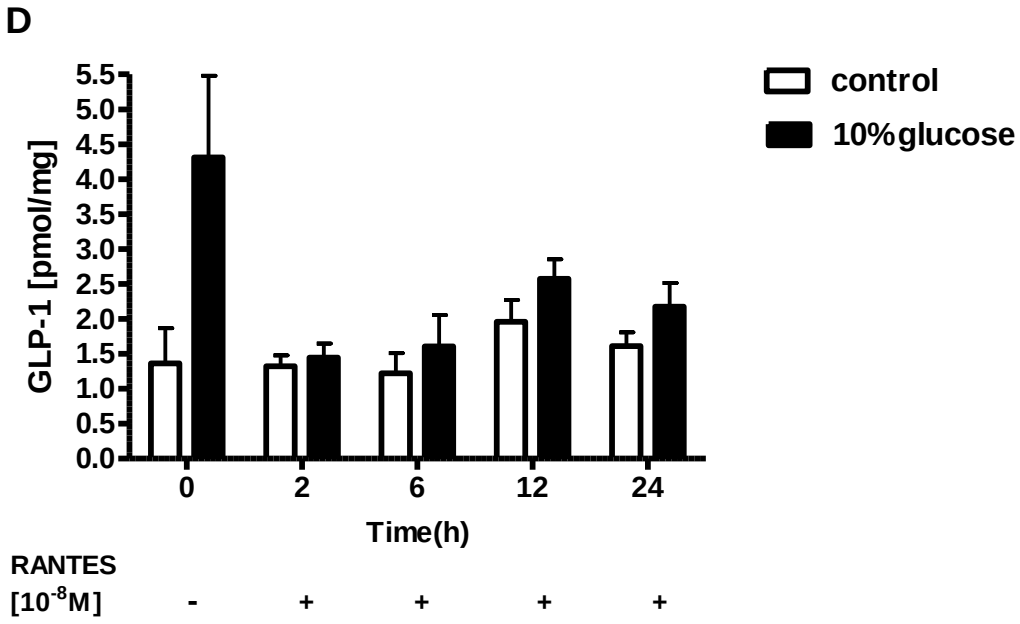

Figure 17D: RANTES [10^{-8}M] was incubated on the NCI-H716 cells for 2, 6, 12 and 24 hours before stimulation with 10% glucose. Data are represented as mean + SEM. Bars represent absolute values of GLP-1 in pmol/mg, n = 4.

3.4 Expression of nutrient transporters on enteroendocrine cells

The inability to isolate enteroendocrine cells (EEC) from mouse intestinal tissue due to its sparse population limited our studies to the use of the NCI-H716 cells in the investigation of nutrient transporters on the L-cells. We aimed at identifying the glucose transporter, SGLT1 and peptide transporter PEPT1 on EEC cells. We used techniques such as RT PCR, Western blot and IF in quest of the transporter.

SGLT1

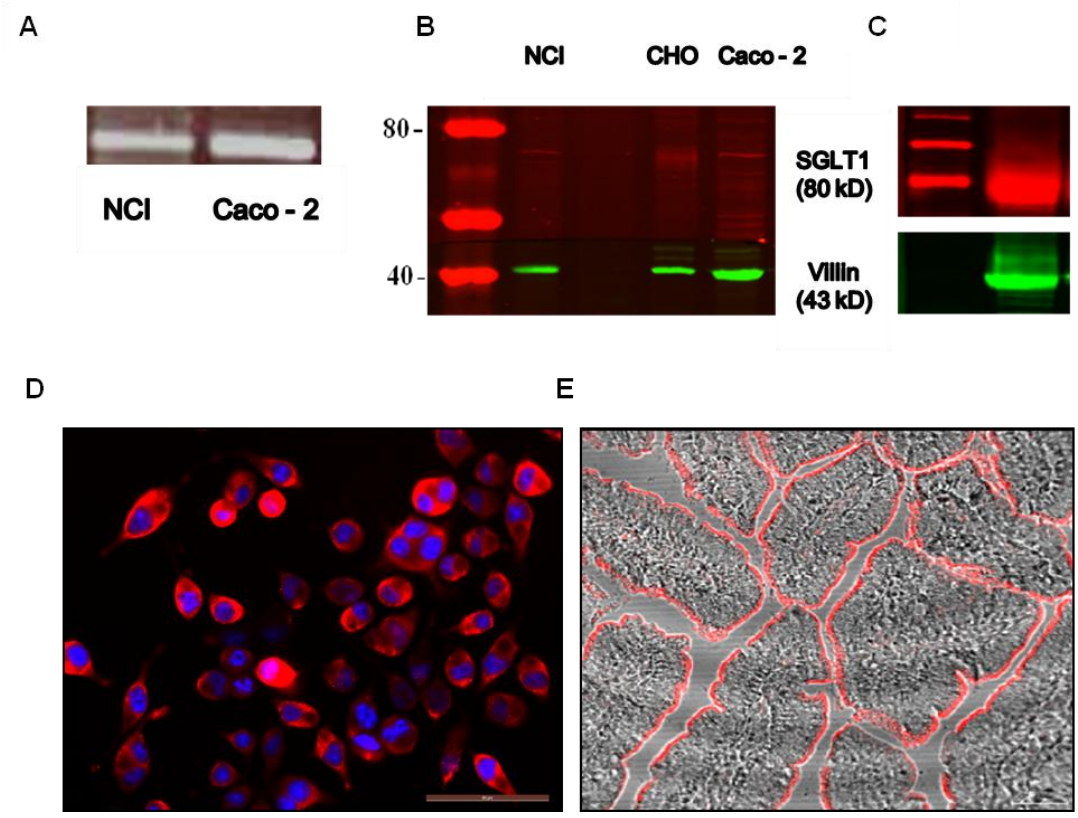

Figure 18: (A) SGLT1 gene expression in NCI-H716 and Caco-2 cells. Western blot was performed on (B) total protein fraction of NCI-H716, CHO cells over expressing SGLT1 and Caco-2 cells and (C) BBM fraction of mouse intestinal tissue with a custom made antibody raised in rabbit recognizing SGLT1 of human, mouse and rat origin (courtesy Prof Joana M. Planas, Barcelona, 1:1,000). (D) & (E) IF on NCI-H716 cell and mouse villi respectively, with anti-SGLT1 (Millipore, cat. #07-147, 1:1,000). Nuclei were stained with propidium iodide.

PEPT1

Further, we looked for the peptide transporter at message and protein level.

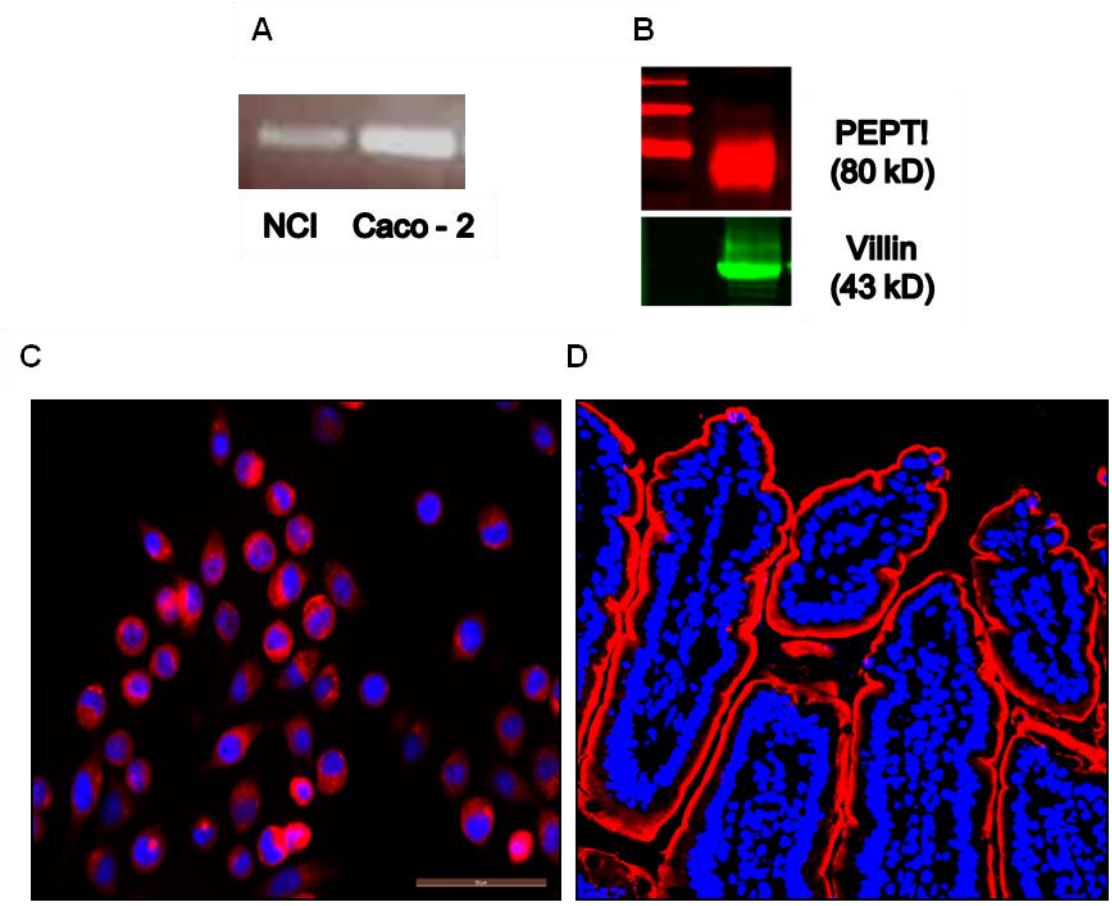

Figure 19: (A) Gene expression of PEPT1 on the NCI-H716 cells and Caco-2 cells. (B) Western blot was performed on BBM fraction of mouse intestinal tissue with a custom made antibody raised in rabbit recognizing PEPT1. IF on (C) NCI-H716 cells for PEPT1 (red) and propidium iodide (blue) and on (D) mouse villi.

From the RT-PCR and western blot analysis, it became clear that the NCI-H716 cells express both the transporters but have lower expression than the Caco-2 cells.

Intracellular calcium imaging in NCI-H716 cells in response to glucose and phlorizin treatment

It is known that secretion of GLP-1 from the EEC cells in response to nutrients succeeds the rise in intracellular calcium and cAMP. Intracellular calcium causes GLP-1 vesicles to fuse to the membrane with consequent exocytosis of the hormone (168). It is also postulated that, SGLT1 that transports glucose into the EEC is crucial for hormone

secretion. Transport of two sodium ions along with glucose causes membrane depolarization and this opens voltage gated calcium channels with subsequent influx of calcium and hormone secretion.

Hence, we tried to monitor changes in intracellular calcium in the NCI-H716 cells after stimulation with glucose. Further, to assess the specific role of SGLT1, we used phlorizin, a highly selective inhibitor of SGLT1 and then challenged the cells with glucose.NCI-H16 cells showed an increase in intracellular calcium which is reflected by the increase in the image ratio of the bound form of Fura-2 to the unbound form upon perfusion of 10 mM glucose solution containing 1.8 mM $CaCl_2$. Cells were perfused with 1 mM phlorizin followed by glucose together with phlorizin. There was a smaller increase in intracellular calcium with glucose when phlorizin was applied on the cells (Figures 20 and 21). Lastly, ionomycin [2 µM] was added to the cells to elicit maximum response.

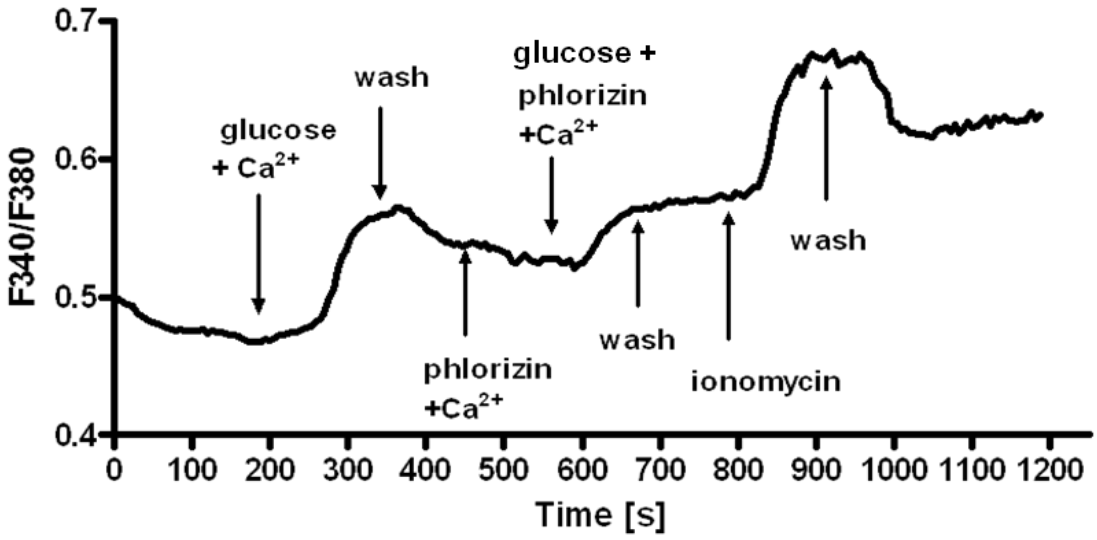

Figure 20: Calcium response in NCI-H716 cells in response to glucose and phlorizin treatment. The above trace is a representative of 6 independent experiments. All solutions were perfused at a rate of 30 ml/h. Glucose 10 mM application (see arrows) induced an increase in $[Ca^{2+}]_i$ which was seen as in increase in the image ratio (first peak) . Phlorizin application caused no change in the ratio. Glucose when applied together with phlorizin brought about a much lower increase in $[Ca^{2+}]_i$ (second small peak). Ionomycin [2 µM] was used as a positive control and cells responded by showing increase in $[Ca^{2+}]_i$.

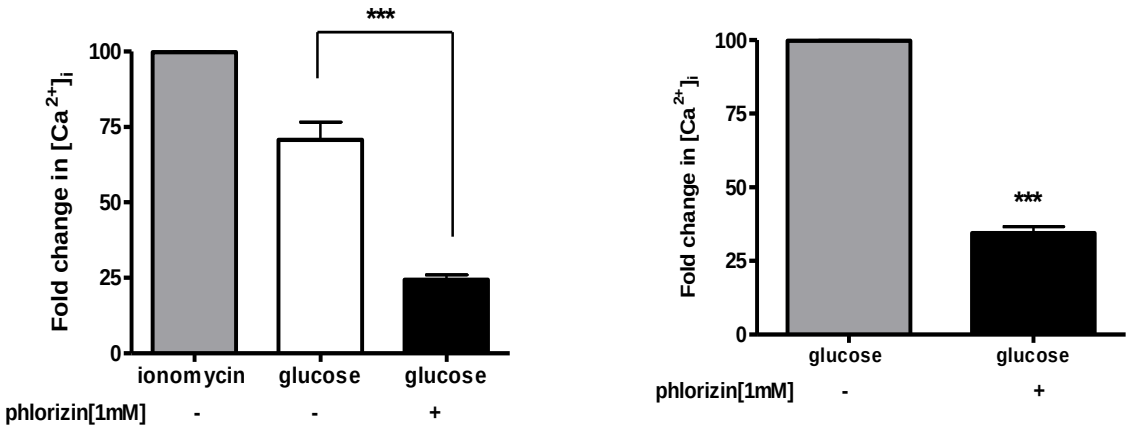

Figure 21: Left panel, Fold increase in $[Ca^{2+}]_{i,}$ taking 2 µM ionomycin induced calcium response as 100%. 10 mM glucose caused a 70.0 ± 5.8% increase in calcium while 10 mM glucose together with 1 mM phlorizin caused only 24.4 ± 1.5% increase. Right panel, Fold increase in $[Ca^{2+}]_{i,}$ taking 10 mM glucose stimulated response as 100%. Phlorizin lowered glucose stimulation by 65.3 ± 2.2%. Data are shown as mean ± SEM from 6 independent experiments. Statistical significance determined by Student's t-test, ***p < 0.001.

In the next chapters, I will focus on RANTES and Angiotensin II and describe their role and effects on GLP-1 secretion and nutrient transporters in different models.

3.5 Role of RANTES

As RANTES, in combination with other chemokines might be predictive for the development of type 2 diabetes we focused on its effects on NCI-cells, *ex vivo* and *in vivo* models in the following experiments.

3.5.1 Direct effects of RANTES on GLP-1 secretion in NCI-H716 cells

To assess dose-dependent effects of RANTES on GLP-1 secretion in the absence of glucose, NCI-H716 cells were incubated with increasing concentrations of rh RANTES in PBS medium containing 1 mM $CaCl_2$ for 1 hour. PBS alone served as a negative control and PMA [10^{-6} M] an activator of protein kinase C and known to cause GLP-1 secretion, served as positive control (169, 170). After the incubation period, supernatants were collected, centrifuged and stored at -80^{o}C. Cells were homogenized in 0.1 M NaOH for protein determination by Bradford assay. While PMA stimulated GLP-1 secretion to 352 ± 31.2% of control values, RANTES in concentrations of 10^{-12}, 10^{-8}, 10^{-4} M caused a small but significant increase in GLP-1 secretion (129.7 ± 15.2%, 173.6 ± 20.2% and 167.2 ± 14.6%) as compared to buffer control (Figure 22).

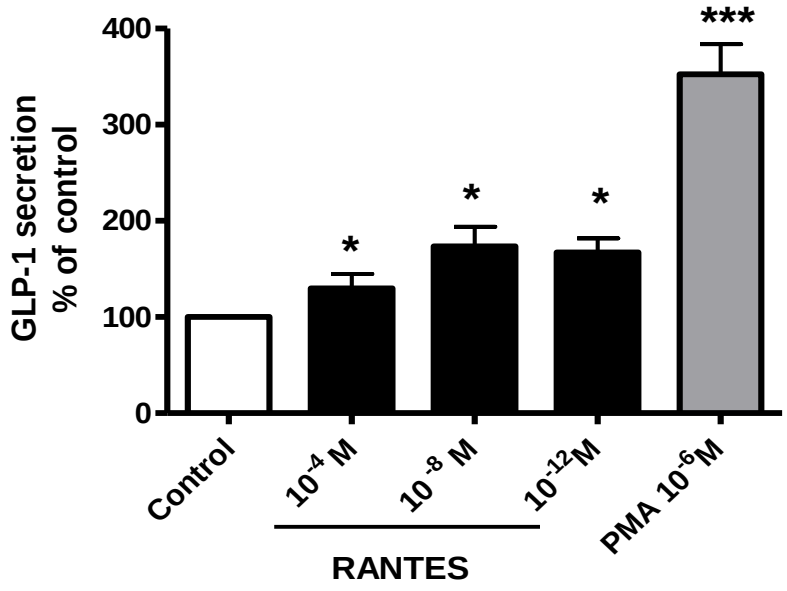

Figure 22: Effect of increasing concentrations of RANTES on GLP-1 secretion. Data are given as mean ± SEM. Statistical significance was calculated by one way ANOVA followed by Dunnett's post test, *$p < 0.05$, ***$p < 0.001$, $n = 4$.

3.5.2 Effect of RANTES on glucose stimulated GLP-1 secretion from NCI-H716 cells

To test the effect of RANTES on glucose stimulated GLP-1 secretion, a near physiological concentration of 10^{-8} M RANTES was used and cells were exposed for 2, 6, 12, and 24 hours to the adipokine at 37^{o}C. After that, the cells were stimulated with glucose for 1 hour and cells not exposed to RANTES served as control. RANTES significantly reduced GLP-1 secretion following glucose stimulation by 63.4 ± 12.4%, 57.5 ± 7.5%, 52.8 ± 27.5% and 54.3 ± 21.0% after 2, 6, 12 and 24 hour treatment, respectively when compared to control (Figure 23).

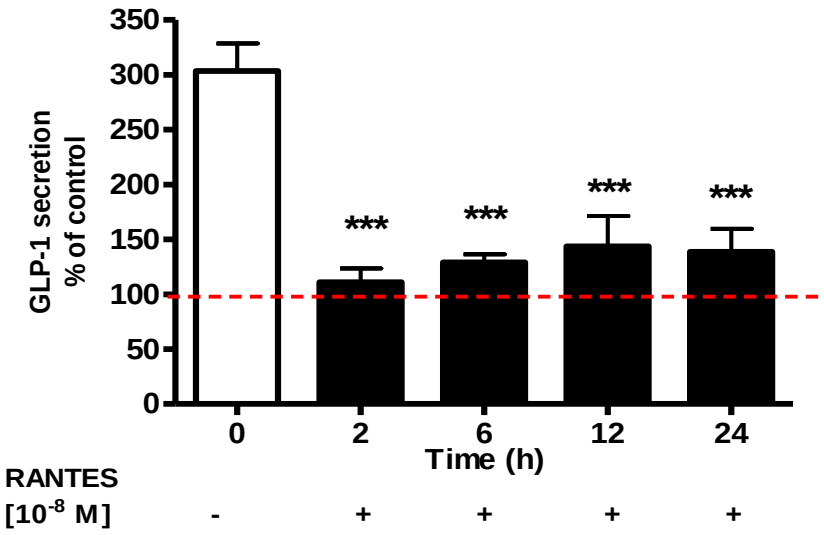

Figure 23: Effect of time dependent inhibition of RANTES on glucose stimulated GLP-1 response in NCI-H716 cells**.** Data are expressed as percentage of control (untreated cells challenged with glucose) Data are given as mean ± SEM. Statistical significance was calculated by one way ANOVA followed by Bonferroni's post test, ***$p < 0.001$, $n = 4$.

3.5.3 Expression of receptors for RANTES on enteroendocrine cells

After consistently demonstrating functional effects of RANTES in cell culture, the next question that arose was to identify how the inhibitory signals from RANTES were being transduced into the enteroendocrine cell. RANTES is known to bind to three types of chemokine receptors, CCR1, CCR3 and CCR5 (47).

mRNA expression of receptors

All the three receptors are expressed at message level (real time PCR) on the NCI-H716 cells (Figure 24). Additionally we looked for the more relevant CCR1 and CCR5 in mouse proximal and distal small intestine. Both CCR1 and CCR5 were found to be expressed in same amounts in the mouse intestine (Figure 24).

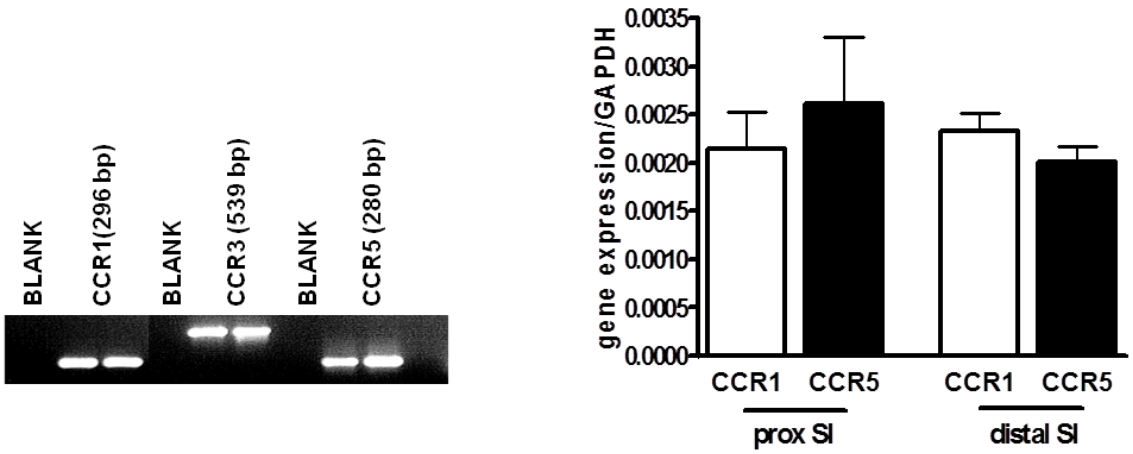

Figure 24: Left panel, expression of CCR1, CCR3 and CCR5 in the NCI-H716 cells. Right panel, expression of CCR1 and CCR5 in mouse proximal and distal small intestine. RT-PCR was used to amplify CCR1, CCR3 and CCR5 mRNA transcript.

Protein expression of the receptors

Western blot

We performed a western blot on whole cellular protein isolated from the NCI-H716 cells. Additionally, we also isolated cellular protein from the Caco-2 cells, an intestinal epithelial cell line. 25 µg of protein was loaded and run on a 10% gel and probed with anti-CCR1 (1:200), anti-CCR5 (1:200) and β-tubulin (1:1,000). Appropriate infra-red dye coupled secondary antibodies, IRDYE 800 and IRDYE 680 (1:20,000) were used and the membrane was scanned with an Odyssey scanner (LICOR). We were able to only detect CCR1 by western blot on both the cell lines (Figure 25).

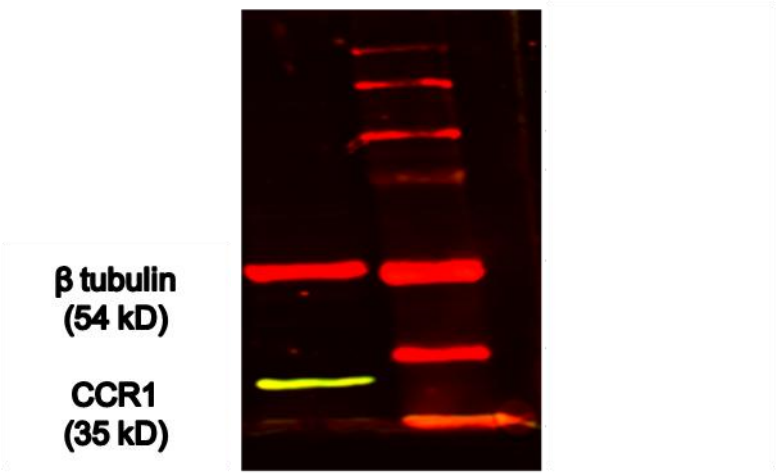

Figure 25: Western blot was performed on total protein fraction of NCI-H716 cells with anti-CCR1 antibody.

Immunofluorescence

NCI-H716 cells and Caco-2 cells were fixed with 4% formalin and then incubated with rabbit anti-CCR1 (1:50), mouse anti-CCR5 (1:50) overnight at 4^{o}C. The next day cells were washed and incubated with appropriate secondary antibodies, donkey anti-rabbit FITC (1:150) donkey anti-mouse cy5 (1:150) and DAPI (1:500) for nuclear staining for 1 hour at room temperature. Omission of secondary antibodies served as negative control. Cells were washed with PBS, mounted and examined with a confocal fluorescent microscope. CCR1 was found to be expressed along the membrane of the cells with a spotty appearance (inside the cytosol which could probably be vesicular CCR1 (Figure 26A, B and C). Negative control stained positive for DAPI alone.

In mouse tissue, CCR1 was found to be present on both epithelial and enteroendocrine cells types. Enteroendocrine cells were distinguished from epithelial cells by co- staining for GLP-1 with a goat anti-GLP-1 antibody (1:50). Interestingly, CCR1 was found to be present on both the apical and basolateral membrane of the cells (Figure 26Dand E).

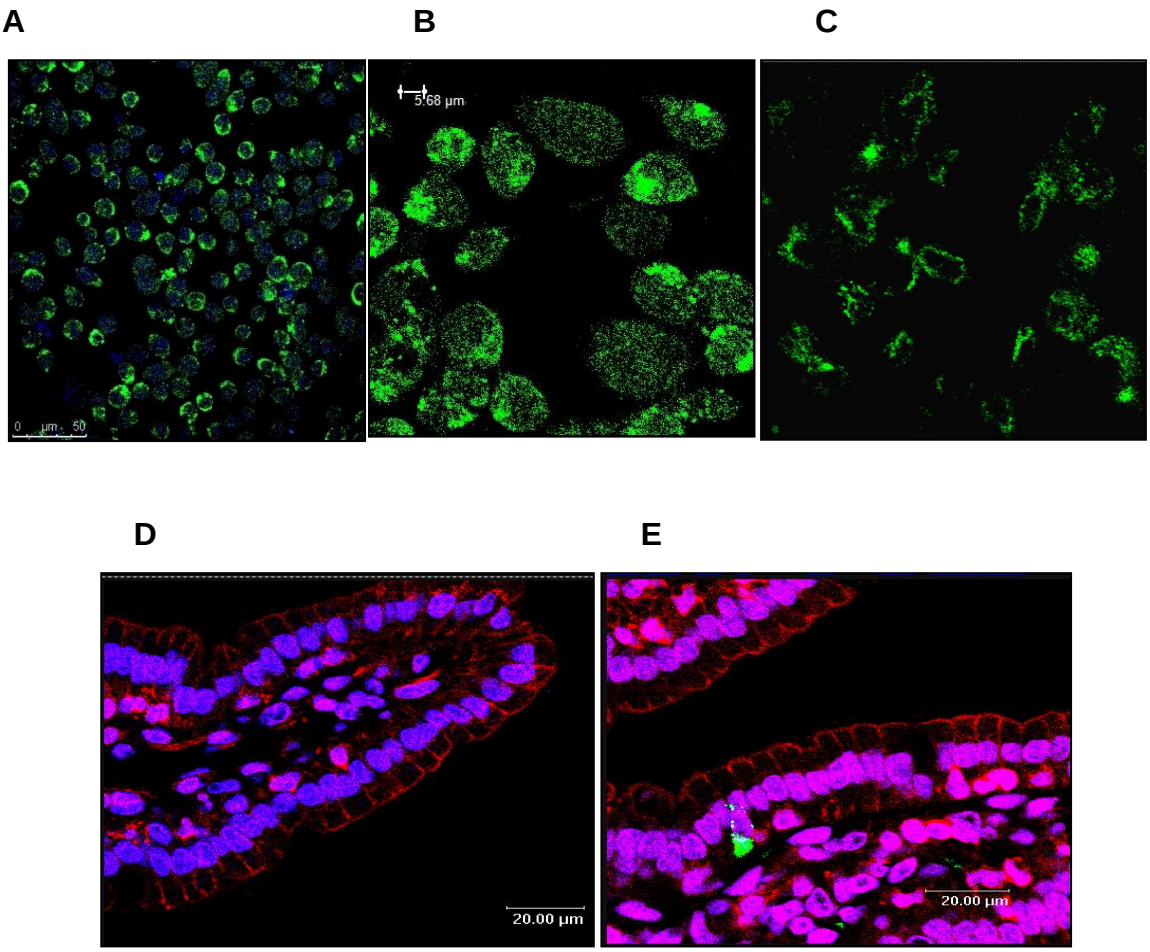

Figure 26: Immunofluorescence staining of formalin fixed (A and B) NCI-H716 and (C) Caco-2cells for CCR1 (green) and DAPI (blue). (D and E) Double–immunofluorescent staining of mouse paraffin embedded 7 µm sections from ileum with anti-GLP-1(green) and anti-CCR1 (red) as visualized by fluorescence microscopy.

3.5.4 *CCR1* gene expression in the intestine of obese animals

We analyzed the mRNA expression of CCR1 and CCR5 in the proximal and distal small intestine of lean and diet-induced obese C57BL/6 mice. CCR1 expression was significantly increased with a 2 and 2.8-fold increase in proximal and distal small intestine, respectively (Figure 27). Additionally, CCR5 showed a trend towards higher expression in the obese group (Figure 27).

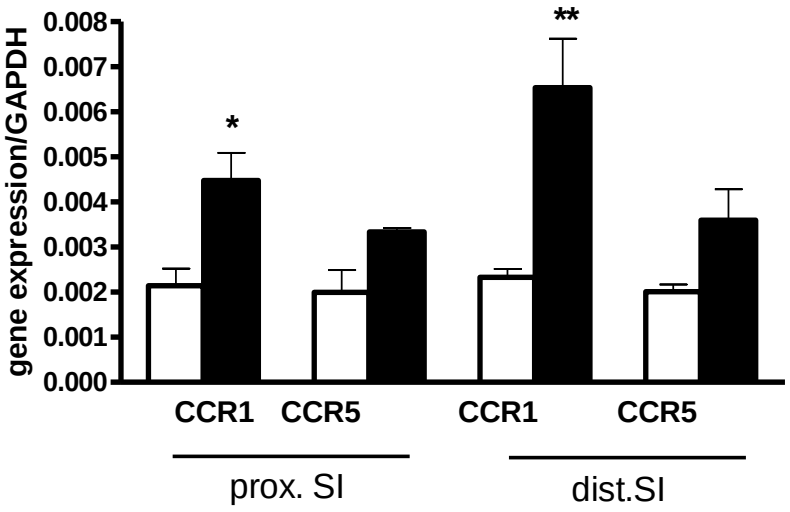

Figure 27: Gene expression of *CCR1* and *CCR5* in lean (white bars) and obese (black bars) mice in proximal and distal small intestine in mice. Statistical significance determined by two way ANOVA followed by Bonferroni's post test. Columns represent mean ± SEM of 6 mice, *$p < 0.05$, ** $p < 0.01$ vs. lean.

3.5.5 Effect of RANTES antibody and Met-RANTES on GLP-1 secretion

To further demonstrate RANTES-induced inhibition of glucose stimulated GLP-1 secretion, we used Met-RANTES which is a CCR1 & CCR5 receptor antagonist and a specific antibody raised against RANTES. NCI-H716 cells were pre-incubated with RANTES ± anti-RANTES or RANTES ± Met-RANTES for 2 hours followed by 1 hour stimulation with glucose. Incubation with anti-RANTES caused a significant recovery of 60 ± 23.9% in GLP-1 secretion (Figure 28A) while antagonism with Met-RANTES resulted in complete recovery of GLP-1 secretion compared to untreated cells (Figure 28B). These data demonstrate that the disturbances in GLP-1 secretion are specific for RANTES and are mediated by the RANTES receptors.

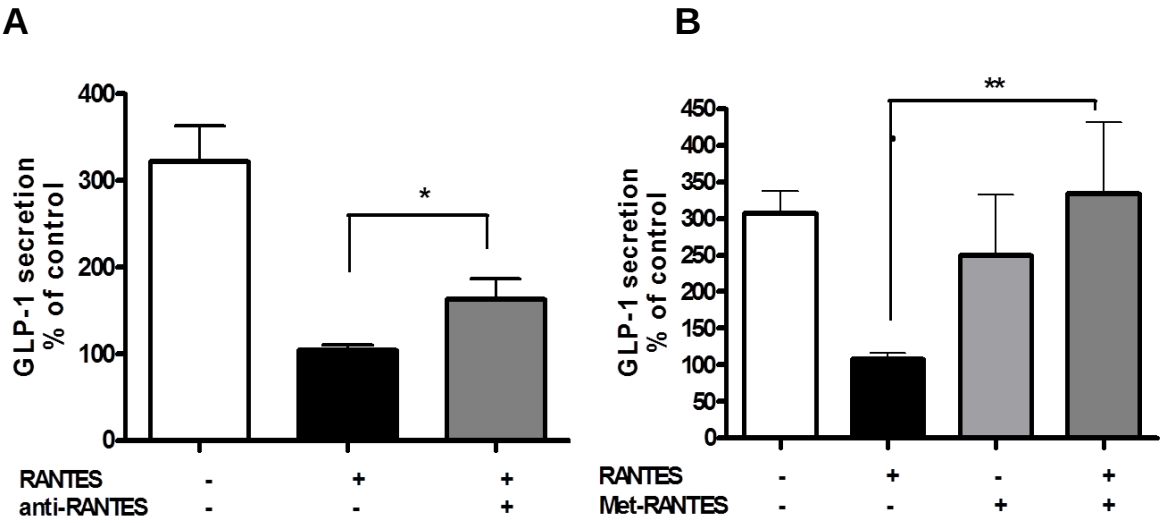

Figure 28: (A) Effect of anti-RANTES [7 µg/ml] on glucose stimulated GLP-1 release by NCI-H716 cells. Cells were treated with 10^{-8} M RANTES and with or without anti-RANTES for 2 hours before stimulating with glucose. (B) Effect of Met-RANTES [$2*10^{-8}$ M] on glucose stimulated GLP-1 release by NCI-H716 cells. Cells were treated with Met-RANTES alone and together with RANTES [10^{-8} M] for 2 hours before stimulating with 500 mM glucose. Data are given as mean ± SEM. Statistical significance was calculated by one way ANOVA followed by Bonferroni's post test, *$p < 0.05$, **$p < 0.01$, vs. control, $n \geq 4$.

3.5.6 siRNA silencing of *CCR1* and its effect on GLP-1 secretion

Subconfluent NCI-H716 cells were transfected with commercially obtained siRNAs targeting the CCR1 receptor. Three different siRNA (a, b, c) and a mixture of the three (abc) were used on the cells along with a mock siRNA (negative control) and monitored by probing for the CCR1 protein by western blot after 24, 48 and 72 hours. Silencing of CCR5 since was not performed as we were unable to detect the protein by both western blot and immunofluorescence. For CCR1, after 24 hours of treatment, an 80.2 ± 6.6% reduction of CCR1 protein levels was obtained with 'a' siRNA (Figure 29). At 48 and 72 hours, protein levels already slightly recovered to levels of untransfected or mock transfected samples. Therefore CCR1 siRNA transfected cell were used after 24 hours to perform GLP-1 secretion experiments. Briefly, untransfected, mock and CCR1 siRNA transfected cells were incubated with 10^{-8} M RANTES for 2 hours followed by glucose stimulation for 1 hour. Cells were homogenized and protein determined by Bradford. Cells not treated with RANTES responded to glucose stimulation with an increase in GLP-1 output of 303 ± 25% over basal levels (buffer alone). In CCR1 siRNA-treated cells, a significant improvement in GLP-1 secretion upon glucose stimulation was observed

accounting to 48.0 ± 12.2% more than in RANTES treated but untransfected cells. A full recovery was not seen in silenced cells which may be explained by remaining functional CCR1 receptors still present.

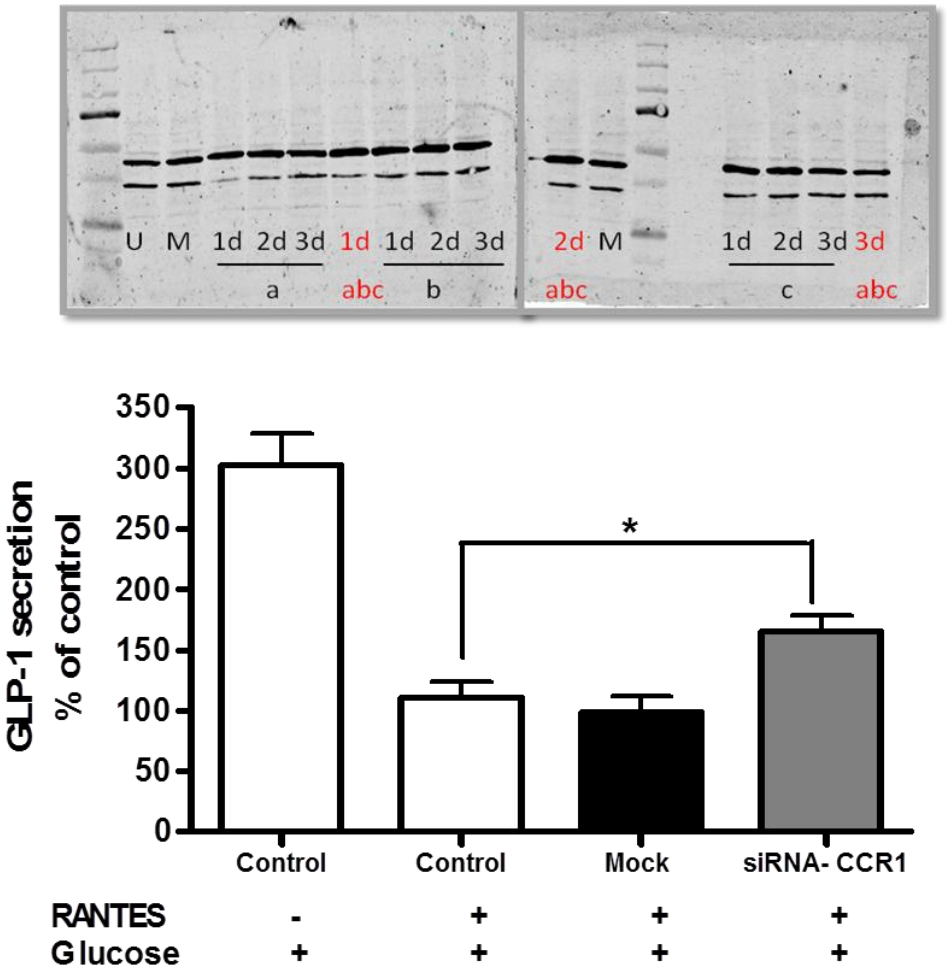

Figure 29: Top panel, western blot analysis showing siRNA mediated diminution of CCR1 protein 24 hours after transfection and recovery after 48 and 72 hours in the NCI-H716 cells. Untransfected (U) and mock transfected (M) cells showed normal CCR1 levels. Bottom panel, GLP-1 secretion in the transfected cells following RANTES treatment and glucose stimulation. Data are given as mean ± SEM. Statistical significance was calculated by one way ANOVA followed by Bonferroni's post test, *$p < 0.05$, vs. control, $n \geq 4$.

3.5.7 RANTES and cAMP

Adenosine 3', 5' cyclic monophosphate (cAMP) is a ubiquitous cellular second messenger that is a critical component of signal transduction pathways linking membrane receptors

and their ligands to the activation of intracellular pathways affecting enzymatic activity and gene expression**.** An elevation of cAMP levels has been repeatedly demonstrated to increase GLP-1 secretion in several models of intestinal EEC (171-174). There are also reports that cAMP via CREB increases *proglucagon*-gene expression in EEC cells (175).

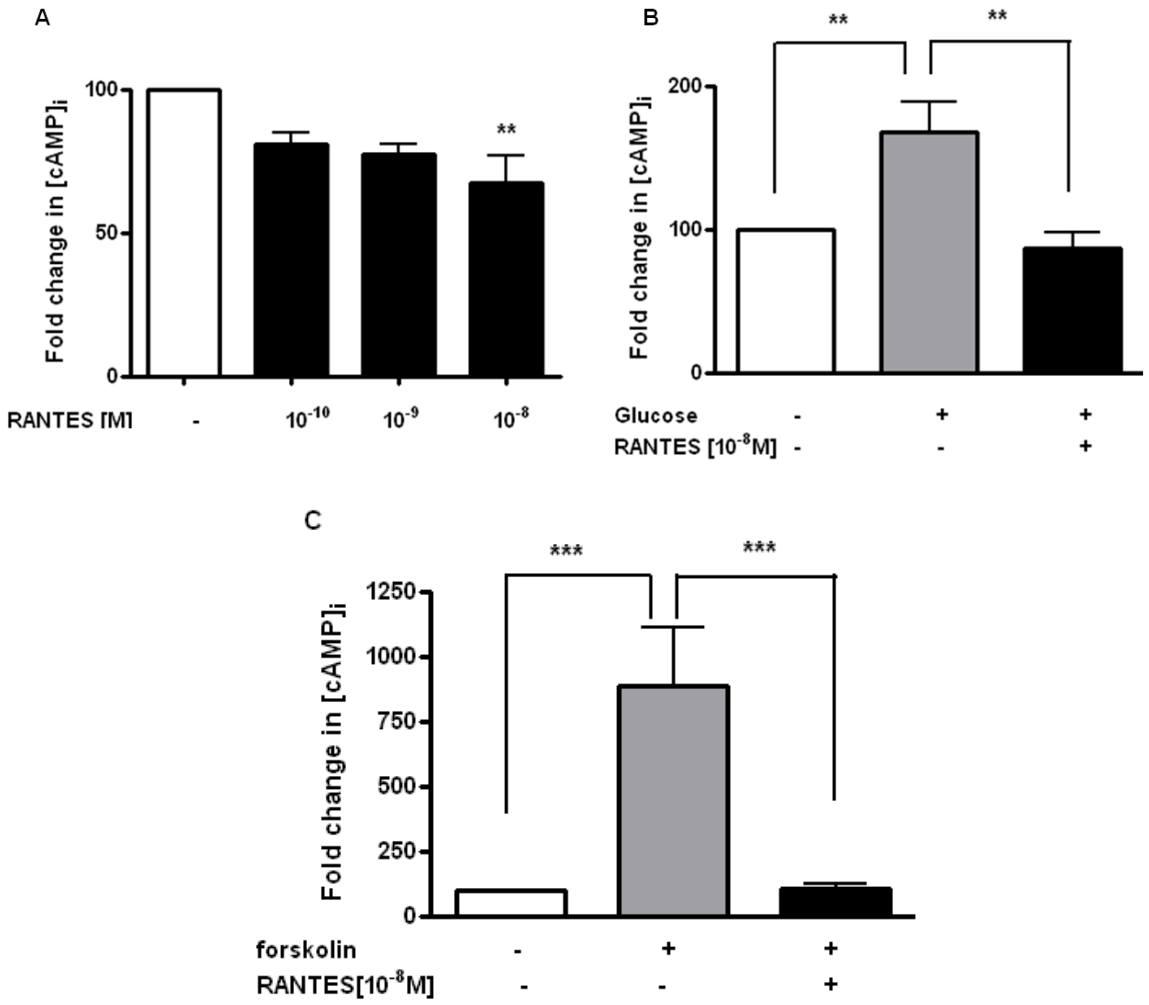

Figure 30: (A) RANTES caused a dose dependent reduction in the accumulation of basal intracellular cAMP after 5 minutes incubation in *in vitro* cultured NCI-H716 cells. (B) RANTES [10^{-8} M] significantly reduced the glucose [500 mM] induced increase in cAMP after 20 minutes incubation. (C) Treatment with forskolin [10 µM] for 1 hour significantly increased $[cAMP]_i$ in NCI-H716 cells whereas RANTES [10^{-8} M] blunted this stimulated increase completely. Data are expressed as mean ± SEM and are expressed as fold change with only buffer treatment taken as 100%. Statistical significance determined by one way ANOVA followed by Bonferroni's post test, **$p < 0.01$, *** $p < 0.001$, $n = 3$.

To assess the involvement of cAMP on RANTES mediated suppression of GLP-1 secretion, NCI-H716 cells were incubated with or without different doses of RANTES

[10^{-8}, 10^{-9} and 10^{-11} M] for 5 minutes. In another set of experiments, cells were first stimulated with 10 µM Forskolin (fsk) for 1 hour and then treated with 10^{-8} M RANTES for 5 minutes. Cells were also treated with 500 mM glucose with and without 10^{-8} M RANTES for 20 minutes. RANTES treatment showed a dose dependent reduction in intracellular cAMP levels accounting to 33 ± 9% at 10^{-8} M RANTES (Figure 30A). Furthermore, 10^{-8}M RANTES significantly reduced the glucose and forskolin induced increase in intracellular cAMP by 48.5 ± 10% and 88.1 ± 20% respectively (Figure 30B and C).

3.5.8 RANTES and PKA

Protein Kinase A (PKA) is the primary mediator of cAMP action and a key regulatory enzyme responsible for many cellular processes by catalyzing phosphorylation in response to hormonal stimuli. As we observed that RANTES lowers cAMP in the NCI-H716 cells at basal conditions and after glucose and forskolin stimulation, we next addressed its effects on PKA activity. PKA was described to mediate the stimulatory effect of cAMP on GLP-1 secretion (173). Everted mouse intestinal tissues were incubated with glucose [50 mM] in the absence or the presence of $7.5*10^{-8}$ M RANTES for 10 minutes. At the end of the incubation period, the mucosa was scraped, homogenized and the cytosolic fraction was obtained after centrifugation. PKA activity was measured in the supernatant with an ELISA. RANTES incubation along with glucose significantly reduced relative PKA activity by 40.4 ± 4.7% after 10 minutes of incubation (Figure 31).

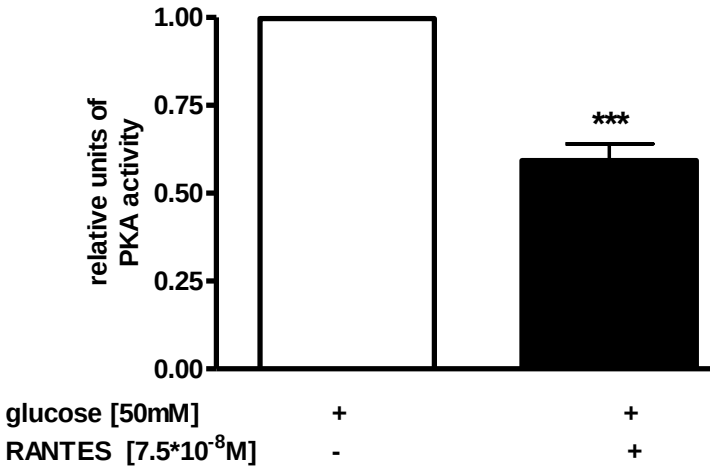

Figure 31: Relative units of protein kinase activity after incubation of glucose [50 mM] with and without RANTES [10^{-8} M] for 10 minutes in mouse everted intestinal rings. Data are expressed as mean ± SEM and statistical significance determined by Student's t-test, *** $p < 0.001$ vs. buffer.

3.5.9 RANTES increases $[Ca^{2+}]_i$ in NCI-H716 cells

In our quest to understand how RANTES lowers GLP-1 secretion, we assessed the effects of RANTES on changes in $[Ca^{2+}]_i$ in the NCI-H716 cells alone and cells exposed to glucose. Levels of $[Ca^{2+}]_i$ were quantified by fluorescence imaging, using the calcium indicator dye, Fura 2-AM employing a Leica Life cell imaging system. Application of 10^{-8} M RANTES in buffer containing 1 mM $CaCl_2$ for 2 minutes produced an increase in $[Ca^{2+}]_{i.}$ which accounted to 63.3 ± 11.3% of the maximal ionomycin [2 µM] induced response that was set to 100% (Figure 32A). To determine if RANTES stimulates Ca^{2+} influx through plasma membrane calcium channels, we first performed experiments using RANTES in calcium-free media (in the presence of 100 µM EGTA). Another set of experiments employed 10 µM Nifedipine (dihydropyridine-sensitive calcium channel blocker) with cells exposed for 15 minutes to the channel blocker prior to adding RANTES. Removal of extracellular Ca^{2+} completed abolished the RANTES response (Figure 32B) and similar effects were obtained for Nifedipine treatment (Figure 32C). This strongly suggested that RANTES can affect L-type channels that mediate a Ca^{2+} influx across the plasma membrane leading to an increase in $[Ca^{2+}]_i$.

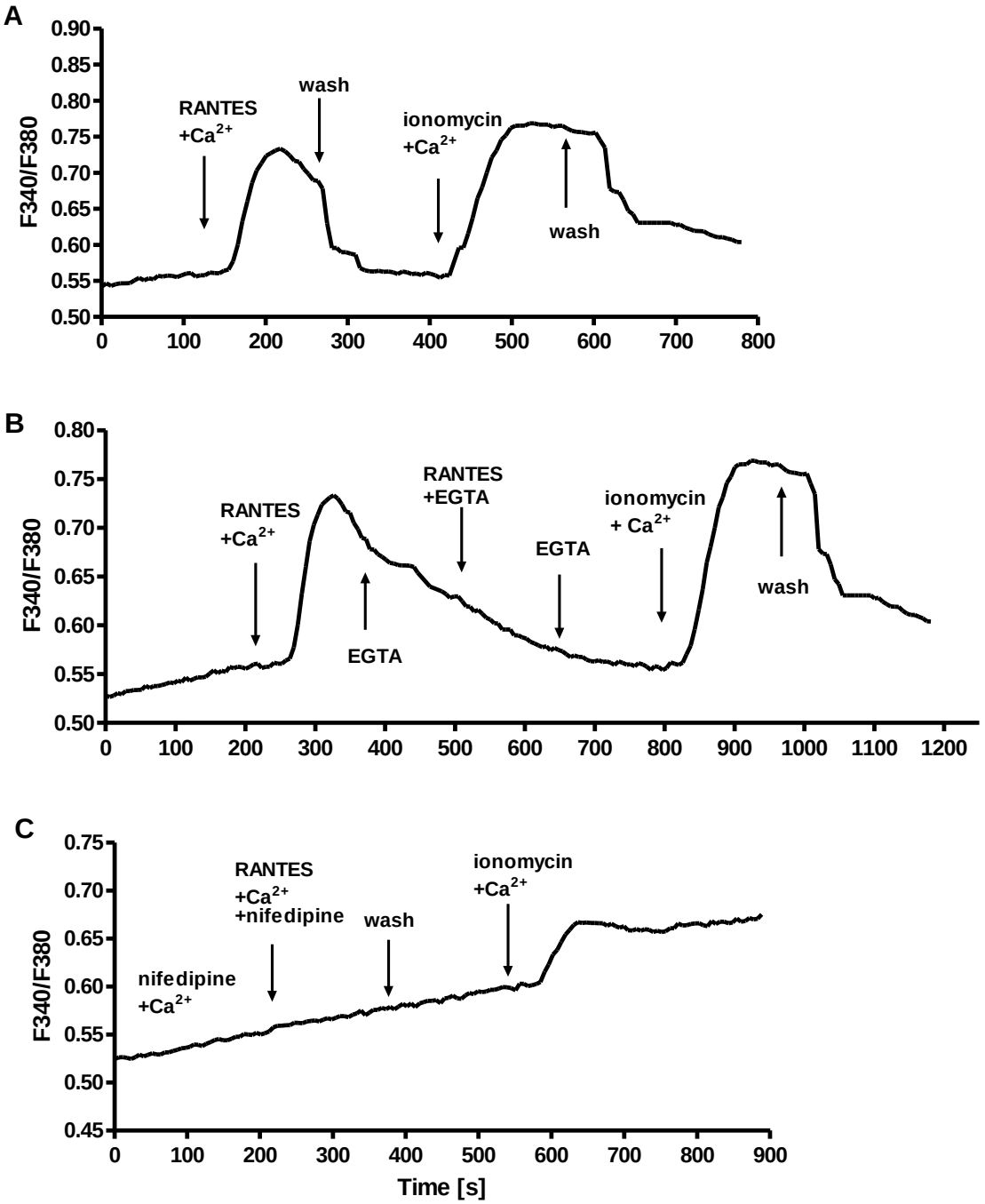

Figure 32: (A) RANTES [10^{-8} M] in a buffer containing 1 mM $CaCl_2$ increases $[Ca^{2+}]_i$ in NCI-H716 cells. Changes in intracellular calcium were measured using FURA-2 based life cell imaging. Addition of effectors to the cells is indicated by arrows. (B) After an initial control response to RANTES with Ca^{2+}, EGTA (100 µM) was applied for 2 minute prior to and during a second application of RANTES without calcium. (C) RANTES applied to the cells after a 15 minute perfusion with 10 µM Nifedipine failed to evoke calcium changes. Traces shown are a representative of 4-6 individual experiments.

3.5.10 RANTES lowers the glucose mediated increase in $[Ca^{2+}]_i$ and Met-RANTES alleviates this effect

When NCI-H716 cells were exposed to glucose, $[Ca^{2+}]_i$ levels increased as shown in Figure 33A and B for an individual recording. This glucose-mediated increase in $[Ca^{2+}]_i$ for various measurements accounted to around 71.8 ± 10.5% of the maximal ionomycin [2 µM] induced response that was set to 100% (Figure 33C & D). When cells after a wash-out of glucose were perfused with 10^{-8} M RANTES for two minutes, we again observed an increase in $[Ca^{2+}]_i$ but a second exposure of cells to glucose following this RANTES pre treatment, caused now a much smaller $[Ca^{2+}]_i$ response (Figure 33A). The average fold-change in $[Ca^{2+}]_i$ induced by RANTES and RANTES plus glucose as compared to ionomycin defined as 100% is provided in Figure 33C. RANTES pre-treatment reduced $[Ca^{2+}]_i$ responses by 74.5 ± 5.4% in comparison to first glucose treatment (Figure 33C).

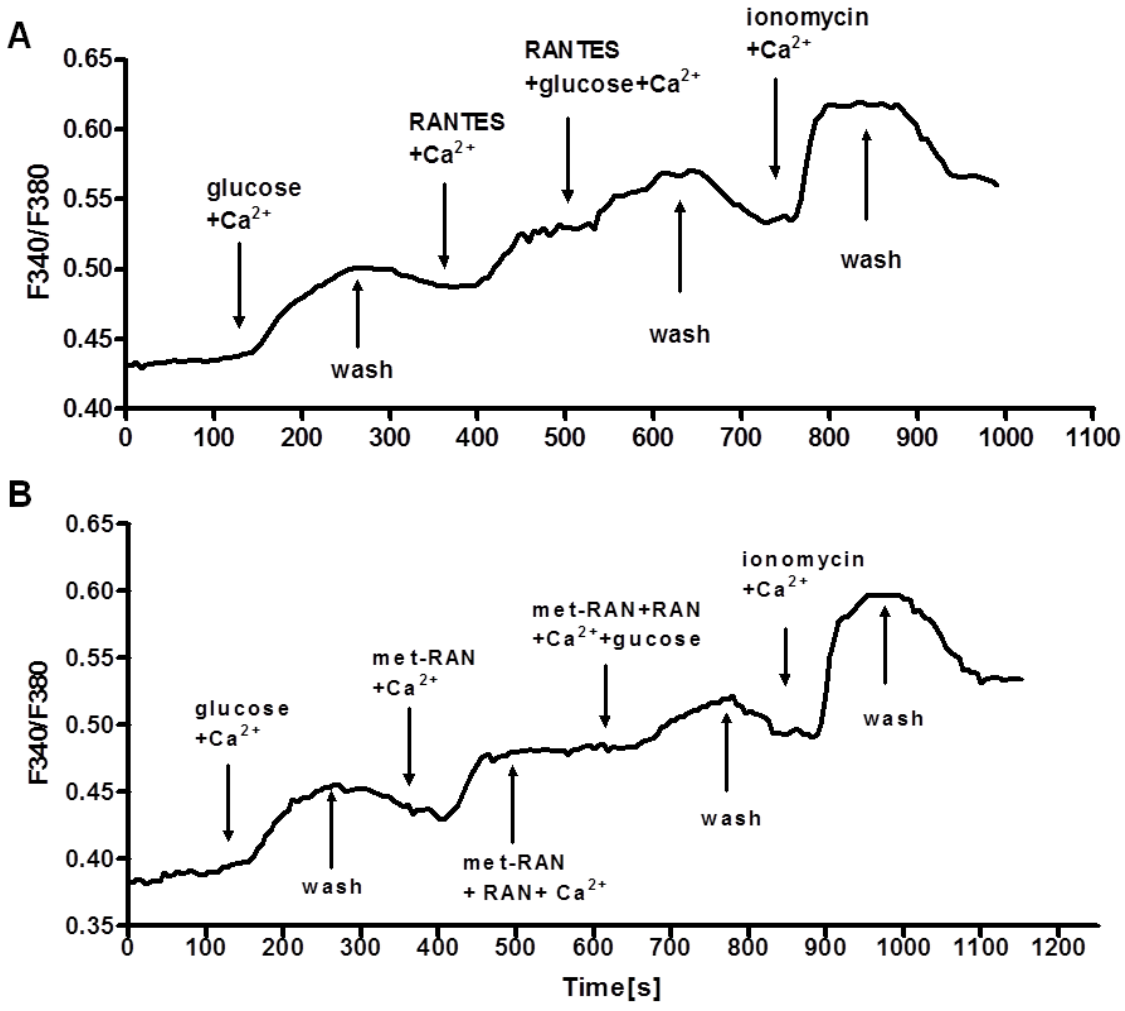

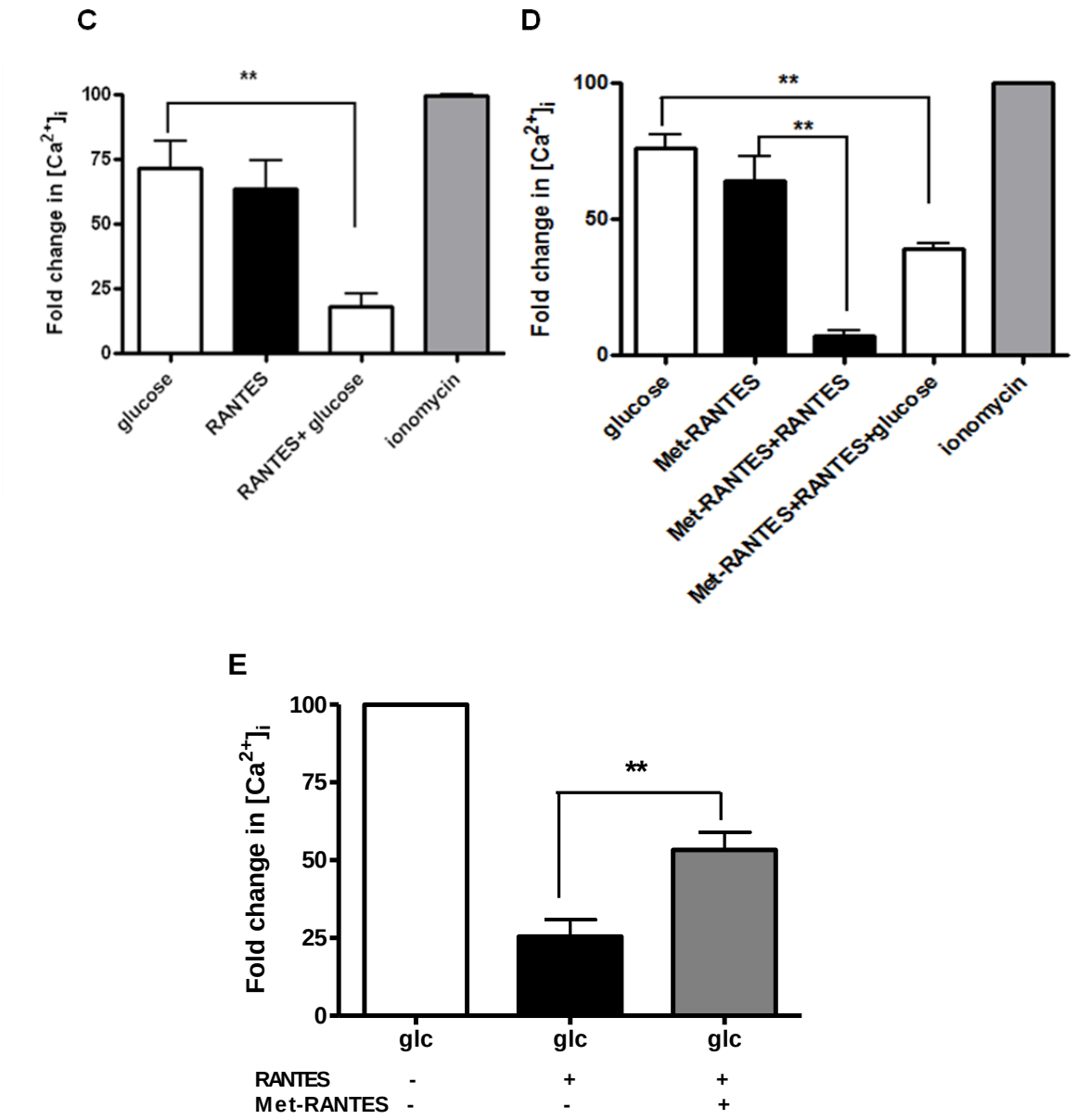

Figure 33: (A) RANTES [10^{-8} M], in a buffer supplemented with 1 mM $CaCl_2$ reduced glucose induced increase in $[Ca^{2+}]_i$. (B) Met-RANTES [$2*10^{-8}$ M] dramatically reduced RANTES evoked increase in $[Ca^{2+}]_i$ and improved glucose induced increase in $[Ca^{2+}]_i$. (C) Fold changes in $[Ca^{2+}]_i$ after glucose, RANTES, glucose + RANTES treatment with ionomycin-induced response set as 100%. (D) Fold changes in $[Ca^{2+}]_i$ after glucose, Met-RANTES, Met-RANTES + RANTES, glucose + Met-RANTES + RANTES treatment with ionomycin response set as 100%. (E) Fold change in glucose after RANTES and Met-RANTES + RANTES treatment with glucose induced response set as 100%. Data are shown as mean ± SEM and statistical significance calculated by one way ANOVA followed by Bonferroni's post test.

We next employed Met-RANTES as a CCR1/CCR5 receptor antagonist. Met-RANTES at $2*10^{-8}$ M was applied on cells 2 minutes either before or together with RANTES followed by glucose administration (Figure 33B). For the mean changes in $[Ca^{2+}]_i$, treatment with

Met-RANTES abolished the RANTES-induced effects on $[Ca^{2+}]_i$ by 89.1 ± 9% (Figure 33D). In repeated experiments the recovery of the glucose mediated $[Ca^{2+}]_i$ change by Met-RANTES accounting to 47.7 ± 4.5% of glucose-control (Figure 33E).

3.5.11 RANTES lowers fsk/IBMX induced increase in $[Ca^{2+}]_i$

cAMP has been demonstrated to directly modulate ion channel activity in the plasma membrane that leads to membrane depolarization and calcium entry in GLUTag enteroendocrine cells (173). When we applied 10 µM forskolin (fsk) and 10 µM IBMX to elevate cAMP levels, glucose-mediated $[Ca^{2+}]_i$ changes in perfused NCI-H716 cells was higher than with glucose treatment alone as shown for an individual recording in Figure 34 A and this effect was maintained even after a wash-out of fsk and IBMX. Whereas fsk/IBMX treatment elevated the mean glucose-mediated change in $[Ca^{2+}]_i$ by two-fold, they modestly reduced the RANTES-effects on intracellular calcium levels as shown in Figure 34B. This experiment further supports the previous findings that RANTES can lower intracellular cAMP levels.

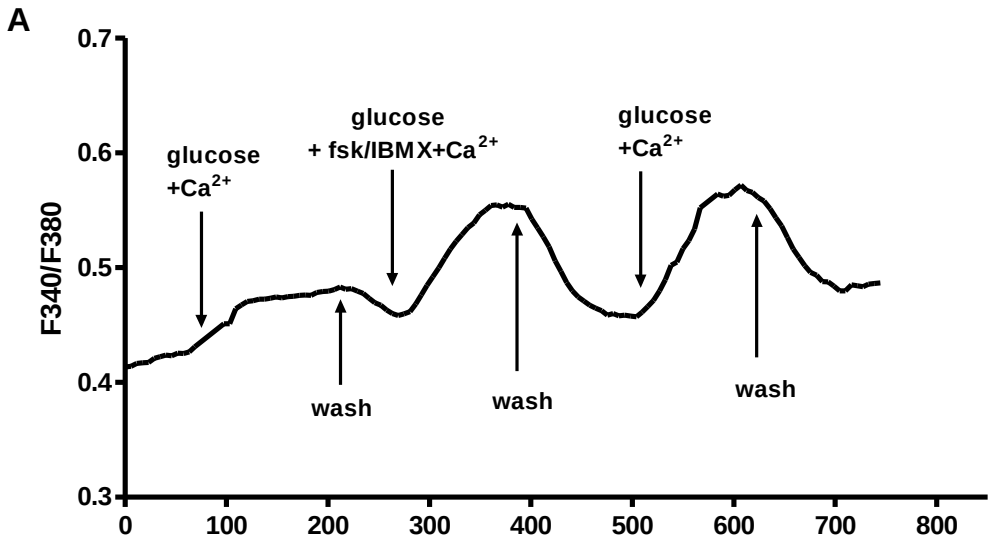

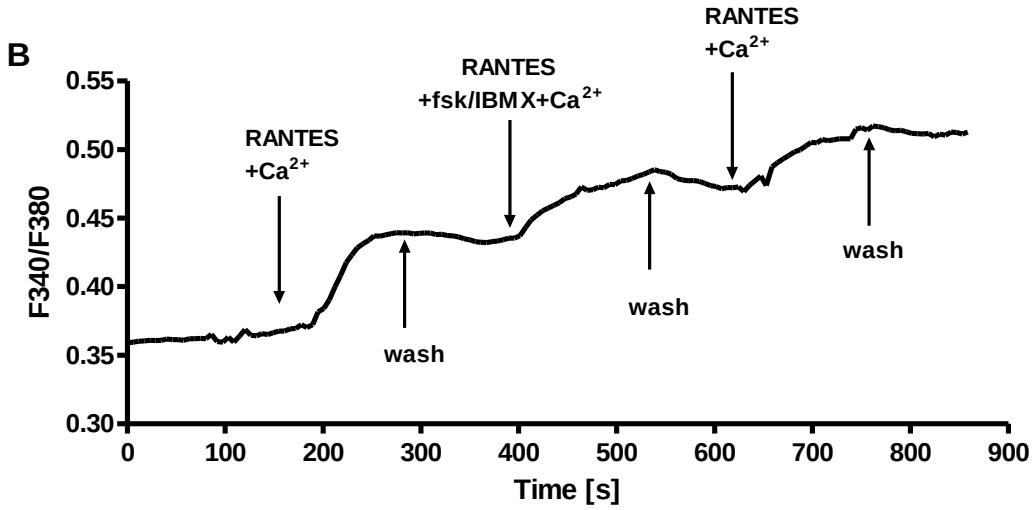

Figure 34: (A) fsk/IBMX enhanced glucose induced increase in $[Ca^{2+}]_{i..}$ (B) RANTES [10^{-8} M] reduced fsk/IBMX induced increase in $[Ca^{2+}]_i$. Traces shown are the image ratio of the calcium bound (F_{340}) to unbound form (F_{380}) of Fura-2AM dye and are a representative of 4-6 experiments.

3.5.12 Effect of RANTES on SGLT1 transport activity

SGLT1 has been demonstrated to be pivotal for GLP-1 secretion and $SGLT1^{-/-}$ mice showed a reduced GLP-1 secretion after an oral glucose bolus (146, 148). These recent findings suggest that the Na^+-dependent glucose transporter SGLT1 may act as a sensor in gut endocrine cells. We therefore studied next whether RANTES has an effect on α-MDG transport mediated by SGLT1in mouse intestine. Everted intestinal rings of mouse jejunum were incubated with 1 mM radiolabeled α-MDG either in the absence or the presence of $7.5*10^{-8}$ M RANTES by pre-exposure for 5 minutes. Specificity for SGLT1 mediated transport was demonstrated by use of 0.5 mM phlorizin that reduced α-MDG uptake by 89.9 ± 3.9%. RANTES pre treatment of mucosal tissues resulted in a dose-dependent reduction of SGLT1-mediated α-MDG uptake with a maximal effect for inhibition by 61.7 ± 4.6% as compared to controls. Further, to elucidate if the inhibitory action of RANTES was specific to SGLT1 or involved other nutrient transporters, we performed similar experiments to investigate the role of RANTES on uptake capacity of PEPT1. No difference was seen in PEPT1 transport when rings were incubated with gly-sar alone (4,523 ± 256 pmol/cm/min) or together with RANTES (4,707 ± 229 pmol/cm/min).

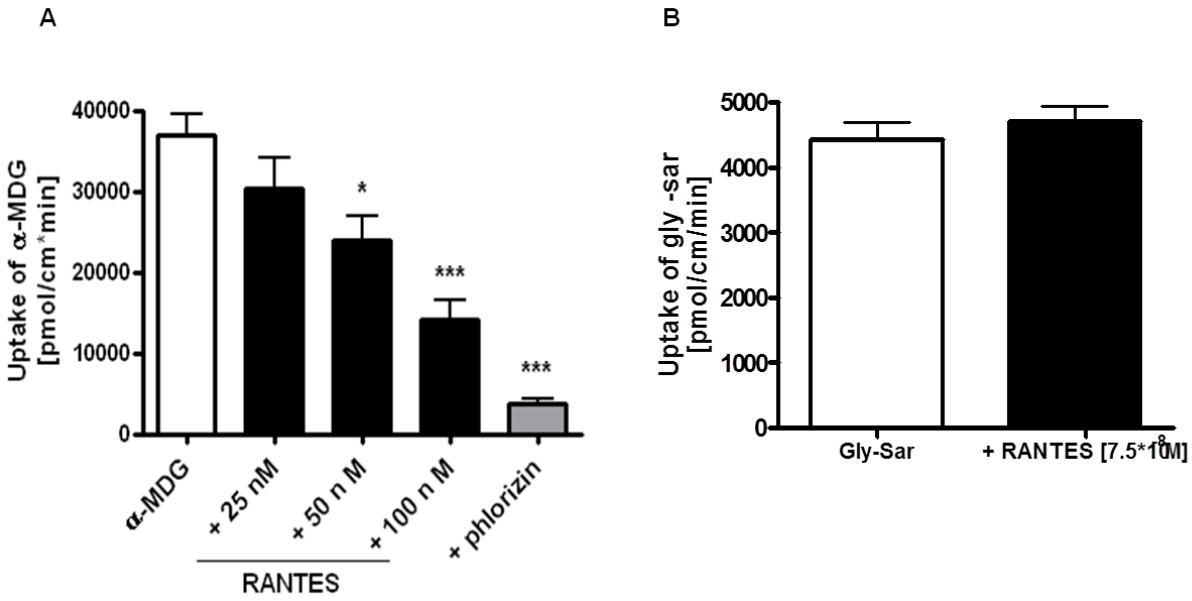

Figure 35: Uptake of α-MDG by SGLT1 in the presence and absence of different concentrations of RANTES. Data are shown as mean ± SEM from 5 independent experiments. Statistical significance determined by one way ANOVA followed by Dunnett's post test, *p < 0.05, **p < 0.01, ***p < 0.001.

3.5.13 *In vivo* experiments

Mice were purchased at 14-15 weeks of age from Charles River, Germany and then allowed two weeks acclimatization at an open facility with ad libitum access to rodent chow and water. We performed two sets of experiments to investigate the acute and chronic effects of RANTES on incretin hormone secretion.

3.5.13.1 Acute RANTES treatment

Following 6 hours of fasting, mice received a single injection of RANTES intraperitoneally [10 µg in 200 µl PBS] (176). Control group received PBS. Immediately after the injection, mice from both groups received either water or glucose as an oral bolus [6 g/kg]. Ten minutes later, blood was collected as described in section 2.2.11.4. Uptake experiments were performed with the intestinal tissue as described in section 2.2.2.

Blood glucose, insulin and gut hormones after chronic treatment

To test if RANTES would show the same inhibitory effect on GLP-1 in mice, we injected mice with 10 µg RANTES in 200 µl PBS and soon after, gavaged them with glucose bolus [6 g/kg]. Blood glucose was measured before and 10 minutes after glucose administration.

Blood was collected and used to measure gut hormones and insulin. RANTES significantly decreased blood glucose levels by 30.9 ± 9.3% in comparison to PBS treated mice that received glucose. However, GLP-1 and GIP levels were unaffected but insulin showed a trend towards lower levels than the control group.

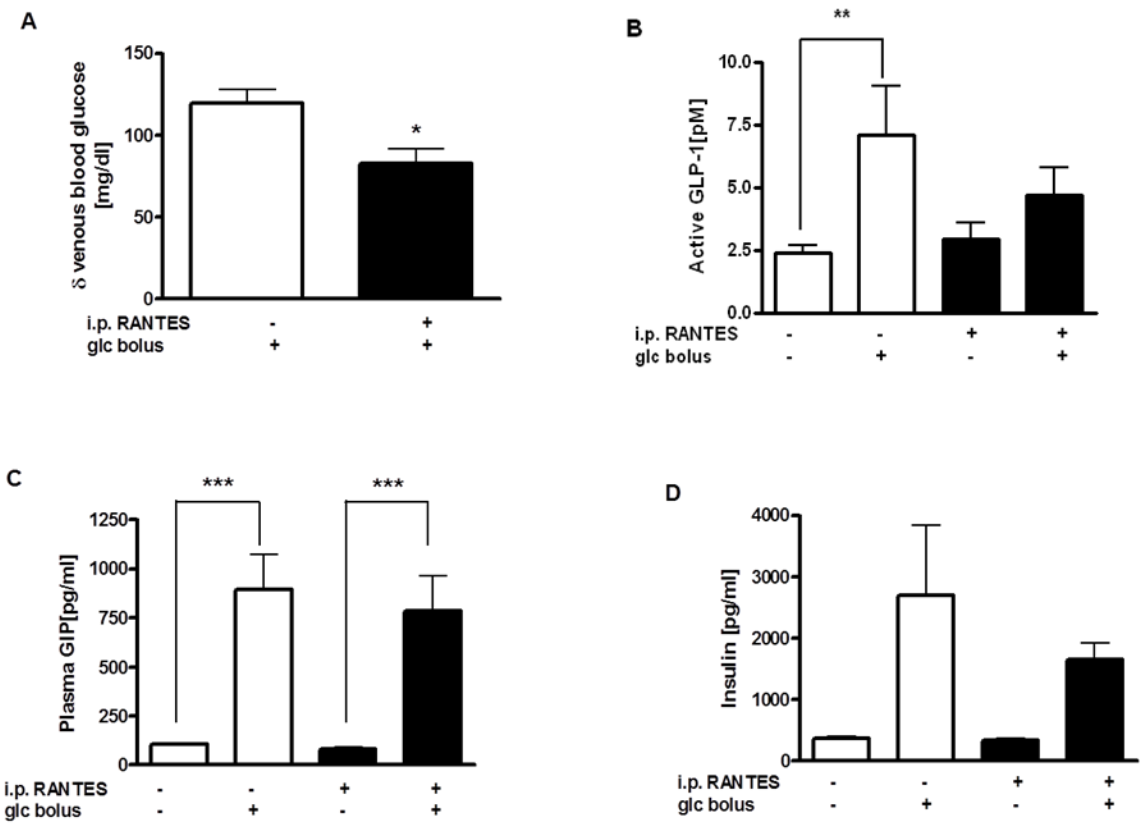

Figure 36: (A) Delta blood glucose ten minutes after receiving glucose bolus [6 g/kg] in saline and RANTES injected mice. Active GLP-1 (B), total GIP (C) and insulin (D) in plasma of saline (white bars) and RANTES injected mice (black bars) at fasting state and 10 minutes after glucose bolus [6 g/kg]. Bars are shown as mean ± SEM. Each group contained 6-10 mice. Statistical significance determined by one way ANOVA, *$p < 0.05$, **$p < 0.01$, ***$p < 0.001$.

3.5.13.2 Chronic RANTES administration

For chronic treatment of RANTES, mice received the same dosage of RANTES as in the acute experiment over consecutive 4 days, 1 injection/day. On the fourth day, immediately after the last injection, they received either water or glucose load by gavage. The rest of the experiment was performed in the same fashion as during the acute treatment (see 3.5.13.1).

Blood glucose, insulin and gut hormones after chronic treatment

We wanted to investigate if the chronic administration of RANTES via intraperitoneal route would cause changes in the secretion pattern of GLP-1 after a glucose bolus.

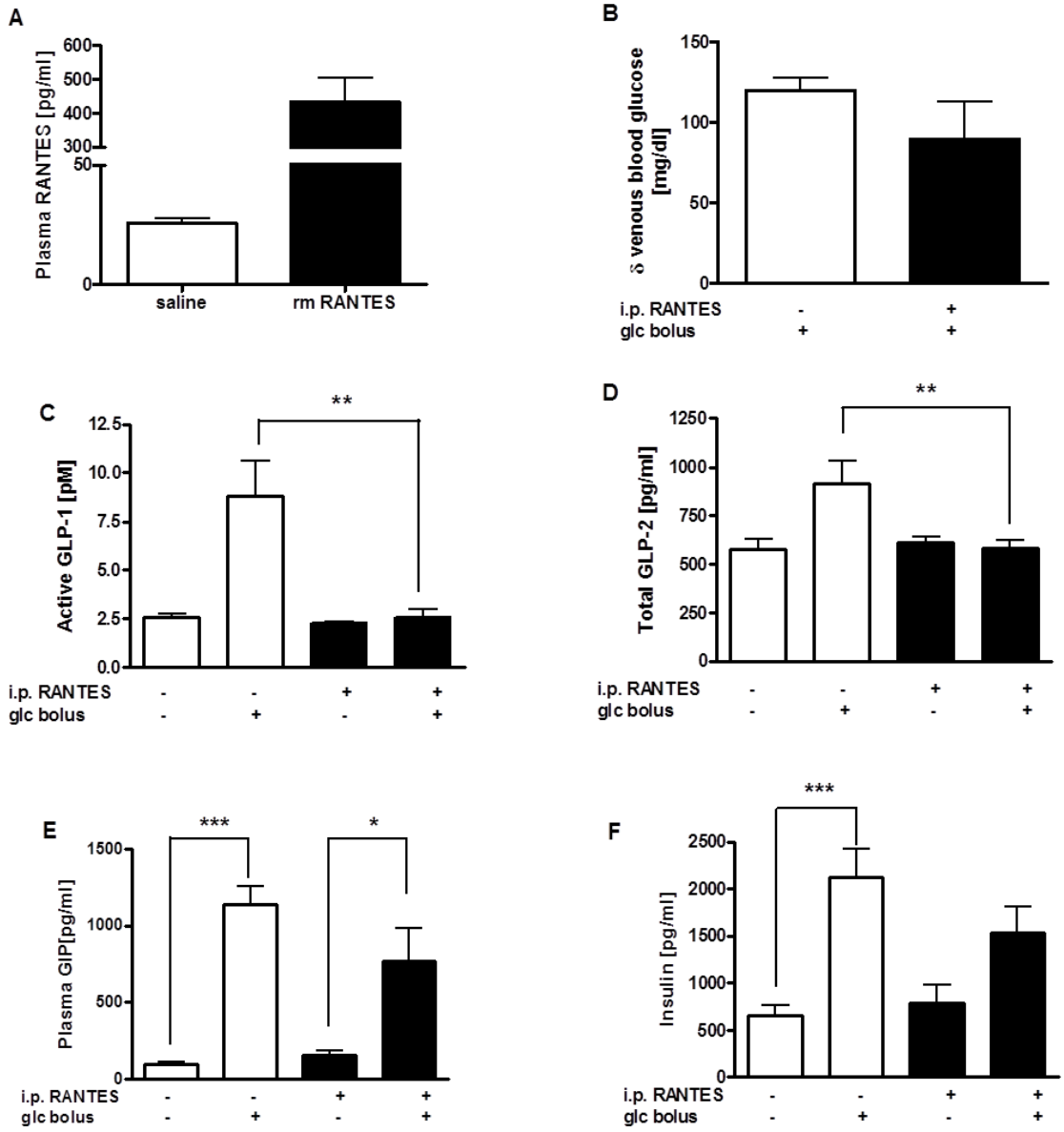

Figure 37: (A) Plasma RANTES levels in saline (white bars) and rm RANTES injected mice (black bars). (B) Delta blood glucose ten minutes after receiving glucose bolus [6 g/kg] in saline and RANTES injected mice. Active GLP-1 (C), total GLP-2 (D), total GIP (E) and insulin (F) in plasma of saline (white bars) and RANTES injected (black bars) mice at fasting state and 10 minutes after glucose bolus. Bars are shown as mean and SEM. Each group contained 6-10 mice. Statistical significance determined by one way ANOVA *$p < 0.05$, **$p < 0.01$, ***$p < 0.001$.

Mice that received rm RANTES over 4 days showed high levels of circulating RANTES in the plasma (432.6 ± 71.3 pg/ml) against saline injected (25.6 ± 1.8 pg/ml) mice (Figure

37A). Along with GLP-1, we also measured GIP, another incretin hormone and GLP-2 which is co-secreted together with GLP-1 from L-cells and also insulin. Blood glucose was also measured in the mice before and after the oral glucose bolus. RANTES treated mice showed no difference in basal blood glucose levels (data not shown) to saline injected mice. However after glucose bolus (6g/kg body weight), the mice that received RANTES showed a trend towards lower blood glucose than saline treated mice (Figure 36B) suggesting a defect in absorption by the intestine. Active GLP-1 and total GLP-2 were not different in the basal state in both groups, however following glucose bolus, both GLP-1 and GLP-2 hormones were significantly lowered in the RANTES group by 70.4 ± 1.3% and 36.3 ± 4.1%, respectively, (Figures 37C and D). Plasma GIP and insulin also showed a trend towards lower levels in the RANTES group after glucose load, but was not significant (Figures 37E and F).

3.5.14 Effect of IP RANTES treatment on the uptake of isotope labelled substrate by SGLT1 and PEPT1

We performed α-MDG uptake experiments in mouse intestinal everted rings from animals that received an IP-injection of RANTES or saline control over 4 consecutive days with or without a subsequent glucose gavage on the last day. No difference was seen in uptake rates of α-MDG in control and RANTES treated mouse tissues *in vitro* as compared to controls.

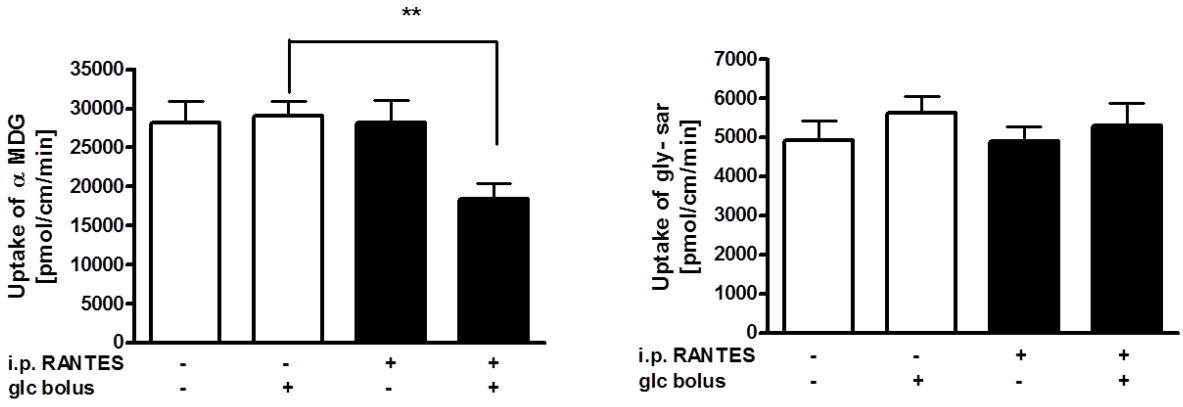

Figure 38: Uptake of α-MDG in untreated (white bars) and RANTES treated animals (black bars) by SGLT1 (left panel) and gly-sar by PEPT1 (right panel) by intestinal everted rings made from mice that received IP saline and RANTES with and without glucose bolus. Columns represent the mean ± SEM of 10 mice. Statistical significance calculated by one way ANOVA followed by Bonferroni's post test, p** < 0.001.

However, when animals received an oral glucose bolus [6g/kg], RANTES treated mice showed a 34.8 ± 2.1% reduction in uptake of α-MDG in comparison to saline treated controls (Figure 38). No such difference was obtained when using gly-sar as a substrate suggesting that the RANTES specifically affects SGLT1.

3.6 Angiotensin II

Angiotensin II is well described as a peptide hormone with distinct pro-inflammatory actions (177) (59). During our screening study with adipokines on GLP-1 secretion on the NCI-H716 cells, Angiotensin II also showed a lowering effect on GLP-1 secretion after glucose stimulation.

In the next part of my results, I will describe findings with Angiotensin II on different models with respect to hormone secretion and nutrient transporters.

3.6.1 Effect of Angiotensin II on glucose stimulated GLP-1 secretion from NCI-H716 cells

To test the effect of Angiotensin II on glucose stimulated GLP-1 secretion, 10^{-6} M Angiotensin II was incubated on the cells along with normal growth medium in a time dependent manner ranging from 2 to 24 hours and maintained at 37^{o}C throughout the incubation period. After that, the cells were stimulated with glucose 10%. Glucose stimulation without any Ang II pre-incubation served as the control. The rest of experiment was performed in a similar fashion as with RANTES and has been previously described. Ang II significantly reduced GLP-1 secretion following glucose stimulation to 67.1 ± 15.2%, 54.2 ± 9.2%, 66.9 ± 5.3 % and 59.8 ± 17.7% after 2, 6, 12 and 24 hour treatment, respectively (Figure 39)

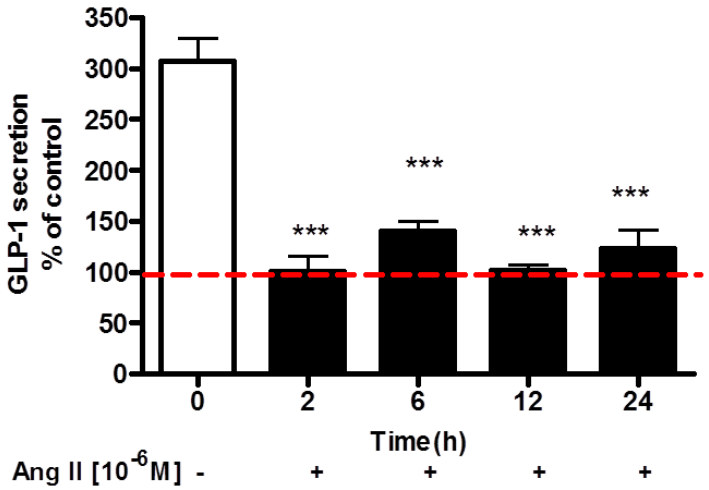

Figure 39: Effect of time dependent inhibition of Angiotensin-II on glucose stimulated GLP-1 secretion in NCI-H716 cells. Data are expressed as percentage of basal secretion (buffer alone) and are given as mean ± SEM. Statistical significance was calculated by one way ANOVA followed by Bonferroni's post test, ***p < 0.001.

3.6.2 Expression of receptors for Ang II on enteroendocrine cells

After demonstrating functional effects of Ang II on cell culture and *ex vivo* models, the next question that arose was to identify the receptors of Ang II on EEC. Effects of Ang II on peripheral tissues are mediated through two receptors, the more prevalent AT_1 receptor and the AT_2 receptor.

mRNA expression of receptors

We identified both AT_1 and AT_2 to be present at message level on the NCI-H716 cells.Additionally we looked for the expression of the receptors in mouse intestinal tissue. Both AT_1 and AT_2 were found to be expressed (Figure 40).

Protein expression of the receptors

Western blot

We performed a western blot on total protein isolated from the NCI-H716 cells. Additionally, we also isolated cellular protein from the Caco-2 cells, an intestinal epithelial cell line. 25 µg of protein was loaded and run on a 10% gel and probed with anti-AT_1

(1:200) and GAPDH (1:1,000). Appropriate infra red dye coupled secondary antibodies, RDYE 800 and IRDYE 680 (1:20,000) were used and the membrane was scanned with an Odyssey scanner (LICOR).

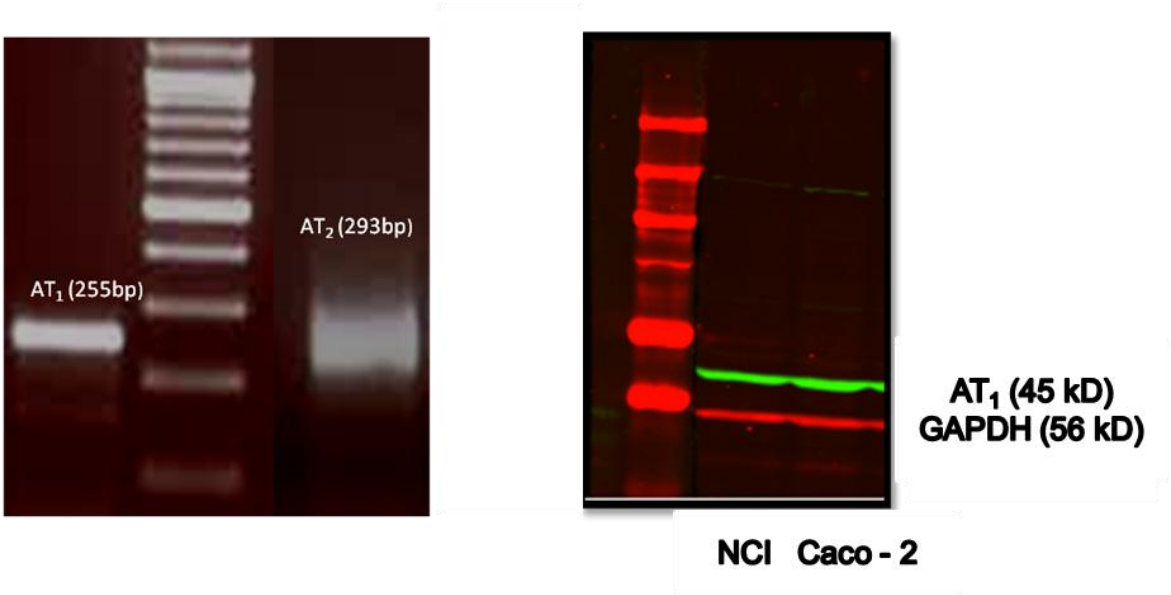

Figure 40: Left panel, expression of AT_1 and AT_2 receptor in NCI-H716 cells. Right panel, western blot analysis of AT_1 in total protein fraction of NCI-H716 and Caco-2 cells.

Immunofluorescence

NCI-H716 cells were fixed with 4% formalin and then incubated with anti-AT_1 (1:50) and anti-AT_2 (1:50) overnight at 4^oC. The next day cells were washed and incubated with appropriate secondary antibodies, donkey anti-goat FITC (1:150) and donkey anti-rabbit FITC (1:150) and DAPI (1:500) for nuclear staining for 1 hour at room temperature. Omission of secondary antibodies served as negative control. Cells were washed with PBS, mounted and examined with a confocal fluorescent microscope. Both AT_1 and AT_2 were abundantly expressed on the NCI-H716 (Figure 41).

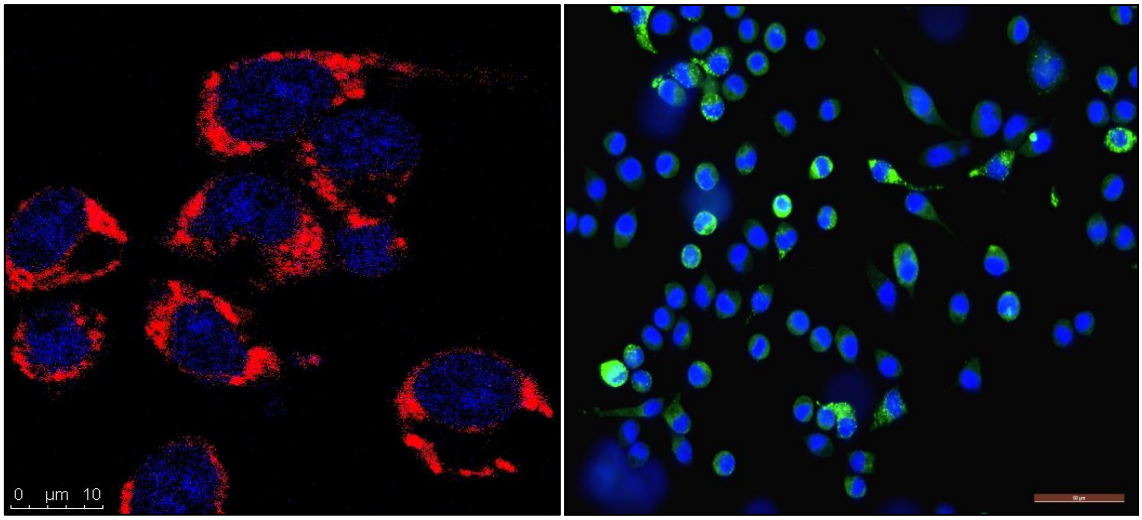

Figure 41: Left panel, IF staining on the NCI-H716 cells for AT_1 (red) and DAPI (blue). Right panel, IF staining on the NCI-H716 cells for AT_2 (green) and DAPI (blue).

In mouse tissue, AT_1 was found to be present on both epithelial and enteroendocrine cells types. Enteroendocrine cells were distinguished from epithelial cells by co-staining for GLP-1 with a goat anti-GLP-1 antibody (1:50). Again, the receptor was found to be present on both the apical and basolateral membrane of the cells (Figure 42).

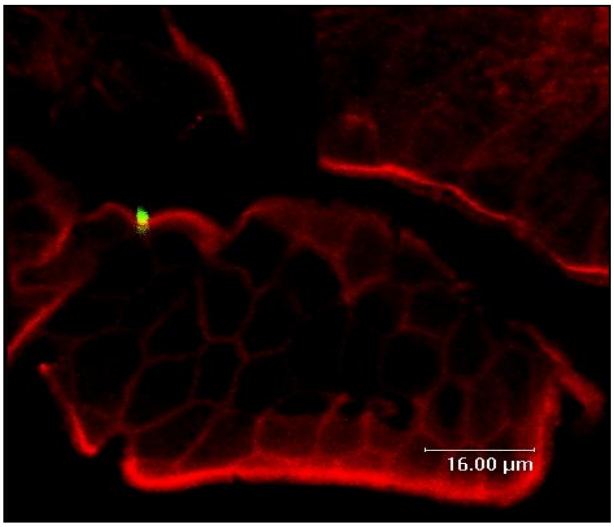

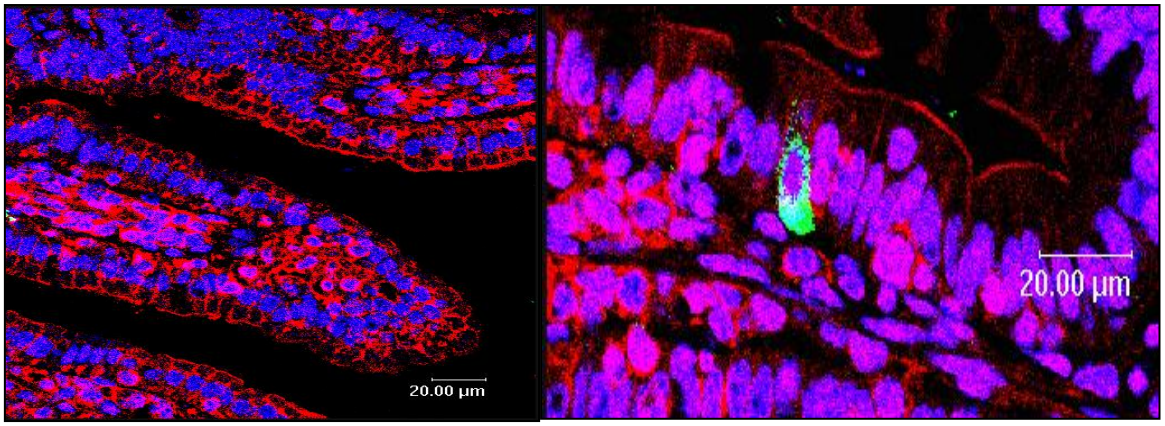

Figure 42: IF staining of mouse villi for AT1 (red), GLP-1 (green) and DAPI (blue)

3.6.3 Effect of AT_1 and AT_2 receptor blockers on GLP-1 secretion

To confirm the role of Ang II on GLP-1 secretion, we wanted to see if the effect could be blocked by using antagonists for its receptors. Since we found both the receptors AT_1 and AT_2 expressed by the NCI-H716 cells at message and protein level, we used Candesartan and PD123 319 which are Ang II- type 1 and 2 receptor antagonists, respectively. Briefly, NCI-H716 cells were pre-incubated with Ang II ± Candesartan or PD123 319 for 2 hours followed by 1 hour stimulation with glucose. Candesartan and PD123 319 treatment seemed to have a beneficial effect on the NCI-H716 cells causing more GLP-1 secretion in comparison to glucose stimulation. Together with Ang II, they recovered the cells from the detrimental effect that was seen in cells when treated with Ang II (Figure 43 A and B). Combination of both the blockers together with Ang II significantly improved the cell's response to glucose (Figure 43C). From these data, it is still quite early to designate which of the two receptors is involved in signal transduction following Ang II activation.

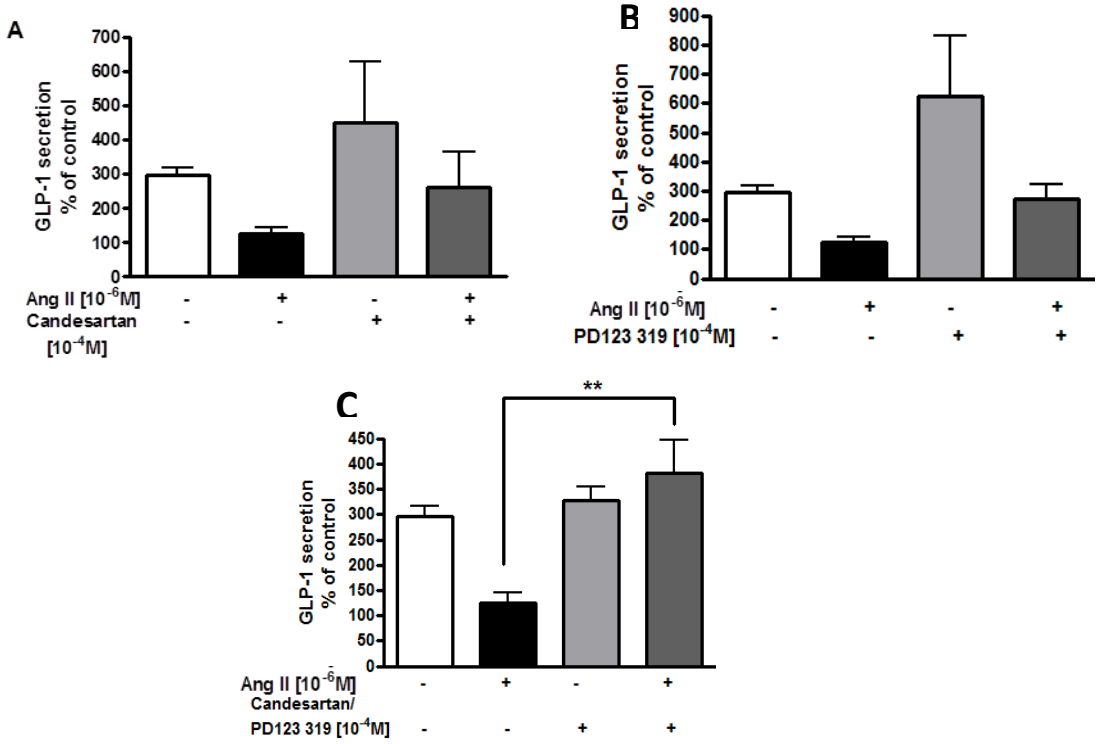

Figure 43: (A) Effect of Candesartan [10^{-4}M] on glucose stimulated GLP-1 release by NCI-H716 cells. (B) Effect of PD123 319 [10^{-4}M] glucose stimulated GLP-1 release by NCI-H716 cells. (C) Effect of Candesartan [10^{-4}M] and PD123 319 [10^{-4}M] on glucose stimulated GLP-1 release by NCI-H716 cells. Cells were treated with 10^{-6} M Ang II and with or without blockers for 2 hours before stimulating with glucose. Data are given as mean ± SEM. Statistical significance was calculated by one way ANOVA followed by Bonferroni's post test, **$p < 0.01$, vs. control, $n = 3$.

3.6.4 Preliminary *in vivo* mice experiments

3.6.4.1 Acute Angiotensin II treatment

To test if Ang II would show the same inhibitory effect on GLP-1 *in vivo*, we injected mice with 10^{-7} M Ang II in 200 µl PBS (178) and soon after, gavaged them with glucose [6 g/kg]. Blood glucose was measured before and 10 minutes after glucose administration. Blood was collected and used to measure gut hormones and insulin. Ang II significantly decreased blood glucose levels by 33.9 ± 8.1% (Figure 44A) in comparison to PBS treated

mice that received glucose. However, GLP-1, GIP and insulin plasma levels were not affected by acute Ang II treatment (Figure 44B, C and D).

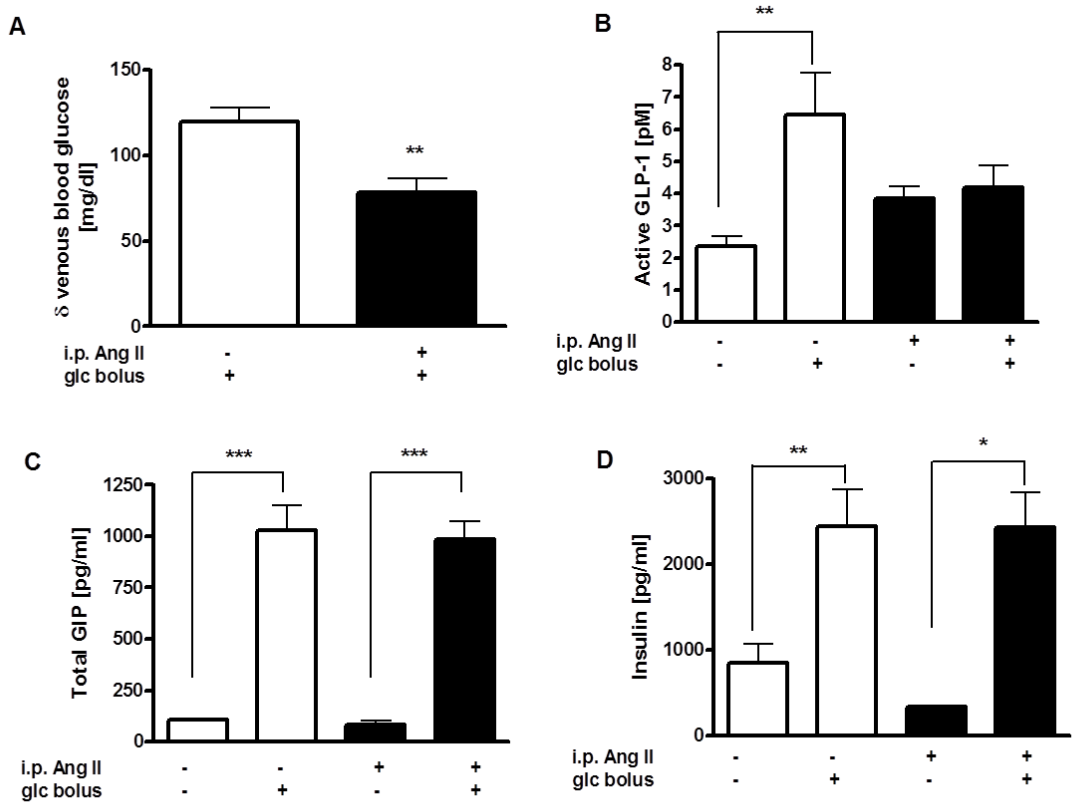

Figure 44: Delta venous blood glucose (A), active GLP-1 (B), total GIP (C) and insulin (D) in plasma of saline (white bars) and Ang II injected mice (black bars) at fasting state and 10 minutes after glucose bolus. Bars are shown as mean ± SEM from 6-10 mice. Statistical significance was determined by one way ANOVA *p < 0.05, **p < 0.01, ***p < 0.001.

3.6.4.2 Chronic Angiotensin II treatment

Since, acute Ang II treatment did not reduce GLP-1; we subjected the mice to a longer duration of Ang II treatment. Mice were injected for 4 consecutive days. On the last day, blood glucose was measured, glucose administered and blood collected after 10 minutes. Mice in the Ang II test group again showed significantly lower blood glucose which was 49.3 ± 3.1% (Figure 45A) lower than control group after glucose administration. Chronically treated mice also showed impaired GLP-1 secretion after glucose gavage which was 56.4 ± 1.0% (Figure 45B) lower than control group. GIP however was not

affected and insulin showed a trend towards lower levels after glucose gavage in the test group (Figures 45C and D).

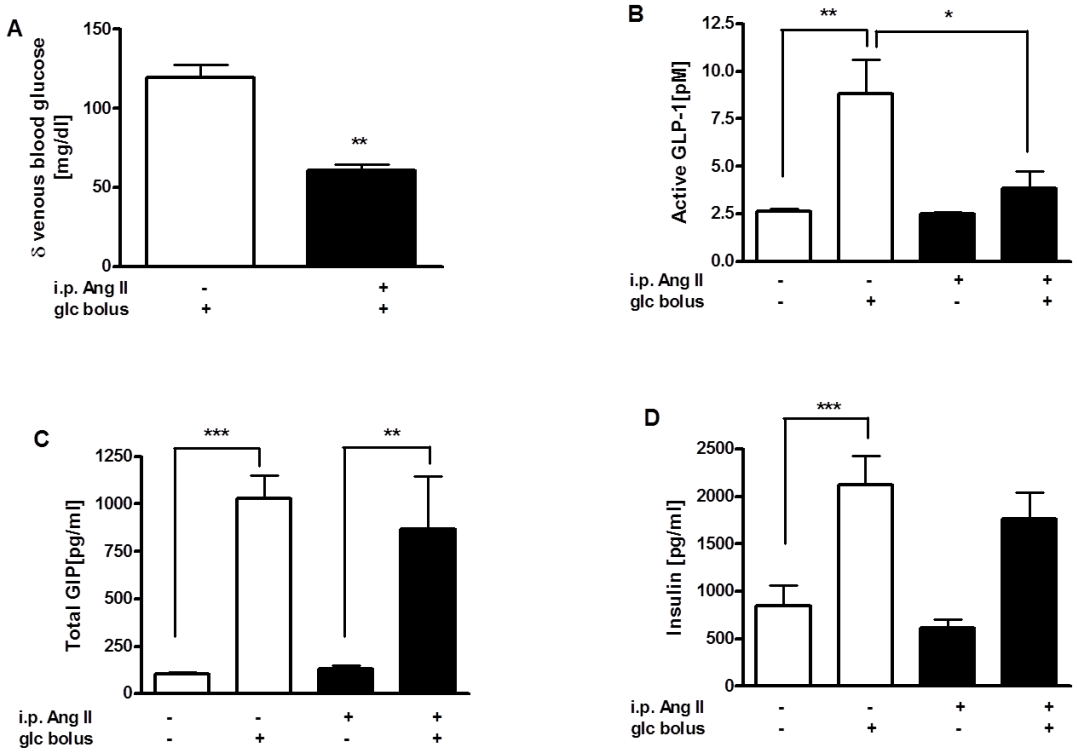

Figure 45: Delta venous blood glucose (A), active GLP-1, (B) total GIP (C) and insulin (D) in plasma of saline (white bars) and Ang II injected mice (black bars) at fasting state and 10 minutes after glucose bolus. Bars are shown as mean ± SEM from 6-10 mice. Statistical significance was determined by one way ANOVA *$p < 0.05$, **$p < 0.01$, ***$p < 0.001$.

4 DISCUSSION

4.1 Impaired GLP-1 secretion from the intestine of obese mice

The *ex vivo* gut ring experiment that was conducted using mouse intestinal tissue from control and diet induced obese mice revealed a clear reduction in GLP-1 secretion from the obese mice's intestinal tissue. It became apparent that this reduction although small at basal state (no nutrient stimulation) became large and significant upon nutrient stimulation (glucose and glycyl-glycyl). This suggested some sort of blockage or inhibition preventing exocytosis of more GLP-1 molecules which is a normal occurrence when the L-cells are stimulated. This experiment helped to reinforce the observation that has already been described in literature demonstrating a decrement in GLP-1 secretion in obese and type 2 diabetic subjects (116, 123, 179), although they have been some literature contrasting this, showing normal GLP-1 responses in type 2 diabetic subjects in comparison to healthy subjects (180). With regard to GIP, the data is rather baffling, showing elevated, normal or even reduced GIP responses in diabetics compared to healthy subjects (181-183) .One reason for this could be the assay techniques that were employed in the early 90s that showed high cross reactivity to substances in plasma unrelated to the peptide (184). But using COOH-terminal GIP assays without such cross-reaction, Toft-Nielsen *et al*. (116) found slightly decreased postprandial GIP concentrations in a large group of type 2 diabetic patients compared with a control group of carefully weight, age and sex matched individuals. In obesity, however, GIP is even increased (185).

4.2.1 Preconditioned adipocyte media and impairment in GLP-1 secretion

The reasons underlying the loss of these incretins are still not completely comprehended and what remains still to be elucidated is, if this defect is the consequence of the diabetic/obese state or primary pathogenetic factors. To answer this question, we simulated conditions in the obese state where the intestine is exposed to pro-inflammatory factors secreted from the adipose tissue, in particular mesenteric adipose stores because of its close proximity to the intestine in a cell culture model of enteroendocrine cells, the NCI-H716 cell line. The NCI-H716 cell line is derived from a poorly differentiated adenocarcinoma of human colon and has been described to display endocrine features, in

particular the formation of secretory granules and chromogranin A expression (186). Furthermore, this cell line expresses several neurohormonal receptors, including receptors for gastrin, serotonin, and somatostatin, nutrient transporters and taste receptors (140, 144) and responds to a host of GLP-1 secretagogues (171, 187). The NCI-H716 cells line has the advantage of being the only GLP-1 secreting cell line of human origin. In the experiment where we treated the NCI-H716 cells with preconditioned media prepared from mature adipocytes of obese and lean subjects, we clearly saw a harmful effect of these media on glucose stimulated GLP-1 secretion and the effect was exacerbated with the media prepared from subjects with BMI $\geq$ 25 kg/m^2. This experiment revealed to us that the reduced GLP-1 came secondary to the disease which was in fact even shown indirectly in a study done with first degree relatives of type 2 diabetic patients, where the former exhibited normal GLP-1 profiles (120). Further studies that were done on GLP-1 secretion in T2D, identified obesity (116), insulin resistance (188) and glucose intolerance (189) as factors associated with decreased secretion. What also came out of other studies were that, long duration and severity of type 2 diabetes are associated with lower GLP-1 responses (189). BMI is a powerful regulator of the GLP-1 response and comes out as a significant determinant in larger studies (123, 190, 191). It has been suggested that it is particularly the GLP-1 response to carbohydrates that is impaired in obesity (123).

4.2.2 Pro-inflammatory factors and GLP-1 secretion

Although a relation between obesity and lowered GLP-1 secretion has been observed in many studies, not much has been done to point out if proinflammatory factors from adipose tissue (chemokines and hormones), collectively known as adipokines, which are secreted from the adipose tissue could interfere with the secretion of incretin hormones. There is data relating adipokines to insulin resistance where they are known to interfere with insulin signal transduction pathways (13, 34, 36, 192, 193). To the best of my knowledge, only two studies have been conducted showing a relation between adipokines and GLP-1. One was done with leptin, where the authors showed the involvement of this adipose tissue derived hormone in GLP-1 secretion in different cell culture models (NCI-H716, GLUTag, FRIC cells) and demonstrated impaired secretion in mice exhibiting insulin and leptin resistance associated with obesity (169). More recently, another cytokine, IL-6 which circulates in higher levels in obesity, diabetes and exercise was shown to increase GLP-1 secretion not only from the intestine but also from the pancreatic

α-cells by increasing GLP-1 exocytosis, proglucagon and prohormone convertase 1/3 gene expression (194). These findings prompted us to explore more in detail the role of other adipokines on GLP-1 secretion, specifically since they display altered patterns in obesity. We started out by screening adipokines which have been described in literature to be involved in the pathogenesis of T2D, such as TNF-α (13, 192, 193), RANTES (53), MCP-1 (34), angiotenisn II (177) and included leptin (169) as a control since its role was already described.

4.3 RANTES and its involvement in GLP-1 regulation

From our own previous work, we have seen that the adipose tissue secretes RANTES in a BMI dependent fashion and the secretion is dependent on adipocyte cell size (50). Our data with RANTES treatment on the NCI-H716 cells revealed two effects. Firstly, RANTES itself caused a small but significant increase in GLP-1 secretion (although not as potently as glucose), secondly, exposure to the chemokine for 2-24 hours caused a dramatic reduction in glucose stimulated GLP-1 from the same cell (which normally responded to glucose with a strong secretion of the incretin). RANTES treatment in mice (4 day intraperitoneal injection) reduced GLP-1 secretion following a glucose bolus and this reduction was significantly reduced in comparison to saline injected mice. RANTES however, did not affect the expression of *proglucagon* since the basal level of GLP-1 in the plasma remained unchanged. This observation raised an interesting point as to whether different signaling pathways could account for this ambiguous effect on the L- cells. Basolateral as well as apical expression of the receptor (CCR1) suggested that RANTES might also be secreted into the lumen from gut micro flora or immune cells. Despite the expression of the RANTES gene and its receptors by the intestine, we were not able to detect the protein from healthy mouse intestine tissue culture supernatants. It is known, however, that the expression of RANTES rises in granulomatous conditions such as colitis and might be involved in the progression from acute to chronic colitis in rats (195). On exposure to *salmonella dublin*, Caco-2 (intestinal epithelial model cell line) cells respond by increasing the expression of cytokines, including RANTES to ward off infection as was also seen in rotavirus infection of HT29 and Caco-2 cells as an immune response to the virus (196). Diet induced obese mice in our study responded with an up regulation in CCR1 in proximal and distal segments of the small intestine. RANTES was described to be secreted from mesenteric adipose tissue and from creeping fat in Crohn's disease (197)

confirming our observation that animals respond to increased RANTES secretion in obesity by up-regulating the receptors for RANTES.

4.4 Mechanism of action

To perceive alterations in signalling that follow RANTES treatment, we first need to understand signalling in normal healthy cells.

4.4.1 Calcium homeostasis in cells

Ionized calcium is an important regulator of a variety of cellular processes, including cell movement, cell differentiation, muscle contraction and secretion of hormones like insulin and GLP-1. The concentration of calcium [Ca^{2+}] in the cytoplasm is maintained in the range of 1-100 nM. Substantial amounts of calcium are associated with intracellular organelles such as the endoplasmic reticulum, mitochondria and lysosomes. In spite of high Ca^{2+} concentrations (2.5-5 mM) in the extracellular fluid, Ca^{2+} is restrained from entering the cell to ensure that the intracellular Ca^{2+} is maintained as prolonged elevations of Ca^{2+} in the cell is very toxic. A considerable amount of energy is expended to ensure that intracellular Ca^{2+} is controlled. A Na^{+}/Ca^{2+} exchange that has high capacity but low affinity pumps Ca^{2+} out of the cell. There also is a Ca^{2+}/proton ATPase-dependent pump that extrudes Ca^{2+} in exchange for H^{+}. This has a high affinity for Ca^{2+} but low capacity and is responsible for fine tuning cytosolic of Ca^{2+}. Furthermore, sarco/endoplasmic reticulum Ca^{2+} ATPases (SERCA) pumps Ca^{2+} from the cytosol to the lumen of the endoplasmic reticulum. Cells also have systems to increase the concentration of free Ca^{2+} in the cytoplasm. These systems generate a diffusion flux of Ca^{2+} either from the extracellular medium or from intracellular compartments, by increasing membrane permeability. These calcium channels are divided into two classes, the voltage – dependent Ca^{2+} channels (VDCC) and ligand gated Ca^{2+} channels (LGCC) are activated by extracellular ligands. There are also cyclic nucleotide –gated Ca^{2+} channels (CNG) that function in response to binding of cAMP. The VDCC are activated by depolarization of the membrane. Different types of voltage-sensitive Ca^{2+} channels can be distinguished on the basis of activation and inactivation voltage, kinetic parameters, single channel conductance and pharmacological properties. At physiological or resting membrane potential, the VDCC are normally closed. They are activated (opened) when the membrane depolarizes. Normally, the resting membrane potential is established when the movement

of K^+ out of the cell equals the K^+ movement into the cell. A summary of calcium homeostasis in cells has been depicted in the figure below.

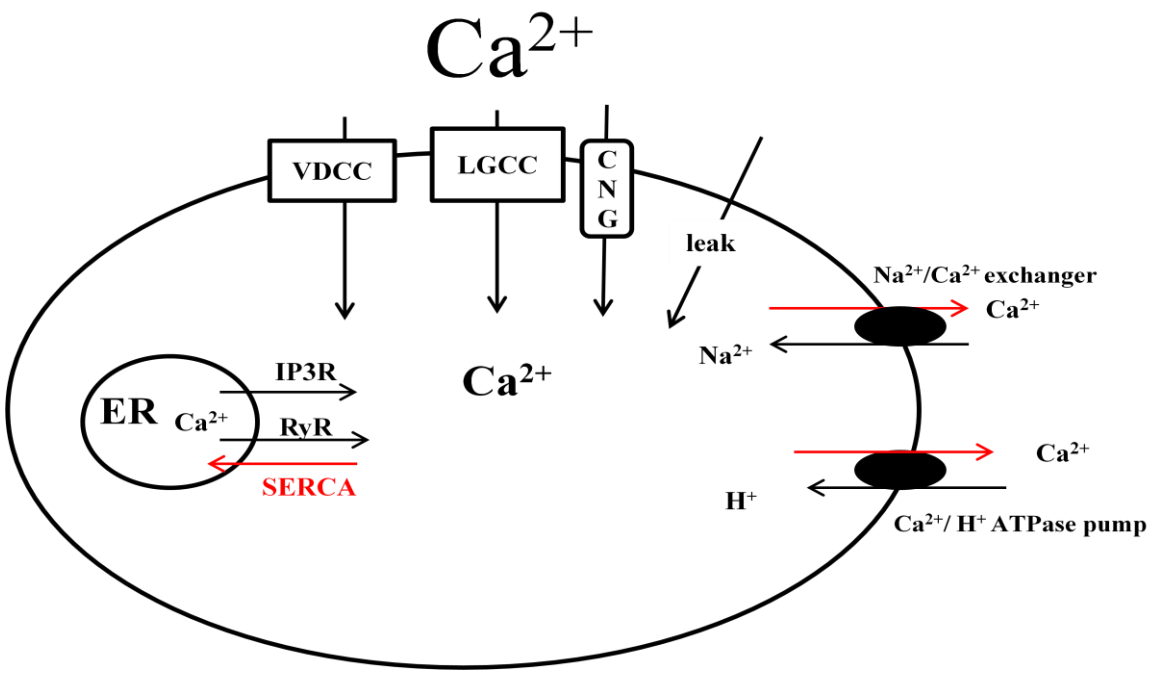

Figure 46: Regulation of intracellular calcium in mammalian cells. Upon receiving appropriate stimuli, Ca^{2+} enters the cell through voltage dependent calcium channels (VDCC), ligand gated calcium channels (LGCC) and cyclic nucleotide gated calcium channels (CNG). Additionally, Ca^{2+} can enter the cytoplasm from intracellular stores (ER) through the activation of inositol triphosphate receptor (IP3R) by inositol triphosphate (IP3) or ryanodine receptor (RyR) by cyclic ADP-ribose and other agonists. Calcium leaves the cell through exchangers or ATPase pumps or re-enters the ER through sarco/endoplasmic reticulum Ca^{2+} ATPase pump (SERCA).

4.4.2 Glucose mediated GLP-1 secretion

Glucose is a potent stimulant of GLP-1 secretion and has been well documented to trigger GLP-1 secretion in *in vivo*, whole intestinal preparations, GLUTag and NCI-H716 cells (198) (132, 171, 199). Glucose stimulation of the L- cell brings about increase in cytosolic calcium concentration, which could arise either by Ca^{2+} release from intracellular stores or by influx across the plasma membrane. There is more evidence pointing towards the influx pathway following glucose application on L-cells which proceeds membrane depolarization and opening of voltage dependent L-type calcium channels (131). Increase in cytosolic calcium causes fusion of GLP-1 vesicles to the plasma membrane and

subsequent GLP-1 exocytosis (132). The group of Ohara-Imaizumi *et al* using total internal reflection fluorescent (TIFR) microscopy strongly validated glucose stimulated GLP-1 secretion by imaging the motion of GLP-1 granules labelled with yellow fluorescent protein (Venus) in the STC-1 enteroendocrine cell line (168). They found that glucose stimulation caused a biphasic GLP-1 granule exocytosis. During the first phase, within 3 minutes of glucose application, fusion events occurred from two types of granules, the previously docked granules and newcomers, and thereafter, continuous fusion was observed mostly from newcomers during the second phase.

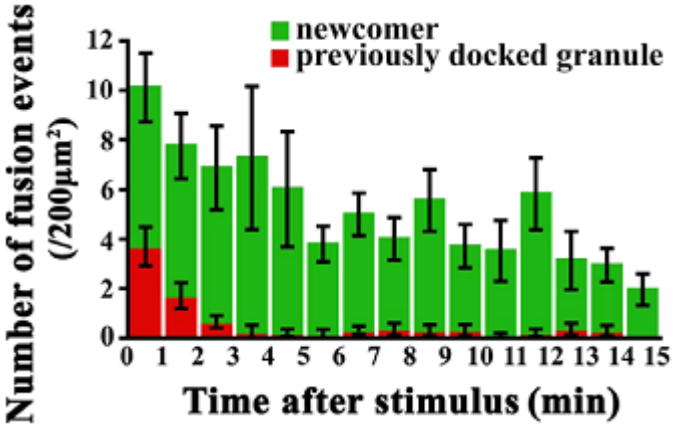

Figure 47: Histogram showing the number of fusion events of GLP-1 granules labeled with Venus at 1-min intervals after 22 mM glucose application viewed by TIFR. The red column shows fusion events from previous docked granules and the green columns shows those from newcomers (168).

We confirmed in our studies on the NCI-H716 cells that glucose in the same concentration as that used in our GLP-1 secretion experiments evoked an increase in intracellular calcium which was monitored by an increase in F340/F380 ratio with the life cell imaging system. In the GLUTag cell line, application of glucose resulted in membrane depolarization, action potential firing, a rise in intracellular calcium and the release of GLP-1, suggesting that L-cells might themselves contain the necessary glucose-sensing machinery to trigger GLP-1 release *in vivo* (147). The L-cell possesses all the glucose sensing machinery as was shown in a detailed study using a transgenic mouse with L-cell-specific expression of fluorescent protein (131). Venus positive L-cells were FACS sorted from the rest of the intestinal cell population and found to express the Kir6.2 and SUR1 subunits of the K_{ATP} channel, glucokinase, facilitative glucose transporters (Glut1, Glut2, Glut5), SGLT1, taste receptors (subunits Tas1R2 and R3) and α-gustducin. Glucose causes

membrane depolarization both by closing the ATP sensitive potassium channel (K_{ATP}) caused by its metabolism and consequent ATP production and by its uptake by Na^+ coupled glucose transporter SGLT1.

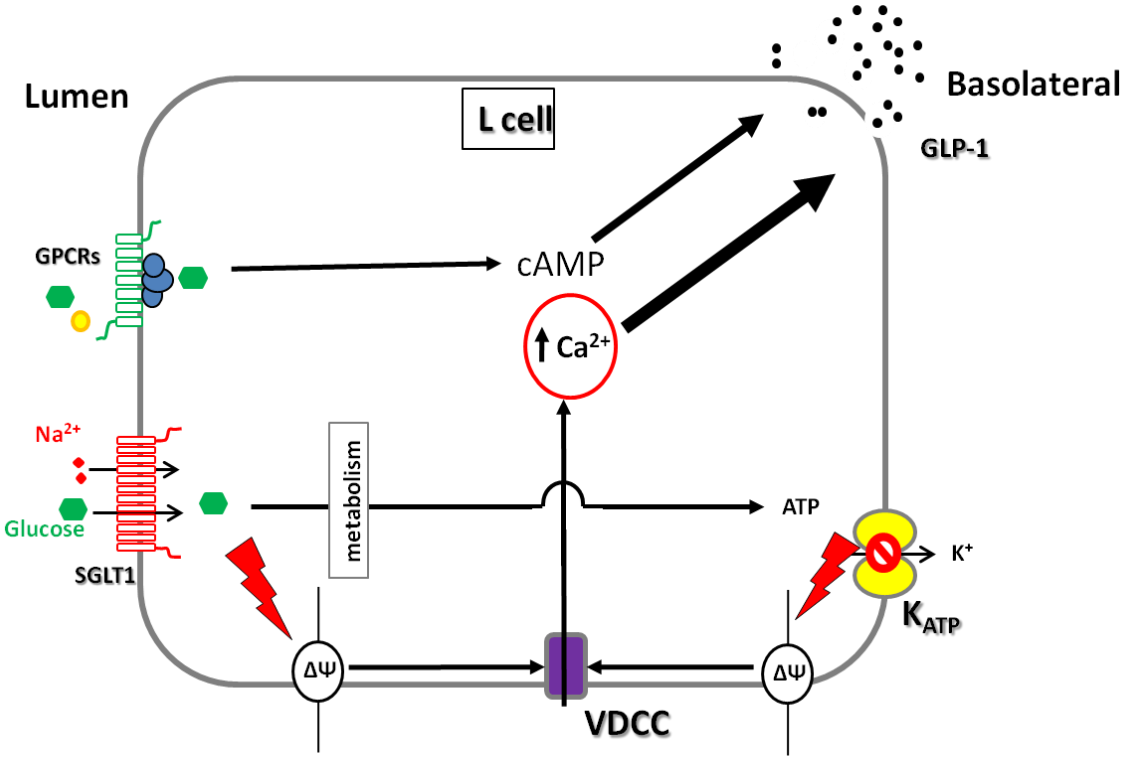

Figure 48: A model of the L-cell showing glucose mediated GLP-1 secretion. Entry of glucose via Na^+ coupled transporters, SGLT1 combines with metabolic signals (ATP) signals to trigger membrane depolarization (ΔΨ) and the opening of voltage gated Ca^{2+}channels (VDCC). The consequent elevated Ca^{2+} concentration stimulates secretion of GLP-1. Hormonal and other nutritional signals enhance secretion downstream of membrane depolarization by, e.g., increasing cAMP production or triggering Ca^{2+} release from intracellular stores.

In the NCI-H716 cells, we required a concentration of 500 mM glucose to stimulate GLP-1 secretion as was reported in previous studies (144). Considering the 2,000-fold lower expression of *Sglt1* mRNA in this cell line compared with the mouse small intestine, the concentration we used is justifiable. Reimann *et al.* reported the GLUTag cells to be responsive to 100 mM α-MDG in contrast to 10 mM which stimulated secretion in primary L-cells and accounted this to the 11-fold lower expression of *Sglt1* mRNA in the GLUTag cells in comparison to primary L-cells (131). In our *in vivo* studies conducted in C57BL/6 mice, an oral bolus of 2g glucose/kg mouse body weight failed to increase GLP-1 in the plasma, however it elicited a good GIP and insulin response, 15 minutes after oral administration. Although, some groups have reported this glucose concentration to

stimulate GLP-1 secretion in mice, there have been other groups, more recently, confirming our observation (148). Accordingly, others also tried higher concentrations of glucose like 3 g/kg (200) and 5 g/kg (144) to stimulate GLP-1 secretion. A glucose bolus of 6 g/kg showed the most promising effects with respect to secretion of both the incretins and insulin (148, 201). We were able to reproduce the same in our experiments. One explanation for this high concentration of glucose that was required to elicit GLP-1 secretion could be deduced from the observation of Tanja J. Little *et al* where they demonstrated in humans that GLP-1 is released in the blood stream when carbohydrates enter the duodenum at rates that exceed the absorptive capacity of the proximal small intestine to reach more GLP-1 bearing mucosa more distal in the small intestine (202). Accordingly, their study revealed that exposure of > 60 cm of the human small intestine to glucose was required for GLP-1 secretion. To the best of my knowledge, no such study was conducted in rodents.

4.4.3 RANTES signalling in L-cells

There have been no reports or studies conducted so far describing any effect of RANTES on enteroendocrine cells, let alone GLP-1 secretion. For this part of my discussion, I will compare RANTES signalling to what is known in other cell types, namely eosinophils, T-cells and microglia to data I obtained in the NCI- cells. The receptors of RANTES (CCR1 and CCR5) have a seven transmembrane domain architecture and are linked to G proteins. Studies conducted with monocytes and granulocytes have suggested that the receptors are associated with pertussis toxin-(PTX) sensitive G proteins. In microglia cells (resident macrophages of the CNS), application of $0.5*10^{-8}$ M RANTES evoked an influx of Ca^{2+} and the authors described a pharmacologically unique voltage-insensitive, nimodipine-sensitive route and channels in the transient receptor potential (TRP) as possible candidates involved (203). The response rapidly desensitized which was indicated by the rapid return of $[Ca^{2+}]_i$ to basal levels in the maintained presence of RANTES. The removal of extracellular Ca^{2+} blocked the RANTES-elicited increase in $[Ca^{2+}]_i$ and nimodipine (L-type channel antagonist belonging to the dihydropyridine family) inhibited RANTES mediated increase in $[Ca^{2+}]_i$ by 80% (203). Six years later, the same group followed up with another paper delineating the signalling pathway linking receptor activation with elevation in $[Ca^{2+}]_i$ .They showed that the RANTES-induced elevation in $[Ca^{2+}]_i$ is mediated by an inhibitory G protein coupled to its receptor CCR5 and demonstrated this

by treating the cells with PTX .They showed a multistep cascade involving phosphatidylinositol 3-kinase (PI3K), Bruton's kinase (Btk), phospholipase C (PLC) mediating calcium release from intracellular stores, and NAD metabolites, ADP ribose evoking calcium influx via a nimodipine-sensitive channel (204). In T-cells, RANTES mediated calcium influx when used at concentrations between 1-100 nM (10^{-10} - 10^{-8}M) and at higher concentration of 1 µM (10^{-7} M) elicited a biphasic $[Ca^{2+}]_i$ profile consisting of a small early transient and a secondary larger and prolonged increase (205).

In our experiments on the NCI-H716 cells, 10^{-8}M RANTES caused an increase in $[Ca^{2+}]_i$ which solely came from extracellular stores via a nifedipine sensitive channel. Interestingly, RANTES mediated calcium entry through the nifedipine sensitive L-channel does not follow cell depolarization as was revealed to us using the membrane potential dye, Di-Bac 3, suggesting it operates via voltage insensitive, nifedipine sensitive L-type channels like in microglial cells. Further, RANTES is known to open Ca^{2+} - activated K^+ channels (CaK) (206). Taking these data into account, it suggests that RANTES fails to cause depolarization of cells because K^+ efflux compensates Ca^{2+} influx keeping the net charge of the membrane unchanged and this accounts for the rather low GLP-1 secretion from the NCI-H716 cells that is seen after RANTES stimulation.

On the other hand, pre-treatment of the NCI-H716 cells with RANTES for as short as 2 minutes lowered the glucose mediated increase in cytosolic calcium. Glucose causes membrane depolarization both by closing the ATP sensitive potassium channel (K_{ATP}) caused by its metabolism and consequent ATP production and by its uptake by Na^{2+} coupled glucose transporter, SGLT1. But, RANTES on account of opening of CaK channels prevents glucose from sufficiently depolarizing the membrane and causing GLP-1 secretion**.**

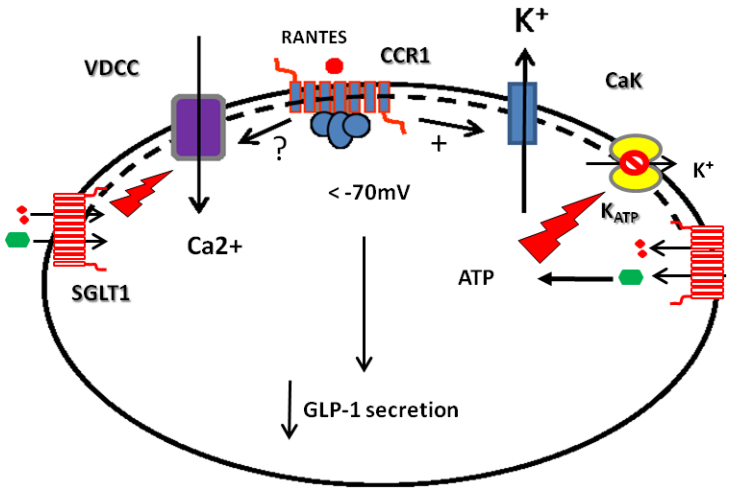

Figure 49: Working model of RANTES signaling in L-cells. Activation of CCR1 by RANTES stimulates Ca^{2+} influx via a nifedipine sensitive calcium channel. Additionally, RANTES activates the calcium activated potassium channel (CaK) causing K^+ efflux hence maintaining the cell at the resting membrane potential state. Glucose causes depolarization of the cell by its entry along with Na^+ via SGLT1 and metabolism to ATP which closes the ATP sensitive potassium channel $K_{ATP.}$ Under normal conditions, this depolarization is strong enough to cause calcium influx via the voltage dependent calcium channel and thereafter GLP-1 secretion. But since RANTES opens CaK channels, efflux of K^+ prevents the cell from sufficiently depolarizing to induce further opening of VDCC and hence the net result is lowered $[Ca^{2+}]_i$ and hence lowered GLP-1 secretion from the cell.

4.4.5 cyclic AMP (cAMP) and GLP-1 secretion

Adenosine 3', 5' cyclic monophosphate (cAMP) is a ubiquitous cellular second messenger that is a critical component of signal transduction pathways linking membrane receptors and their ligands to the activation of internal cellular enzymatic activity and gene expression**.** cAMP is synthesized from ATP by adenylyl cyclase located on the inner side of the membrane. Adenylyl cyclase is activated by a range of signalling molecules through the activation of adenylyl cyclase stimulatory G (G_s)-protein-coupled receptors and inhibited by agonists of adenylyl cyclase inhibitory G (G_i)-protein-coupled receptors. cAMP decomposition into AMP is catalyzed by the enzyme phosphodiesterase. Elevation of cAMP has been repeatedly demonstrated to increase GLP-1 secretion in several models of intestinal EEC (171-174). Further, there are also reports that cAMP via CREB (cAMP response element-binding) increases *proglucagon*-gene expression in EEC cells (175). cAMP has been demonstrated to directly modulate ion channel activity in the plasma

membrane, leading to membrane depolarization and calcium entry in GLUTag cells and thereafter GLP-1 secretion (173). Elevation of cAMP produces a very rapid increase in the number of L-type channels available for voltage activation during excitation and increases the probability of a Ca^{2+} channel opening and the mean open time of the channel (207). In our calcium imaging experiments with the NCI-H716 cells, cAMP elevating agents, forskolin (activator of adenylyl cyclase) and IBMX (inhibitor of phosphodiesterase) potentiated glucose induced increase in $[Ca^{2+}]_i$ and the effect on glucose lasted even after fsk/IBMX was washed out. This experiment proved that cAMP indeed has an effect on the VDCC and increases calcium influx in enteroendocrine cells. Cellular targets of cAMP are protein kinase A (PKA, cAMP-dependent protein kinase), nucleotide gated channels (CNG) and the more recently described exchange proteins activated by cAMP (Epac). PKA is the primary mediator of cAMP action and a key regulatory enzyme responsible for many cellular processes by catalyzing phosphorylation in response to hormonal stimuli. PKA is normally inactive as a tetrameric holoenzyme, consisting of two catalytic and two regulatory units (C_2R_2), with the regulatory units blocking the catalytic centres of the catalytic units. cAMP binds to specific locations on the regulatory units of the protein kinase, and causes dissociation between the regulatory and catalytic subunits, thus activating the catalytic units and enabling them to phosphorylate substrate proteins. PKA was described to mediate the stimulatory effect of cAMP on GLP-1 secretion (173). In mouse pancreatic islets, PKA rapidly senses glucose and brings about insulin exocytosis (208). Additionally, PKA has been found to modulate $[Ca^{2+}]_i$ by affecting voltage-gated Ca^{2+} channels (209, 210). The other target of cAMP, Epac (Exchange protein activated by cAMP) mediates cAMP-dependent mobilization of Ca^{2+} from intracellular Ca^{2+} stores. This is a process of Ca^{2+}-induced Ca^{2+} release (CICR), and it generates an increase of $[Ca^{2+}]_i$ that may serve as a direct stimulus for insulin secretory granule exocytosis from pancreatic β-cells (211). In intestinal L-cells, Epac mediates the stimulatory effects of cAMP on proglucagon transcription and was shown to stimulate the production but not the release of glucagon and GLP-1 in cultured endocrine cell lines, in contrast to PKA which enhances the production and secretion of both the hormones (212). Considering the importance of this molecule in GLP-1 secretion, it warranted interest to assess the effect of RANTES on cAMP accumulation in the L-cells.

4.4.6 RANTES and cAMP

The receptors of chemokines are seven transmembrane spanning G protein coupled receptors and are typically linked to inhibitory (G_i) G proteins (213). Activation of CCR5 releases G_i which inhibits adenylyl cyclase and reduces accumulation of intracellular cAMP (213). In a previous study conducted in primary cultures of mouse astrocytes, RANTES stimulation was shown to modulate intracellular cAMP levels and its downstream target PKA (214). In our experiments, we showed that RANTES dose dependently reduced basal cAMP concentrations in the NCI-H716 cells after just 5 minutes of incubation. Further, 10^{-8} M RANTES even reduced glucose induced cAMP levels and forskolin stimulated cAMP. PKA was also reduced after incubation of mouse intestinal tissue with RANTES. The activity of calcium channels is regulated by protein kinases. cAMP-dependent phosphorylation, initiated by protein kinase A (PKA), are one pathway implicated in the control of ion channels, including the dihydropyridine-sensitive Ca^{2+} channels of many excitable cells (207, 215). Whether Epac is reduced after RANTES treatment has still to be investigated. Taking into account the above pathways, it appears that although RANTES evokes calcium signal in the NCI-H716 cells, its inhibitory effect on cAMP overplays its stimulatory effect and hence lowers the overall calcium current in the cells after glucose stimulation.

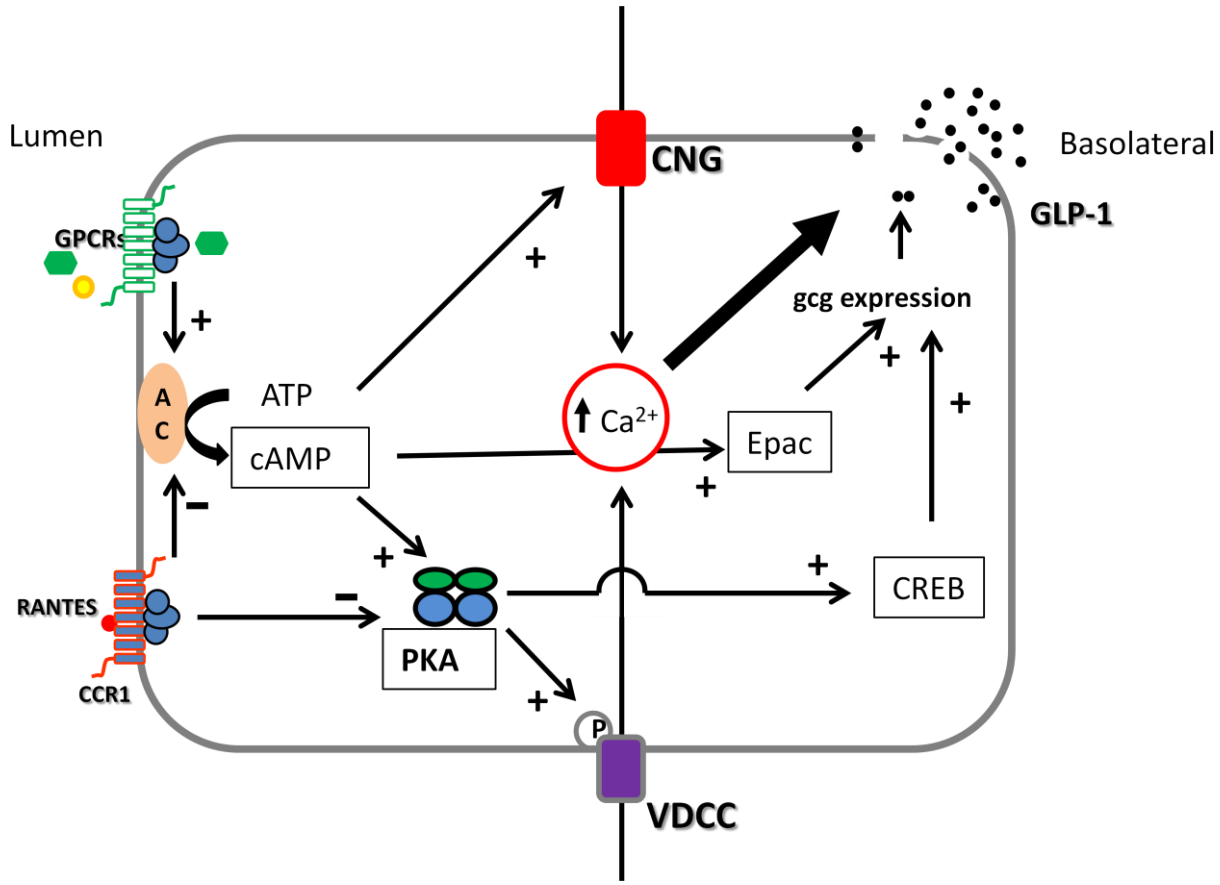

Figure 50: A working hypothesis of the disruption of cAMP mediated GLP-1 secretion by RANTES in the intestinal L-cells. RANTES binding to its receptor inhibits adenylyl cyclase via a G_i protein and thereby lowers accumulation of intracellular cAMP. The targets of cAMP include protein kinase A, which phosphorylates VDCC and increases the open probability of the channel causing more calcium influx (215). Additionally, PKA activates proglucagon gene (*gcg*) transcription and thereby GLP-1 production by phosphorylating CREB, which stimulates *gcg* transcription via binding to CRE or CRE-like elements (216). The other target of cAMP, Epac stimulates the expression of transcriptional activators of *gcg*, such as Cdx-2 (217, 218). cAMP directly activates cyclic nucleotide gated channel (CNG) and can cause calcium influx. The net effect of these pathways activated by cAMP is increased intracellular calcium, proglucagon gene expression and GLP-1 secretion. Inhibition of cAMP production by RANTES hence results in lowered GLP-1 secretion from the L-cell.

4.4.7 Involvement of SGLT1 in GLP-1 secretion

Dietary sugars are transported from the intestinal lumen into absorptive enterocytes by the sodium-dependent glucose transporter (SGLT1). SGLT1 mediates glucose transport and triggers incretin secretion in mice (148). Co-administration of the SGLT1 inhibitor phlorizin and glucose in the upper intestine completely inhibited glucose absorption and glucose-induced incretin secretion, demonstrating that glucose absorption via SGLT1 is essential for glucose-induced GLP-1 secretion (146). Our data show that luminal

application of RANTES to mouse intestine reduced the transport of α-MDG by SGLT1 and suggests that RANTES could contribute to the malabsorption which is characteristic of inflammatory bowel diseases since RANTES is up regulated in colitis (195). There have been other cytokines described in literature to influence SGLT1 activity. In 2000, Hardin *et al* described the effect of 3 pro-inflammatory cytokines (IL-6, IL-1α and IL-8) and the anti-inflammatory IL-10 on jejunal nutrient transport and expression of SGLT1 (219) and demonstrated that while IL-6, IL-1α and IL-8 significantly increased glucose transport, IL-10 had no effect. They concluded that the increase was due to an increase in mucosal to serosal flux and found no difference in the brush border membrane abundance of SGLT1. Barrenetxe *et al* showed that leptin inhibited galactose absorption *in vitro* by acting on SGLT1 (220-222). Another study demonstrated that while luminal leptin induced rapid inhibition of glucose entry into enterocytes which was associated with a parallel decrease in brush border membrane abundance of SGLT1, serosal leptin on the other hand acted more slowly and inhibited SGLT1 indirectly most likely by endogenous CCK (222). TNF-α also was also shown to decreases D-galactose absorption both in rabbit intestinal tissue preparations and brush-border membrane vesicles by reducing the amounts of the SGLT1 protein in the plasma membrane attributable to the cytokine (223). The above mentioned studies show that pro-inflammatory factors influence SGLT1 either positively or negatively and thereby could regulate the secretion of GLP-1.

The role of protein kinases in the regulation of SGLT1 has been well documented. In oocytes expressing rabbit SGLT1, the activation of PKA increased the maximum rate of SGLT1 by 30%, and the activation of protein kinase C (PKC) decreased the maximum rate of transport by 60%. Changes in maximum transport rates were accompanied by proportional changes in the number of co-transporters in the plasma membrane and by changes in the area of the membrane protein (224, 225). Since RANTES reduced PKA activity in mice intestinal tissue, it could suggest that lower kinase activity brought upon by RANTES treatment reduces the transport rate of SGLT1 seen by reduced uptake of α-MDG.

GLP-2 is another enteroendocrine hormone which is co-secreted with GLP-1 from L-cells upon nutrient ingestion. Proglucagon undergoes post-translational proteolytic cleavage to liberate GLP-1 and GLP-2. Unlike GLP-1, GLP-2 is not an incretin but an intestinal growth factor and induces intestinal epithelial proliferation and bestows protective function by inhibition of enterocyte and crypt cell apoptosis (81). GLP-2 increases hexose absorption via GLUT2 and SGLT1 (226, 227). A study in rats demonstrated that a 1 hour

vascular infusion of GLP-2 was sufficient to insert GLUT2 in the BBM and doubled the rate of fructose absorption (226). The same positive effect was seen with SGLT1 in rats where 30 minutes of vascular infusion was sufficient to increase SGLT1 transport activity. In animals treated with RANTES, we observed that glucose-dependent GLP-2 secretion is blunted which in turn could prevent the increase of SGLT1 activity thereby causing the reduction in glucose uptake into the epithelium as shown in mice with α-MDG and hence the slightly lowered blood glucose levels in the RANTES group following glucose bolus.These finding suggest that there may be a feed-forward loop by which SGLT1-mediated glucose transport increases GLP-1 and GLP-2 secretion with GLP-2 increasing sugar uptake capacity while GLP-1 simultaneously affects ß-cells to increase insulin secretion to control glucose disposal.

4.5 Angiotensin II and GLP-1

Angiotensin II (Ang II) is the main effector of the renin-angiotensin system (RAS). A local renin-angiotensin-system was described to be present in the gastrointestinal tract (56, 57). The effects of Ang II on peripheral tissues are mediated by two receptors, the more prevalent AT_1, and the AT_2 receptor. The wide distribution of the receptors (type 1 and 2) in the GIT is an indication of potential physiological actions of Ang II in this tissue (228). Although groups have found the receptors to be expressed on the enterocytes, there is no study till date demonstrating them on the EEC. In our study, we found both the receptors AT_1 and AT_2 at message (mRNA) and protein level (western blot and immunofluorescence) on the model EEC line NCI-H716. Additionally, by co-staining AT_1 with GLP-1, we confirmed that EECs in mouse intestine also express the receptor on their apical and basolateral membrane raising questions as to the possible effects of Ang II on the endocrine cells. Ang II pre exposure (2-24 hours) significantly inhibited glucose stimulated GLP-1 secretion from the NCI-H716 cell and we able to partially abolish the inhibition when AT_1 and AT_2 receptor blockers were used individually and completely when used together, suggesting the involvement of both the receptors in Ang II mediated disruption of GLP-1 secretion.

In vivo, Ang II exerts a dose-dependent dual action upon intestinal absorption. At low doses, Ang II stimulates sodium and water absorption from the intestine and at high doses, Ang II inhibits absorption (229). Further, depending on the site of contact (apical or basolateral), Ang II shows different effects as well (230). With regard to the glucose

transporter SGLT1, there has been a lot of work done. Application of Ang II to the mucosal fluid dose dependently inhibited jejunal glucose uptake and antagonism with losartan (specific AT_1 receptor blocker) abolished the inhibitory effect (228). Furthermore, Ang II treatment reduced the brush border membrane (BBM) expression of SGLT1 within 4 minutes of exposure (228). The effect was specific to glucose, since uptake of L-leucine was unaffected. In a previous study, where the authors observed a much greater reduction in glucose uptake, Ang II was treated *in vitro* and given in the luminal fluid. This hints that basolateral Ang II acts much slower or, that other signalling pathways are activated when basolateral Ang II receptors are activated. With respect to signalling involved with Ang II and decreased SGLT1 activity, Kawano *et al*. demonstrated in renal proximal epithelial cell line LLC-PK that Ang II prevented translocation of SGLT1 to the membrane indicated by reduced BBM abundance of the protein but unaltered total SGLT1. Further they saw that Ang II blocked the formation of cAMP and thereby inhibited translocation of SGLT1 to the membrane by inactivation of cAMP dependent protein kinase A (PKA) and decrease in phosphatidylinositol 3- kinase (PI3) (231).

Ang II evokes increase in intracellular calcium which comes from extracellular or intracellular stores depending on cell type. In cardiac myocytes, Ang II mediates extracellular calcium influx through transient receptor potential channels. In vascular smooth muscle, Ang II binding to AT_1 receptors activates phospholipase C (PLC). PLC breaks down phosphoinositol into diacylglycerol (DAG) and IP3 and IP3 goes on to stimulate the release of Ca^{2+} from intracellular stores (232).

Chronic administration of Ang II intraperitoneally to mice (basolateral exposure of Ang II to the EEC) showed a significant trend towards lowered GLP-1 after glucose gavage administration, but the effect was not as big as compared to chronic RANTES treatment. Plasma insulin on the other hand was only slightly reduced in the chronic group vs. saline. The other incretin GIP was unaffected in both acute and chronic groups.

Looking back at the experiments that were conducted and results obtained so far, it undeniably argues to a significant effect of Ang II on GLP-1 secretion and further investigations will have to be conducted to confirm the effect.

5 CONCLUSION AND OUTLOOK

To the best of our knowledge, this study is the first to demonstrate an effect of RANTES (CCL5) on the secretion of GLP-1 from enteroendocrine cells in mammalian intestine via CCR1 receptors. The mechanisms of action of RANTES are dual by affecting intracellular $[Ca^{2+}]_i$ causing a modest stimulation of GLP-1 output but blocking completely and specifically the GLP-1 secretion in response to glucose and thus to nutrient intake most likely via a reduced PKA activation by preventing a proper increase in cAMP levels. Our findings suggest that the rheogenic glucose transporter SGLT1 in the intestinal epithelium is a target of RANTES that could counteract on a feed-forward loop on glucose transport via GLP-2 while GLP-1 elicits its incretin effects. As circulating RANTES levels are increased in obese and insulin-resistant individuals, this chemokine could contribute to the reduced secretion of incretins following meal-stimulation in these subjects and antagonism of its receptors could serve as a potential target in diabetes therapy.

Angiotensin II, as well seems like a prospective candidate to be further studied since its effect in causing disturbances in GLP-1 secretion has already been recognized in the NCI-H716 cell line. Further *in vivo* experiments in mice will need to be conducted with a higher concentration of Ang II or by prolonging the duration of treatment to see more pronounced and significant effects. Intracellular signalling upon Ang II activation of its receptors will have to be investigated. $[Ca^{2+}]_i$ and cAMP are two likely candidates that need further examination in the NCI-H716 cells to elucidate possible mechanisms by which Ang II causes GLP-1 reduction. Other targets worth studying are PKA and PI3-K. Lastly, a human study has been proposed wherein drug naive hypertensive patients will be challenged with nutrients and GLP-1 output measured.

In the end, I would like to conclude that while the above two mentioned adipokines seem most promising in the course of GLP-1 disturbances in obesity/T2D, there are still many more adipokines to be explored and provide exciting ventures for future research.

6 APPENDIX

6.1 NCI-H716 cells

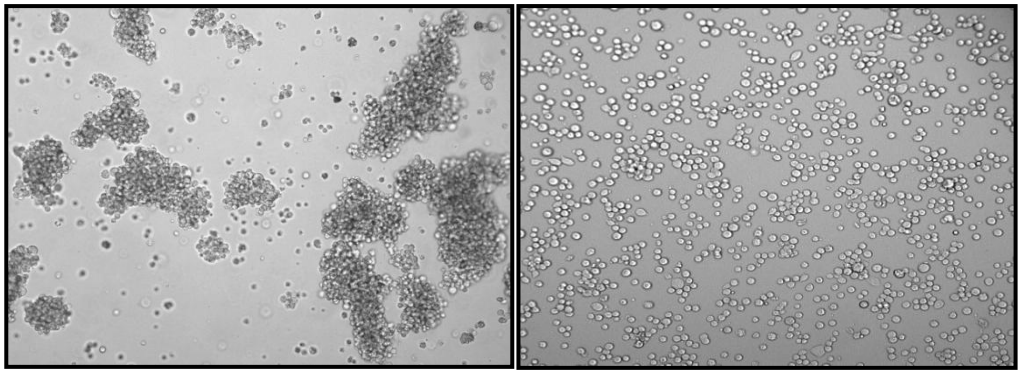

Figure 51: Left panel, NCI-H716 cells in suspension culture and right panel, seeded on Matrigel.

6.2 Isolated primary mouse adipocytes

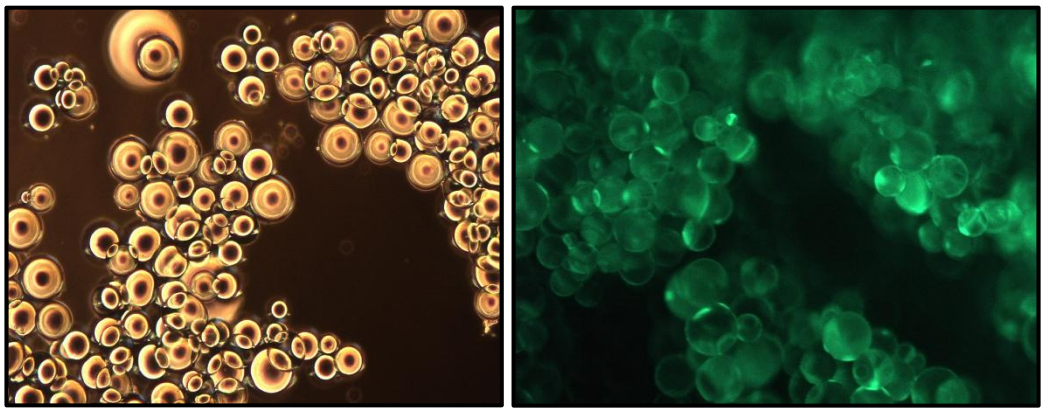

Figure 52: Left panel, primary adipocytes isolated from mouse epididymal fat pads and right panel, primary adipocytes stained with Calcien-AM to determine cell viability.

6.4. CCR1, CCR3 and CCR5 gene expression in NCI-H716 cells after 24 hour incubation with 10^{-8} M RANTES

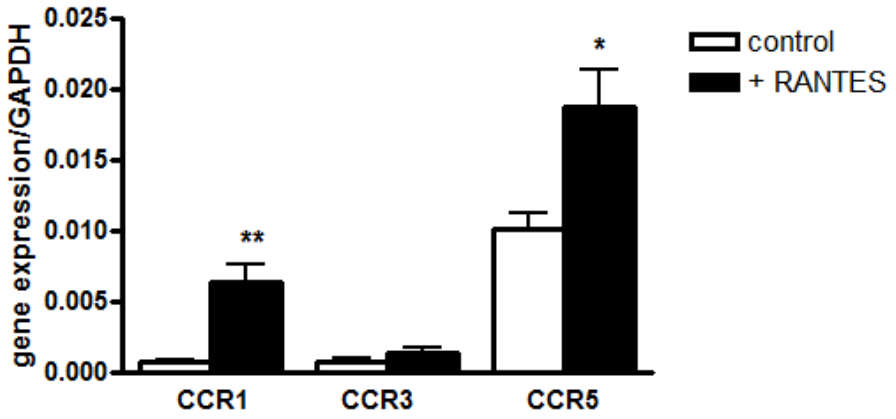

Figure 53: Gene expression of CCR1, CCR3 and CCR5 in control (white) and 10^{-8} M RANTES treated NCI-H716 cells for 24 hours. CCR1 was increased by 8 fold and CCR5 by 2 fold. CCR3 showed no difference after RANTES treatment. Statistical significance determined by One way ANOVA followed by Students t-test, *$p < 0.05$, **$p < 0.01$, $n = 4$.

6.5 GLP-1 secretion along the length of the small intestine

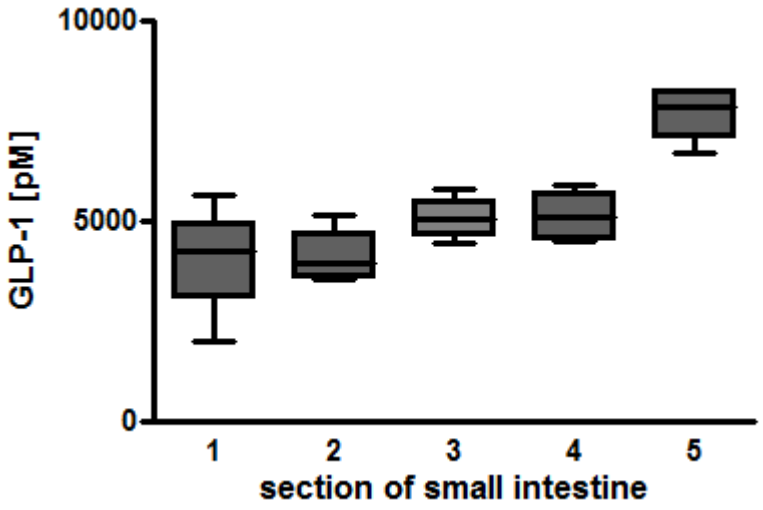

Figure 54: GLP-1 secretion along the length of the small intestine. The small intestine was isolated and cut into 5 cm section starting from the duodenum to the ileum. Sections were incubated in PBS for 45 minutes and GLP-1 measured in the supernatant by ELISA. GLP-1 secretion was highest in section 5 which corresponded to the distal most part of the small intestine and is in accordance with literature.

LIST OF FIGURES

REFERENCES

1. Kershaw, E.E., and Flier, J.S. 2004. Adipose tissue as an endocrine organ. *J Clin Endocrinol Metab* 89:2548-2556.
2. Gesta, S., Tseng, Y.H., and Kahn, C.R. 2007. Developmental origin of fat: tracking obesity to its source. *Cell* 131:242-256.
3. Jo, J., Gavrilova, O., Pack, S., Jou, W., Mullen, S., Sumner, A.E., Cushman, S.W., and Periwal, V. 2009. Hypertrophy and/or Hyperplasia: Dynamics of Adipose Tissue Growth. *PLoS Comput Biol* 5:e1000324.
4. Barsh, G.S., Farooqi, I.S., and O'Rahilly, S. 2000. Genetics of body-weight regulation. *Nature* 404:644-651.
5. Marti, A., Martinez-Gonzalez, M.A., and Martinez, J.A. 2008. Interaction between genes and lifestyle factors on obesity. *Proc Nutr Soc* 67:1-8.
6. Johnson, P.R., and Hirsch, J. 1972. Cellularity of adipose depots in six strains of genetically obese mice. *J Lipid Res* 13:2-11.
7. Drolet, R., Richard, C., Sniderman, A.D., Mailloux, J., Fortier, M., Huot, C., Rheaume, C., and Tchernof, A. 2008. Hypertrophy and hyperplasia of abdominal adipose tissues in women. *Int J Obes (Lond)* 32:283-291.
8. Spalding, K.L., Arner, E., Westermark, P.O., Bernard, S., Buchholz, B.A., Bergmann, O., Blomqvist, L., Hoffstedt, J., Naslund, E., Britton, T., *et al*. 2008. Dynamics of fat cell turnover in humans. *Nature* 453:783-787.
9. Faust, I.M., Johnson, P.R., Stern, J.S., and Hirsch, J. 1978. Diet-induced adipocyte number increase in adult rats: a new model of obesity. *Am J Physiol* 235:E279-286.
10. Bornstein, S.R., Abu-Asab, M., Glasow, A., Path, G., Hauner, H., Tsokos, M., Chrousos, G.P., and Scherbaum, W.A. 2000. Immunohistochemical and ultrastructural localization of leptin and leptin receptor in human white adipose tissue and differentiating human adipose cells in primary culture. *Diabetes* 49:532-538.
11. Xu, H., Barnes, G.T., Yang, Q., Tan, G., Yang, D., Chou, C.J., Sole, J., Nichols, A., Ross, J.S., Tartaglia, L.A., *et al*. 2003. Chronic inflammation in fat plays a crucial role in the development of obesity-related insulin resistance. *J Clin Invest* 112:1821-1830.

12. Weisberg, S.P., McCann, D., Desai, M., Rosenbaum, M., Leibel, R.L., and Ferrante, A.W., Jr. 2003. Obesity is associated with macrophage accumulation in adipose tissue. *J Clin Invest* 112:1796-1808.
13. Hotamisligil, G.S., Shargill, N.S., and Spiegelman, B.M. 1993. Adipose expression of tumor necrosis factor-alpha: direct role in obesity-linked insulin resistance. *Science* 259:87-91.
14. Zhang, Y., Proenca, R., Maffei, M., Barone, M., Leopold, L., and Friedman, J.M. 1994. Positional cloning of the mouse obese gene and its human homologue. *Nature* 372:425-432.
15. Lonnqvist, F., Arner, P., Nordfors, L., and Schalling, M. 1995. Overexpression of the obese (ob) gene in adipose tissue of human obese subjects. *Nat Med* 1:950-953.
16. Hauner, H. 2004. The new concept of adipose tissue function. *Physiol Behav* 83:653-658.
17. Bastard, J.P., Jardel, C., Bruckert, E., Vidal, H., and Hainque, B. 2000. Variations in plasma soluble tumour necrosis factor receptors after diet-induced weight loss in obesity. *Diabetes Obes Metab* 2:323-325.
18. Festa, A., D'Agostino, R., Jr., Williams, K., Karter, A.J., Mayer-Davis, E.J., Tracy, R.P., and Haffner, S.M. 2001. The relation of body fat mass and distribution to markers of chronic inflammation. *Int J Obes Relat Metab Disord* 25:1407-1415.
19. Meier, C.A., Bobbioni, E., Gabay, C., Assimacopoulos-Jeannet, F., Golay, A., and Dayer, J.M. 2002. IL-1 receptor antagonist serum levels are increased in human obesity: a possible link to the resistance to leptin? *J Clin Endocrinol Metab* 87:1184-1188.
20. Bullo, M., Garcia-Lorda, P., Megias, I., and Salas-Salvado, J. 2003. Systemic inflammation, adipose tissue tumor necrosis factor, and leptin expression. *Obes Res* 11:525-531.
21. Hanusch-Enserer, U., Cauza, E., Spak, M., Dunky, A., Rosen, H.R., Wolf, H., Prager, R., and Eibl, M.M. 2003. Acute-phase response and immunological markers in morbid obese patients and patients following adjustable gastric banding. *Int J Obes Relat Metab Disord* 27:355-361.
22. Field, A.E., Coakley, E.H., Must, A., Spadano, J.L., Laird, N., Dietz, W.H., Rimm, E., and Colditz, G.A. 2001. Impact of overweight on the risk of developing common chronic diseases during a 10-year period. *Arch Intern Med* 161:1581-1586.

23. Visscher, T.L., and Seidell, J.C. 2001. The public health impact of obesity. *Annu Rev Public Health* 22:355-375.

24. Ford, E.S., Williamson, D.F., and Liu, S. 1997. Weight change and diabetes incidence: findings from a national cohort of US adults. *Am J Epidemiol* 146:214-222.

25. Zimmet, P., Alberti, K.G., and Shaw, J. 2001. Global and societal implications of the diabetes epidemic. *Nature* 414:782-787.

26. Pickup, J.C., Mattock, M.B., Chusney, G.D., and Burt, D. 1997. NIDDM as a disease of the innate immune system: association of acute-phase reactants and interleukin-6 with metabolic syndrome X. *Diabetologia* 40:1286-1292.

27. Feinstein, R., Kanety, H., Papa, M.Z., Lunenfeld, B., and Karasik, A. 1993. Tumor necrosis factor-alpha suppresses insulin-induced tyrosine phosphorylation of insulin receptor and its substrates. *J Biol Chem* 268:26055-26058.

28. Obeid, L.M., Linardic, C.M., Karolak, L.A., and Hannun, Y.A. 1993. Programmed cell death induced by ceramide. *Science* 259:1769-1771.

29. Unger, R.H., and Orci, L. 2002. Lipoapoptosis: its mechanism and its diseases. *Biochim Biophys Acta* 1585:202-212.

30. Kamata, H., Honda, S., Maeda, S., Chang, L., Hirata, H., and Karin, M. 2005. Reactive oxygen species promote TNFalpha-induced death and sustained JNK activation by inhibiting MAP kinase phosphatases. *Cell* 120:649-661.

31. Dominguez, H., Storgaard, H., Rask-Madsen, C., Steffen Hermann, T., Ihlemann, N., Baunbjerg Nielsen, D., Spohr, C., Kober, L., Vaag, A., and Torp-Pedersen, C. 2005. Metabolic and vascular effects of tumor necrosis factor-alpha blockade with etanercept in obese patients with type 2 diabetes. *J Vasc Res* 42:517-525.

32. Aljada, A., Ghanim, H., Saadeh, R., and Dandona, P. 2001. Insulin inhibits NFkappaB and MCP-1 expression in human aortic endothelial cells. *J Clin Endocrinol Metab* 86:450-453.

33. Sartipy, P., and Loskutoff, D.J. 2003. Monocyte chemoattractant protein 1 in obesity and insulin resistance. *Proc Natl Acad Sci U S A* 100:7265-7270.

34. Kanda, H., Tateya, S., Tamori, Y., Kotani, K., Hiasa, K., Kitazawa, R., Kitazawa, S., Miyachi, H., Maeda, S., Egashira, K., *et al*. 2006. MCP-1 contributes to macrophage infiltration into adipose tissue, insulin resistance, and hepatic steatosis in obesity. *J Clin Invest* 116:1494-1505.

35. Krook, A. 2008. IL-6 and metabolism-new evidence and new questions. *Diabetologia* 51:1097-1099.

36. Rotter, V., Nagaev, I., and Smith, U. 2003. Interleukin-6 (IL-6) induces insulin resistance in 3T3-L1 adipocytes and is, like IL-8 and tumor necrosis factor-alpha, overexpressed in human fat cells from insulin-resistant subjects. *J Biol Chem* 278:45777-45784.

37. Wallenius, V., Wallenius, K., Ahren, B., Rudling, M., Carlsten, H., Dickson, S.L., Ohlsson, C., and Jansson, J.O. 2002. Interleukin-6-deficient mice develop mature-onset obesity. *Nat Med* 8:75-79.

38. Houseknecht, K.L., Baile, C.A., Matteri, R.L., and Spurlock, M.E. 1998. The biology of leptin: a review. *J Anim Sci* 76:1405-1420.

39. Fei, H., Okano, H.J., Li, C., Lee, G.H., Zhao, C., Darnell, R., and Friedman, J.M. 1997. Anatomic localization of alternatively spliced leptin receptors (Ob-R) in mouse brain and other tissues. *Proc Natl Acad Sci U S A* 94:7001-7005.

40. Hamann, A., and Matthaei, S. 1996. Regulation of energy balance by leptin. *Exp Clin Endocrinol Diabetes* 104:293-300.

41. Kamohara, S., Burcelin, R., Halaas, J.L., Friedman, J.M., and Charron, M.J. 1997. Acute stimulation of glucose metabolism in mice by leptin treatment. *Nature* 389:374-377.

42. Minokoshi, Y., Kim, Y.B., Peroni, O.D., Fryer, L.G., Muller, C., Carling, D., and Kahn, B.B. 2002. Leptin stimulates fatty-acid oxidation by activating AMP-activated protein kinase. *Nature* 415:339-343.

43. Meurer, R., Van Riper, G., Feeney, W., Cunningham, P., Hora, D., Jr., Springer, M.S., MacIntyre, D.E., and Rosen, H. 1993. Formation of eosinophilic and monocytic intradermal inflammatory sites in the dog by injection of human RANTES but not human monocyte chemoattractant protein 1, human macrophage inflammatory protein 1 alpha, or human interleukin 8. *J Exp Med* 178:1913-1921.

44. Schall, T.J., Bacon, K., Toy, K.J., and Goeddel, D.V. 1990. Selective attraction of monocytes and T lymphocytes of the memory phenotype by cytokine RANTES. *Nature* 347:669-671.

45. Conti, P., Reale, M., Barbacane, R.C., Letourneau, R., and Theoharides, T.C. 1998. Intramuscular injection of hrRANTES causes mast cell recruitment and increased transcription of histidine decarboxylase in mice: lack of effects in genetically mast cell-deficient W/WV mice. *FASEB J* 12:1693-1700.

46. Das, A.M., Ajuebor, M.N., Flower, R.J., Perretti, M., and McColl, S.R. 1999. Contrasting roles for RANTES and macrophage inflammatory protein-1 alpha (MIP-1 alpha) in a murine model of allergic peritonitis. *Clin Exp Immunol* 117:223-229.

47. Struyf, S., Menten, P., Lenaerts, J.P., Put, W., D'Haese, A., De Clercq, E., Schols, D., Proost, P., and Van Damme, J. 2001. Diverging binding capacities of natural LD78beta isoforms of macrophage inflammatory protein-1alpha to the CC chemokine receptors 1, 3 and 5 affect their anti-HIV-1 activity and chemotactic potencies for neutrophils and eosinophils. *Eur J Immunol* 31:2170-2178.

48. Daugherty, B.L., Siciliano, S.J., DeMartino, J.A., Malkowitz, L., Sirotina, A., and Springer, M.S. 1996. Cloning, expression, and characterization of the human eosinophil eotaxin receptor. *J Exp Med* 183:2349-2354.

49. Madani, R., Karastergiou, K., Ogston, N.C., Miheisi, N., Bhome, R., Haloob, N., Tan, G.D., Karpe, F., Malone-Lee, J., Hashemi, M., *et al*. 2009. RANTES release by human adipose tissue *in vivo* and evidence for depot-specific differences. *Am J Physiol Endocrinol Metab* 296:E1262-1268.

50. Skurk, T., Mack, I., Kempf, K., Kolb, H., Hauner, H., and Herder, C. 2009. Expression and secretion of RANTES (CCL5) in human adipocytes in response to immunological stimuli and hypoxia. *Horm Metab Res* 41:183-189.

51. Wu, H., Ghosh, S., Perrard, X.D., Feng, L., Garcia, G.E., Perrard, J.L., Sweeney, J.F., Peterson, L.E., Chan, L., Smith, C.W., *et al*. 2007. T-cell accumulation and regulated on activation, normal T cell expressed and secreted upregulation in adipose tissue in obesity. *Circulation* 115:1029-1038.

52. Keophiphath, M., Rouault, C., Divoux, A., Clement, K., and Lacasa, D. CCL5 promotes macrophage recruitment and survival in human adipose tissue. *Arterioscler Thromb Vasc Biol* 30:39-45.

53. Herder, C., Haastert, B., Muller-Scholze, S., Koenig, W., Thorand, B., Holle, R., Wichmann, H.E., Scherbaum, W.A., Martin, S., and Kolb, H. 2005. Association of systemic chemokine concentrations with impaired glucose tolerance and type 2 diabetes: results from the Cooperative Health Research in the Region of Augsburg Survey S4 (KORA S4). *Diabetes* 54 Suppl 2:S11-17.

54. Paul, M., Poyan Mehr, A., and Kreutz, R. 2006. Physiology of local renin-angiotensin systems. *Physiol Rev* 86:747-803.

55. Karlsson, C., Lindell, K., Ottosson, M., Sjostrom, L., Carlsson, B., and Carlsson, L.M. 1998. Human adipose tissue expresses angiotensinogen and enzymes required for its conversion to angiotensin II. *J Clin Endocrinol Metab* 83:3925-3929.

56. Hirasawa, K., Sato, Y., Hosoda, Y., Yamamoto, T., and Hanai, H. 2002. Immunohistochemical localization of angiotensin II receptor and local renin-angiotensin system in human colonic mucosa. *J Histochem Cytochem* 50:275-282.

57. Park, W.K., Regoli, D., and Rioux, F. 1973. Characterization of angiotensin receptors in vascular and intestinal smooth muscles. *Br J Pharmacol* 48:288-301.

58. Yvan-Charvet, L., and Quignard-Boulange, A. Role of adipose tissue renin-angiotensin system in metabolic and inflammatory diseases associated with obesity. *Kidney Int* 79:162-168.

59. Chu, K.Y., Lau, T., Carlsson, P.O., and Leung, P.S. 2006. Angiotensin II type 1 receptor blockade improves beta-cell function and glucose tolerance in a mouse model of type 2 diabetes. *Diabetes* 55:367-374.

60. 1964. The constitution and properties of two gastrins extracted from hog antral mucosa: Part II The properties of two gastrins isolated from hog antral mucosa. *Gut* 5:107-117.

61. Castell, D.O. 1978. Gastrin and lower esophageal sphincter tone. *Arch Intern Med* 138:196.

62. Buffa, R., Solcia, E., and Go, V.L. 1976. Immunohistochemical identification of the cholecystokinin cell in the intestinal mucosa. *Gastroenterology* 70:528-532.

63. Liddle, R.A., Goldfine, I.D., Rosen, M.S., Taplitz, R.A., and Williams, J.A. 1985. Cholecystokinin bioactivity in human plasma. Molecular forms, responses to feeding, and relationship to gallbladder contraction. *J Clin Invest* 75:1144-1152.

64. Asin, K.E., Bednarz, L., Nikkel, A.L., Gore, P.A., Jr., and Nadzan, A.M. 1992. A-71623, a selective CCK-A receptor agonist, suppresses food intake in the mouse, dog, and monkey. *Pharmacol Biochem Behav* 42:699-704.

65. Moran, T.H. 2000. Cholecystokinin and satiety: current perspectives. *Nutrition* 16:858-865.

66. Kojima, M., Hosoda, H., Date, Y., Nakazato, M., Matsuo, H., and Kangawa, K. 1999. Ghrelin is a growth-hormone-releasing acylated peptide from stomach. *Nature* 402:656-660.

67. Date, Y., Murakami, N., Toshinai, K., Matsukura, S., Niijima, A., Matsuo, H., Kangawa, K., and Nakazato, M. 2002. The role of the gastric afferent vagal nerve

in ghrelin-induced feeding and growth hormone secretion in rats. *Gastroenterology* 123:1120-1128.

68. Bado, A., Levasseur, S., Attoub, S., Kermorgant, S., Laigneau, J.P., Bortoluzzi, M.N., Moizo, L., Lehy, T., Guerre-Millo, M., Le Marchand-Brustel, Y., *et al*. 1998. The stomach is a source of leptin. *Nature* 394:790-793.
69. Hacki, W.H. 1980. Secretin. *Clin Gastroenterol* 9:609-632.
70. Dupre, J., Ross, S.A., Watson, D., and Brown, J.C. 1973. Stimulation of insulin secretion by gastric inhibitory polypeptide in man. *J Clin Endocrinol Metab* 37:826-828.
71. Parker, H.E., Habib, A.M., Rogers, G.J., Gribble, F.M., and Reimann, F. 2009. Nutrient-dependent secretion of glucose-dependent insulinotropic polypeptide from primary murine K cells. *Diabetologia* 52:289-298.
72. Ehses, J.A., Casilla, V.R., Doty, T., Pospisilik, J.A., Winter, K.D., Demuth, H.U., Pederson, R.A., and McIntosh, C.H. 2003. Glucose-dependent insulinotropic polypeptide promotes beta-(INS-1) cell survival via cyclic adenosine monophosphate-mediated caspase-3 inhibition and regulation of p38 mitogen-activated protein kinase. *Endocrinology* 144:4433-4445.
73. Trumper, A., Trumper, K., and Horsch, D. 2002. Mechanisms of mitogenic and anti-apoptotic signaling by glucose-dependent insulinotropic polypeptide in beta(INS-1)-cells. *J Endocrinol* 174:233-246.
74. Trumper, A., Trumper, K., Trusheim, H., Arnold, R., Goke, B., and Horsch, D. 2001. Glucose-dependent insulinotropic polypeptide is a growth factor for beta (INS-1) cells by pleiotropic signaling. *Mol Endocrinol* 15:1559-1570.
75. Adrian, T.E., Ferri, G.L., Bacarese-Hamilton, A.J., Fuessl, H.S., Polak, J.M., and Bloom, S.R. 1985. Human distribution and release of a putative new gut hormone, peptide YY. *Gastroenterology* 89:1070-1077.
76. Batterham, R.L., Cowley, M.A., Small, C.J., Herzog, H., Cohen, M.A., Dakin, C.L., Wren, A.M., Brynes, A.E., Low, M.J., Ghatei, M.A., *et al*. 2002. Gut hormone PYY(3-36) physiologically inhibits food intake. *Nature* 418:650-654.
77. Van Citters, G.W., and Lin, H.C. 2006. Ileal brake: neuropeptidergic control of intestinal transit. *Curr Gastroenterol Rep* 8:367-373.
78. Mojsov, S., Heinrich, G., Wilson, I.B., Ravazzola, M., Orci, L., and Habener, J.F. 1986. Preproglucagon gene expression in pancreas and intestine diversifies at the level of post-translational processing. *J Biol Chem* 261:11880-11889.

79. Drucker, D.J. 2001. Minireview: the glucagon-like peptides. *Endocrinology* 142:521-527.

80. Drucker, D.J. 2002. Biological actions and therapeutic potential of the glucagon-like peptides. *Gastroenterology* 122:531-544.

81. Drucker, D.J., Erlich, P., Asa, S.L., and Brubaker, P.L. 1996. Induction of intestinal epithelial proliferation by glucagon-like peptide 2. *Proc Natl Acad Sci U S A* 93:7911-7916.

82. Jeppesen, P.B., Hartmann, B., Thulesen, J., Graff, J., Lohmann, J., Hansen, B.S., Tofteng, F., Poulsen, S.S., Madsen, J.L., Holst, J.J., *et al*. 2001. Glucagon-like peptide 2 improves nutrient absorption and nutritional status in short-bowel patients with no colon. *Gastroenterology* 120:806-815.

83. Meier, J.J., Nauck, M.A., Pott, A., Heinze, K., Goetze, O., Bulut, K., Schmidt, W.E., Gallwitz, B., and Holst, J.J. 2006. Glucagon-like peptide 2 stimulates glucagon secretion, enhances lipid absorption, and inhibits gastric acid secretion in humans. *Gastroenterology* 130:44-54.

84. McIntyre, N., Holdsworth, C.D., and Turner, D.S. 1964. New Interpretation of Oral Glucose Tolerance. *Lancet* 2:20-21.

85. Holst, J.J., and Gromada, J. 2004. Role of incretin hormones in the regulation of insulin secretion in diabetic and nondiabetic humans. *Am J Physiol Endocrinol Metab* 287:E199-206.

86. Kreymann, B., Williams, G., Ghatei, M.A., and Bloom, S.R. 1987. Glucagon-like peptide-1 7-36: a physiological incretin in man. *Lancet* 2:1300-1304.

87. Parker, H., Habib, A., Rogers, G., Gribble, F., and Reimann, F. 2009. Nutrient-dependent secretion of glucose-dependent insulinotropic polypeptide from primary murine K cells. *Diabetologia* 52:289-298.

88. Rolf, M., Baptist, G., and Wolfgang, E.S. 1993. Dipeptidyl-peptidase IV hydrolyses gastric inhibitory polypeptide, glucagon-like peptide-1(7–36)amide, peptide histidine methionine and is responsible for their degradation in human serum. *European Journal of Biochemistry* 214:829-835.

89. Cataland, S., Crockett, S.E., Brown, J.C., and Mazzaferri, E.L. 1974. Gastric Inhibitory Polypeptide (GIP) Stimulation by Oral Glucose in Man. *J Clin Endocrinol Metab* 39:223-228.

90. Sirinek, K., Crockett, S., Mazzaferri, E., Cataland, S., and Thomford, N. 1974. Release of gastric inhibitory polypeptide: comparison of glucose and fat as stimuli. *Surg Forum* 25:361-363.

91. Dupre, J., Ross, S.A., Watson, D., and Brown, J.C. 1973. STIMULATION OF INSULIN SECRETION BY GASTRIC INHIBITORY POLYPEPTIDE IN MAN. *J Clin Endocrinol Metab* 37:826-828.

92. Trumper, A., Trumper, K., and Horsch, D. 2002. Mechanisms of mitogenic and anti-apoptotic signaling by glucose-dependent insulinotropic polypeptide in beta(INS-1)-cells. *J Endocrinol* 174:233-246.

93. Trumper, A., Trumper, K., Trusheim, H., Arnold, R., Goke, B., and Horsch, D. 2001. Glucose-Dependent Insulinotropic Polypeptide Is a Growth Factor for {beta} (INS-1) Cells by Pleiotropic Signaling. *Mol Endocrinol* 15:1559-1570.

94. Ehses, J.A., Casilla, V.R., Doty, T., Pospisilik, J.A., Winter, K.D., Demuth, H.-U., Pederson, R.A., and McIntosh, C.H.S. 2003. Glucose-Dependent Insulinotropic Polypeptide Promotes {beta}-(INS-1) Cell Survival via Cyclic Adenosine Monophosphate-Mediated Caspase-3 Inhibition and Regulation of p38 Mitogen-Activated Protein Kinase. *Endocrinology* 144:4433-4445.

95. Nyberg, J., Anderson, M.F., Meister, B., Alborn, A.-M., Strom, A.-K., Brederlau, A., Illerskog, A.-C., Nilsson, O., Kieffer, T.J., Hietala, M.A., *et al*. 2005. Glucose-Dependent Insulinotropic Polypeptide Is Expressed in Adult Hippocampus and Induces Progenitor Cell Proliferation. *J. Neurosci.* 25:1816-1825.

96. Tsukiyama, K., Yamada, Y., Yamada, C., Harada, N., Kawasaki, Y., Ogura, M., Bessho, K., Li, M., Amizuka, N., Sato, M., *et al*. 2006. Gastric Inhibitory Polypeptide as an Endogenous Factor Promoting New Bone Formation after Food Ingestion. *Mol Endocrinol* 20:1644-1651.

97. Miyawaki, K. 2002. Inhibition of gastric inhibitory polypeptide signaling prevents obesity. *Nature Medicine* 8:738 - 742.

98. Yip, R.G., Boylan, M.O., Kieffer, T.J., and Wolfe, M.M. 1998. Functional GIP receptors are present on adipocytes. *Endocrinology* 139:4004-4007.

99. Weaver, R.E., Donnelly, D., Wabitsch, M., Grant, P.J., and Balmforth, A.J. 2008. Functional expression of glucose-dependent insulinotropic polypeptide receptors is coupled to differentiation in a human adipocyte model. *Int J Obes (Lond)* 32:1705-1711.

100. Asmar, M., Simonsen, L., Madsbad, S., Stallknecht, B., Holst, J.J., and Bulow, J. Glucose-dependent insulinotropic polypeptide may enhance fatty acid re-esterification in subcutaneous abdominal adipose tissue in lean humans. *Diabetes* 59:2160-2163.

101. Ebert, R., Nauck, M., and Creutzfeldt, W. 1991. Effect of exogenous or endogenous gastric inhibitory polypeptide (GIP) on plasma triglyceride responses in rats. *Horm Metab Res* 23:517-521.

102. Hauner, H., Glatting, G., Kaminska, D., and Pfeiffer, E.F. 1988. Effects of gastric inhibitory polypeptide on glucose and lipid metabolism of isolated rat adipocytes. *Ann Nutr Metab* 32:282-288.

103. Kindmark, H., Pigon, J., and Efendic, S. 2001. Glucose-dependent insulinotropic hormone potentiates the hypoglycemic effect of glibenclamide in healthy volunteers: evidence for an effect on insulin extraction. *J Clin Endocrinol Metab* 86:2015-2019.

104. Elliott, R. 1993. Glucagon-like peptide -1 (7-36) amide and glucose-dependent insulinotropic polypeptide secretion in response to nutrient ingertion in man: acute post-prandial and 24-h secretion patterns. *J Endocrinol* 138:159-166.

105. Herrmann, H. 1995. Glucago-like peptide-1 and glucose-dependent insulin-releasing polypeptide plasma levels in response ton nutrients. *Digestion* 56:117-126.

106. Cani, P., Holst, J., Drucker, D., Delzenne, N., Thorens, B., Burcelin, R., and Knauf, C. 2007. GLUT2 and the incretin receptors are involved in glucose-induced incretin secretion. *Mol Cekk Endocrinol* 276(1-2):18-23.

107. Merida, E., Delgado, E., Molina, L.M., Villanueva-Penacarrillo, M.L., and Valverde, I. 1993. Presence of glucagon and glucagon-like peptide-1-(7-36)amide receptors in solubilized membranes of human adipose tissue. *J Clin Endocrinol Metab* 77:1654-1657.

108. Fehmann, H., Jiang, J., Pitt, D., Schweinfurth, J., and Göke, B. 1996. Ligand-induced regulation of glucagon-like peptide-I receptor function and expression in insulin-secreting beta cells. *Pancreas* 13:273-282.

109. Turton, M., O'Shea, D., Gunn, I., Beak, S., Edwards, C., Meeran, K., Choi, S., Taylor, G., Heath, M., Lambert, P., *et al*. 1996. A role for glucagon-like peptide-1 in the central regulation of feeding. *Nature* 379:69-72.

110. Verdich, C., Flint, A., Gutzwiller, J.P., Naslund, E., Beglinger, C., Hellstrom, P.M., Long, S.J., Morgan, L.M., Holst, J.J., and Astrup, A. 2001. A Meta-Analysis of the Effect of Glucagon-Like Peptide-1 (7-36) Amide on Ad Libitum Energy Intake in Humans. *J Clin Endocrinol Metab* 86:4382-4389.

111. Näslund, E., King, N., Mansten, S., Adner, N., Holst, J., Mutniak, G., and Hellström, P. 2004. Prandial subcutaneous injections of glucagon-like peptide-1 cause weight loss in obese human subjects. *Br J Nutr* 91:439-446.

112. Salvatore, T., Carbonara, O., Cozzolino, D., Torella, R., and Sasso, F. 2009. Progress in the oral treatment of type 2 diabetes: update on DPP-IV inhibitors. *Curr Diabetes Rev* 5:92-101.

113. Drucker, D.J. 2006. The biology of incretin hormones. *Cell Metab* 3:153-165.

114. Baggio, L.L., and Drucker, D.J. 2007. Biology of incretins: GLP-1 and GIP. *Gastroenterology* 132:2131-2157.

115. Nauck, M., Stockmann, F., Ebert, R., and Creutzfeldt, W. 1986. Reduced incretin effect in type 2 (non-insulin-dependent) diabetes. *Diabetologia* 29:46-52.

116. Toft-Nielsen, M.B., Damholt, M.B., Madsbad, S., Hilsted, L.M., Hughes, T.E., Michelsen, B.K., and Holst, J.J. 2001. Determinants of the impaired secretion of glucagon-like peptide-1 in type 2 diabetic patients. *J Clin Endocrinol Metab* 86:3717-3723.

117. Vilsboll, T., Knop, F.K., Krarup, T., Johansen, A., Madsbad, S., Larsen, S., Hansen, T., Pedersen, O., and Holst, J.J. 2003. The pathophysiology of diabetes involves a defective amplification of the late-phase insulin response to glucose by glucose-dependent insulinotropic polypeptide-regardless of etiology and phenotype. *J Clin Endocrinol Metab* 88:4897-4903.

118. Kjems, L.L., Holst, J.J., Volund, A., and Madsbad, S. 2003. The influence of GLP-1 on glucose-stimulated insulin secretion: effects on beta-cell sensitivity in type 2 and nondiabetic subjects. *Diabetes* 52:380-386.

119. Vaag, A.A., Holst, J.J., Volund, A., and Beck-Nielsen, H.B. 1996. Gut incretin hormones in identical twins discordant for non-insulin-dependent diabetes mellitus (NIDDM)--evidence for decreased glucagon-like peptide 1 secretion during oral glucose ingestion in NIDDM twins. *Eur J Endocrinol* 135:425-432.

120. Nyholm, B., Walker, M., Gravholt, C.H., Shearing, P.A., Sturis, J., Alberti, K.G., Holst, J.J., and Schmitz, O. 1999. Twenty-four-hour insulin secretion rates, circulating concentrations of fuel substrates and gut incretin hormones in healthy

offspring of Type II (non-insulin-dependent) diabetic parents: evidence of several aberrations. *Diabetologia* 42:1314-1323.

121. Vilsboll, T., Krarup, T., Deacon, C.F., Madsbad, S., and Holst, J.J. 2001. Reduced postprandial concentrations of intact biologically active glucagon-like peptide 1 in type 2 diabetic patients. *Diabetes* 50:609-613.
122. Vilsboll, T., Agerso, H., Krarup, T., and Holst, J.J. 2003. Similar elimination rates of glucagon-like peptide-1 in obese type 2 diabetic patients and healthy subjects. *J Clin Endocrinol Metab* 88:220-224.
123. Ranganath, L.R., Beety, J.M., Morgan, L.M., Wright, J.W., Howland, R., and Marks, V. 1996. Attenuated GLP-1 secretion in obesity: cause or consequence? *Gut* 38:916-919.
124. le Roux, C.W., Aylwin, S.J., Batterham, R.L., Borg, C.M., Coyle, F., Prasad, V., Shurey, S., Ghatei, M.A., Patel, A.G., and Bloom, S.R. 2006. Gut hormone profiles following bariatric surgery favor an anorectic state, facilitate weight loss, and improve metabolic parameters. *Ann Surg* 243:108-114.
125. Vincent, R.P., and le Roux, C.W. 2008. Changes in gut hormones after bariatric surgery. *Clin Endocrinol (Oxf)* 69:173-179.
126. Lugari, R., Dei Cas, A., Ugolotti, D., Barilli, A.L., Camellini, C., Ganzerla, G.C., Luciani, A., Salerni, B., Mittenperger, F., Nodari, S., *et al*. 2004. Glucagon-like peptide 1 (GLP-1) secretion and plasma dipeptidyl peptidase IV (DPP-IV) activity in morbidly obese patients undergoing biliopancreatic diversion. *Horm Metab Res* 36:111-115.
127. Carr, R.D., Larsen, M.O., Jelic, K., Lindgren, O., Vikman, J., Holst, J.J., Deacon, C.F., and Ahren, B. Secretion and dipeptidyl peptidase-4-mediated metabolism of incretin hormones after a mixed meal or glucose ingestion in obese compared to lean, nondiabetic men. *J Clin Endocrinol Metab* 95:872-878.
128. Ranganath, L., Norris, F., Morgan, L., Wright, J., and Marks, V. 1999. Inhibition of carbohydrate-mediated glucagon-like peptide-1 (7-36)amide secretion by circulating non-esterified fatty acids. *Clin Sci (Lond)* 96:335-342.
129. Goke, B., Herrmann, C., Goke, R., Fehmann, H.C., Berghofer, P., Richter, G., and Arnold, R. 1994. Intestinal effects of alpha-glucosidase inhibitors: absorption of nutrients and enterohormonal changes. *Eur J Clin Invest* 24 Suppl 3:25-30.

130. Besterman, H.S., Bloom, S.R., Sarson, D.L., Blackburn, A.M., Johnston, D.I., Patel, H.R., Stewart, J.S., Modigliani, R., Guerin, S., and Mallinson, C.N. 1978. Gut-hormone profile in coeliac disease. *Lancet* 1:785-788.

131. Reimann, F., Habib, A.M., Tolhurst, G., Parker, H.E., Rogers, G.J., and Gribble, F.M. 2008. Glucose sensing in L cells: a primary cell study. *Cell Metab* 8:532-539.

132. Reimann, F., and Gribble, F.M. 2002. Glucose-sensing in glucagon-like peptide-1-secreting cells. *Diabetes* 51:2757-2763.

133. Rogers, G.J., Tolhurst, G., Ramzan, A., Habib, A.M., Parker, H.E., Gribble, F.M., and Reimann, F. Electrical activity-triggered glucagon-like peptide-1 secretion from primary murine L-cells. *J Physiol* 589:1081-1093.

134. Tolhurst, G., Heffron, H., Lam, Y.S., Parker, H.E., Habib, A.M., Diakogiannaki, E., Cameron, J., Grosse, J., Reimann, F., and Gribble, F.M. Short-Chain Fatty Acids Stimulate Glucagon-Like Peptide-1 Secretion via the G-Protein-Coupled Receptor FFAR2. *Diabetes*.

135. Tolhurst, G., Zheng, Y., Parker, H.E., Habib, A.M., Reimann, F., and Gribble, F.M. Glutamine triggers and potentiates glucagon-like peptide-1 secretion by raising cytosolic Ca2+ and cAMP. *Endocrinology* 152:405-413.

136. Elliott, R.M., Morgan, L.M., Tredger, J.A., Deacon, S., Wright, J., and Marks, V. 1993. Glucagon-like peptide-1 (7-36)amide and glucose-dependent insulinotropic polypeptide secretion in response to nutrient ingestion in man: acute post-prandial and 24-h secretion patterns. *J Endocrinol* 138:159-166.

137. Nielsen, L.B., Ploug, K.B., Swift, P., Orskov, C., Jansen-Olesen, I., Chiarelli, F., Holst, J.J., Hougaard, P., Porksen, S., Holl, R., *et al*. 2007. Co-localisation of the Kir6.2/SUR1 channel complex with glucagon-like peptide-1 and glucose-dependent insulinotrophic polypeptide expression in human ileal cells and implications for glycaemic control in new onset type 1 diabetes. *Eur J Endocrinol* 156:663-671.

138. Ma, J., Chang, J., Checklin, H.L., Young, R.L., Jones, K.L., Horowitz, M., and Rayner, C.K. Effect of the artificial sweetener, sucralose, on small intestinal glucose absorption in healthy human subjects. *Br J Nutr* 104:803-806.

139. Flatt, P.R., Kwasowski, P., and Bailey, C.J. 1989. Stimulation of gastric inhibitory polypeptide release in ob/ob mice by oral administration of sugars and their analogues. *J Nutr* 119:1300-1303.

140. Kokrashvili, Z., Mosinger, B., and Margolskee, R.F. 2009. T1r3 and α-Gustducin in Gut Regulate Secretion of Glucagon-like Peptide-1. *Annals of the New York Academy of Sciences* 1170:91-94.

141. Wong, G.T., Gannon, K.S., and Margolskee, R.F. 1996. Transduction of bitter and sweet taste by gustducin. *Nature* 381:796-800.

142. Dyer, J., Salmon, K.S., Zibrik, L., and Shirazi-Beechey, S.P. 2005. Expression of sweet taste receptors of the T1R family in the intestinal tract and enteroendocrine cells. *Biochem Soc Trans* 33:302-305.

143. Rozengurt, N., Wu, S.V., Chen, M.C., Huang, C., Sternini, C., and Rozengurt, E. 2006. Colocalization of the alpha-subunit of gustducin with PYY and GLP-1 in L cells of human colon. *Am J Physiol Gastrointest Liver Physiol* 291:G792-802.

144. Jang, H.J., Kokrashvili, Z., Theodorakis, M.J., Carlson, O.D., Kim, B.J., Zhou, J., Kim, H.H., Xu, X., Chan, S.L., Juhaszova, M., *et al*. 2007. Gut-expressed gustducin and taste receptors regulate secretion of glucagon-like peptide-1. *Proc Natl Acad Sci U S A* 104:15069-15074.

145. Ma, J., Bellon, M., Wishart, J.M., Young, R., Blackshaw, L.A., Jones, K.L., Horowitz, M., and Rayner, C.K. 2009. Effect of the artificial sweetener, sucralose, on gastric emptying and incretin hormone release in healthy subjects. *Am J Physiol Gastrointest Liver Physiol* 296:G735-739.

146. Moriya, R., Shirakura, T., Ito, J., Mashiko, S., and Seo, T. 2009. Activation of sodium-glucose cotransporter 1 ameliorates hyperglycemia by mediating incretin secretion in mice. *Am J Physiol Endocrinol Metab* 297:E1358-1365.

147. Gribble, F.M., Williams, L., Simpson, A.K., and Reimann, F. 2003. A novel glucose-sensing mechanism contributing to glucagon-like peptide-1 secretion from the GLUTag cell line. *Diabetes* 52:1147-1154.

148. Gorboulev, V., Schurmann, A., Vallon, V., Kipp, H., Jaschke, A., Klessen, D., Friedrich, A., Scherneck, S., Rieg, T., Cunard, R., *et al*. Na+-D-glucose Cotransporter SGLT1 is Pivotal for Intestinal Glucose Absorption and Glucose-Dependent Incretin Secretion. *Diabetes* 61:187-196.

149. Rocca, A.S., and Brubaker, P.L. 1995. Stereospecific effects of fatty acids on proglucagon-derived peptide secretion in fetal rat intestinal cultures. *Endocrinology* 136:5593-5599.

150. Briscoe, C.P., Tadayyon, M., Andrews, J.L., Benson, W.G., Chambers, J.K., Eilert, M.M., Ellis, C., Elshourbagy, N.A., Goetz, A.S., Minnick, D.T., *et al*. 2003. The

Orphan G Protein-coupled Receptor GPR40 Is Activated by Medium and Long Chain Fatty Acids. *Journal of Biological Chemistry* 278:11303-11311.

151. Itoh, Y., Kawamata, Y., Harada, M., Kobayashi, M., Fujii, R., Fukusumi, S., Ogi, K., Hosoya, M., Tanaka, Y., Uejima, H., *et al*. 2003. Free fatty acids regulate insulin secretion from pancreatic [beta] cells through GPR40. *Nature* 422:173-176.
152. Reimann, F., Habib, A., Tolhurst, G., Parker, H., Rogers, G., and Gribble, F. 2008. Glucose sensing in L cells: a primary cell study. *Cell Metabolism* 8:532-539.
153. Hara, T., Hirasawa, A., Sun, Q., Sadakane, K., Itsubo, C., Iga, T., Adachi, T., Koshimizu, T.-a., Hashimoto, T., Asakawa, Y., *et al*. 2009. Novel selective ligands for free fatty acid receptors GPR120 and GPR40. *Naunyn-Schmiedeberg's Archives of Pharmacology* 380:247-255.
154. Tazoe, H., Otomo, Y., Karaki, S.-i., Kato, I., Fukami, Y., Terasaki, M., and Kuwahara, A. 2009. Expression of short-chain fatty acid receptor GPR41 in the human colon. *Biomedical Research* 30:149-156.
155. Karaki, S.-i., Tazoe, H., Hayashi, H., Kashiwabara, H., Tooyama, K., Suzuki, Y., and Kuwahara, A. 2008. Expression of the short-chain fatty acid receptor, GPR43, in the human colon. *Journal of Molecular Histology* 39:135-142.
156. Lauffer, L.M., Iakoubov, R., and Brubaker, P.L. 2009. GPR119 Is Essential for Oleoylethanolamide-Induced Glucagon-Like Peptide-1 Secretion From the Intestinal Enteroendocrine L-Cell. *Diabetes* 58:1058-1066.
157. Kawamata, Y., Fujii, R., Hosoya, M., Harada, M., Yoshida, H., Miwa, M., Fukusumi, S., Habata, Y., Itoh, T., Shintani, Y., *et al*. 2003. A G Protein-coupled Receptor Responsive to Bile Acids. *Journal of Biological Chemistry* 278:9435-9440.
158. Chu, Z.-L., Carroll, C., Alfonso, J., Gutierrez, V., He, H., Lucman, A., Pedraza, M., Mondala, H., Gao, H., Bagnol, D., *et al*. 2008. A Role for Intestinal Endocrine Cell-Expressed G Protein-Coupled Receptor 119 in Glycemic Control by Enhancing Glucagon-Like Peptide-1 and Glucose-Dependent Insulinotropic Peptide Release. *Endocrinology* 149:2038-2047.
159. Thomas, C., Gioiello, A., Noriega, L., Strehle, A., Oury, J., Rizzo, G., Macchiarulo, A., Yamamoto, H., Mataki, C., Pruzanski, M., *et al*. 2009. TGR5-mediated bile acid sensing controls glucose homeostasis. *Cell Metab.* 10:167-177.
160. Lan, H., Vassileva, G., Corona, A., Liu, L., Baker, H., Golovko, A., Abbondanzo, S.J., Hu, W., Yang, S., Ning, Y., *et al*. 2009. GPR119 is required for physiological

regulation of glucagon-like peptide-1 secretion but not for metabolic homeostasis. *J Endocrinol* 201:219-230.

161. Thomas, F.B., Sinar, D., Mazzaferri, E.L., Cataland, S., Mekhjian, H.S., Caldwell, J.H., and Fromkes, J.J. 1978. Selective release of gastric inhibitory polypeptide by intraduodenal amino acid perfusion in man. *Gastroenterology* 74:1261-1265.
162. Thomas, F.B., Mazzaferri, E.L., Crockett, S.E., Mekhjian, H.S., Gruemer, H.D., and Cataland, S. 1976. Stimulation of secretion of gastric inhibitory polypeptide and insulin by intraduodenal amino acid perfusion. *Gastroenterology* 70:523-527.
163. Greenfield, J.R., Farooqi, I.S., Keogh, J.M., Henning, E., Habib, A.M., Blackwood, A., Reimann, F., Holst, J.J., and Gribble, F.M. 2009. Oral glutamine increases circulating glucagon-like peptide 1, glucagon, and insulin concentrations in lean, obese, and type 2 diabetic subjects. *Am J Clin Nutr* 89:106-113.
164. Reimer, R.A. 2006. Meat hydrolysate and essential amino acid-induced glucagon-like peptide-1 secretion, in the human NCI-H716 enteroendocrine cell line, is regulated by extracellular signal-regulated kinase1/2 and p38 mitogen-activated protein kinases. *J Endocrinol* 191:159-170.
165. Matsumura, K., Miki, T., Jhomori, T., Gonoi, T., and Seino, S. 2005. Possible role of PEPT1 in gastrointestinal hormone secretion. *Biochemical and Biophysical Research Communications* 336:1028-1032.
166. Darcel, N.P., Liou, A.P., Tome, D., and Raybould, H.E. 2005. Activation of Vagal Afferents in the Rat Duodenum by Protein Digests Requires PepT1. *J. Nutr.* 135:1491-1495.
167. Naif, H.M., Li, S., Alali, M., Sloane, A., Wu, L., Kelly, M., Lynch, G., Lloyd, A., and Cunningham, A.L. 1998. CCR5 expression correlates with susceptibility of maturing monocytes to human immunodeficiency virus type 1 infection. *J Virol* 72:830-836.
168. Ohara-Imaizumi, M., Aoyagi, K., Akimoto, Y., Nakamichi, Y., Nishiwaki, C., Kawakami, H., and Nagamatsu, S. 2009. Imaging exocytosis of single glucagon-like peptide-1 containing granules in a murine enteroendocrine cell line with total internal reflection fluorescent microscopy. *Biochem Biophys Res Commun* 390:16-20.
169. Anini, Y., and Brubaker, P.L. 2003. Role of leptin in the regulation of glucagon-like peptide-1 secretion. *Diabetes* 52:252-259.

170. Anini, Y., and Brubaker, P.L. 2003. Muscarinic receptors control glucagon-like peptide 1 secretion by human endocrine L cells. *Endocrinology* 144:3244-3250.

171. Reimer, R.A., Darimont, C., Gremlich, S., Nicolas-Metral, V., Ruegg, U.T., and Mace, K. 2001. A human cellular model for studying the regulation of glucagon-like peptide-1 secretion. *Endocrinology* 142:4522-4528.

172. Brubaker, P.L., Schloos, J., and Drucker, D.J. 1998. Regulation of glucagon-like peptide-1 synthesis and secretion in the GLUTag enteroendocrine cell line. *Endocrinology* 139:4108-4114.

173. Simpson, A.K., Ward, P.S., Wong, K.Y., Collord, G.J., Habib, A.M., Reimann, F., and Gribble, F.M. 2007. Cyclic AMP triggers glucagon-like peptide-1 secretion from the GLUTag enteroendocrine cell line. *Diabetologia* 50:2181-2189.

174. Friedlander, R.S., Moss, C.E., Mace, J., Parker, H.E., Tolhurst, G., Habib, A.M., Wachten, S., Cooper, D.M., Gribble, F.M., and Reimann, F. Role of phosphodiesterase and adenylate cyclase isozymes in murine colonic glucagon-like peptide 1 secreting cells. *Br J Pharmacol* 163:261-271.

175. Drucker, D.J., and Brubaker, P.L. 1989. Proglucagon gene expression is regulated by a cyclic AMP-dependent pathway in rat intestine. *Proc Natl Acad Sci U S A* 86:3953-3957.

176. Chvatchko, Y., Proudfoot, A.E., Buser, R., Juillard, P., Alouani, S., Kosco-Vilbois, M., Coyle, A.J., Nibbs, R.J., Graham, G., Offord, R.E., *et al*. 2003. Inhibition of airway inflammation by amino-terminally modified RANTES/CC chemokine ligand 5 analogues is not mediated through CCR3. *J Immunol* 171:5498-5506.

177. Ogihara, T., Asano, T., Ando, K., Chiba, Y., Sakoda, H., Anai, M., Shojima, N., Ono, H., Onishi, Y., Fujishiro, M., *et al*. 2002. Angiotensin II-induced insulin resistance is associated with enhanced insulin signaling. *Hypertension* 40:872-879.

178. Keidar, S., and Attias, J. 1997. Angiotensin II injection into mice increases the uptake of oxidized LDL by their macrophages via a proteoglycan-mediated pathway. *Biochem Biophys Res Commun* 239:63-67.

179. Holst, J.J., Knop, F.K., Vilsboll, T., Krarup, T., and Madsbad, S. Loss of incretin effect is a specific, important, and early characteristic of type 2 diabetes. *Diabetes Care* 34 Suppl 2:S251-257.

180. Orskov, C., Jeppesen, J., Madsbad, S., and Holst, J.J. 1991. Proglucagon products in plasma of noninsulin-dependent diabetics and nondiabetic controls in the fasting state and after oral glucose and intravenous arginine. *J Clin Invest* 87:415-423.

181. Crockett, S.E., Mazzaferri, E.L., and Cataland, S. 1976. Gastric inhibitory polypeptide (GIP) in maturity-onset diabetes mellitus. *Diabetes* 25:931-935.

182. Krarup, T. 1988. Immunoreactive gastric inhibitory polypeptide. *Endocr Rev* 9:122-134.

183. Krarup, T., Holst, J.J., and Madsbad, S. 1987. Heterogeneity of immunoreactive gastric inhibitory polypeptide in the plasma of newly diagnosed type 1 (insulin-dependent) diabetics. *Acta Endocrinol (Copenh)* 114:74-83.

184. Krarup, T., and Holst, J.J. 1984. The heterogeneity of gastric inhibitory polypeptide in porcine and human gastrointestinal mucosa evaluated with five different antisera. *Regul Pept* 9:35-46.

185. Yip, R.G., and Wolfe, M.M. 2000. GIP biology and fat metabolism. *Life Sci* 66:91-103.

186. de Bruine, A.P., Dinjens, W.N., van der Linden, E.P., Pijls, M.M., Moerkerk, P.T., and Bosman, F.T. 1993. Extracellular matrix components induce endocrine differentiation *in vitro* in NCI-H716 cells. *Am J Pathol* 142:773-782.

187. Hirasawa, A., Tsumaya, K., Awaji, T., Katsuma, S., Adachi, T., Yamada, M., Sugimoto, Y., Miyazaki, S., and Tsujimoto, G. 2005. Free fatty acids regulate gut incretin glucagon-like peptide-1 secretion through GPR120. *Nat Med* 11:90-94.

188. Rask, E., Olsson, T., Soderberg, S., Johnson, O., Seckl, J., Holst, J.J., and Ahren, B. 2001. Impaired incretin response after a mixed meal is associated with insulin resistance in nondiabetic men. *Diabetes Care* 24:1640-1645.

189. Muscelli, E., Mari, A., Casolaro, A., Camastra, S., Seghieri, G., Gastaldelli, A., Holst, J.J., and Ferrannini, E. 2008. Separate impact of obesity and glucose tolerance on the incretin effect in normal subjects and type 2 diabetic patients. *Diabetes* 57:1340-1348.

190. Vollmer, K., Holst, J.J., Baller, B., Ellrichmann, M., Nauck, M.A., Schmidt, W.E., and Meier, J.J. 2008. Predictors of incretin concentrations in subjects with normal, impaired, and diabetic glucose tolerance. *Diabetes* 57:678-687.

191. Verdich, C., Toubro, S., Buemann, B., Lysgard Madsen, J., Juul Holst, J., and Astrup, A. 2001. The role of postprandial releases of insulin and incretin hormones in meal-induced satiety--effect of obesity and weight reduction. *Int J Obes Relat Metab Disord* 25:1206-1214.

192. Borst, S.E. 2004. The role of TNF-alpha in insulin resistance. *Endocrine* 23:177-182.

193. Hotamisligil, G.S. 1999. Mechanisms of TNF-alpha-induced insulin resistance. *Exp Clin Endocrinol Diabetes* 107:119-125.

194. Ellingsgaard, H., Hauselmann, I., Schuler, B., Habib, A.M., Baggio, L.L., Meier, D.T., Eppler, E., Bouzakri, K., Wueest, S., Muller, Y.D., *et al*. Interleukin-6 enhances insulin secretion by increasing glucagon-like peptide-1 secretion from L cells and alpha cells. *Nat Med* 17:1481-1489.

195. Ajuebor, M.N., Hogaboam, C.M., Kunkel, S.L., Proudfoot, A.E., and Wallace, J.L. 2001. The chemokine RANTES is a crucial mediator of the progression from acute to chronic colitis in the rat. *J Immunol* 166:552-558.

196. Casola, A., Estes, M.K., Crawford, S.E., Ogra, P.L., Ernst, P.B., Garofalo, R.P., and Crowe, S.E. 1998. Rotavirus infection of cultured intestinal epithelial cells induces secretion of CXC and CC chemokines. *Gastroenterology* 114:947-955.

197. Schaffler, A., Furst, A., Buchler, C., Paul, G., Rogler, G., Scholmerich, J., and Herfarth, H. 2006. Secretion of RANTES (CCL5) and interleukin-10 from mesenteric adipose tissue and from creeping fat in Crohn's disease: regulation by steroid treatment. *J Gastroenterol Hepatol* 21:1412-1418.

198. Herrmann, C., Goke, R., Richter, G., Fehmann, H.C., Arnold, R., and Goke, B. 1995. Glucagon-like peptide-1 and glucose-dependent insulin-releasing polypeptide plasma levels in response to nutrients. *Digestion* 56:117-126.

199. Plaisancie, P., Dumoulin, V., Chayvialle, J.A., and Cuber, J.C. 1995. Luminal glucagon-like peptide-1(7-36) amide-releasing factors in the isolated vascularly perfused rat colon. *J Endocrinol* 145:521-526.

200. Cani, P.D., Holst, J.J., Drucker, D.J., Delzenne, N.M., Thorens, B., Burcelin, R., and Knauf, C. 2007. GLUT2 and the incretin receptors are involved in glucose-induced incretin secretion. *Mol Cell Endocrinol* 276:18-23.

201. Persson, K., Gingerich, R.L., Nayak, S., Wada, K., Wada, E., and Ahren, B. 2000. Reduced GLP-1 and insulin responses and glucose intolerance after gastric glucose in GRP receptor-deleted mice. *Am J Physiol Endocrinol Metab* 279:E956-962.

202. Little, T.J., Doran, S., Meyer, J.H., Smout, A.J., O'Donovan, D.G., Wu, K.L., Jones, K.L., Wishart, J., Rayner, C.K., Horowitz, M., *et al*. 2006. The release of GLP-1 and ghrelin, but not GIP and CCK, by glucose is dependent upon the length of small intestine exposed. *Am J Physiol Endocrinol Metab* 291:E647-655.

203. Hegg, C.C., Hu, S., Peterson, P.K., and Thayer, S.A. 2000. Beta-chemokines and human immunodeficiency virus type-1 proteins evoke intracellular calcium increases in human microglia. *Neuroscience* 98:191-199.

204. Shideman, C.R., Hu, S., Peterson, P.K., and Thayer, S.A. 2006. CCL5 evokes calcium signals in microglia through a kinase-, phosphoinositide-, and nucleotide-dependent mechanism. *J Neurosci Res* 83:1471-1484.

205. Bacon, K.B., Premack, B.A., Gardner, P., and Schall, T.J. 1995. Activation of dual T cell signaling pathways by the chemokine RANTES. *Science* 269:1727-1730.

206. Saito, M., Sato, R., Hisatome, I., and Narahashi, T. 1996. RANTES and platelet-activating factor open Ca^{2+}-activated K^{+} channels in eosinophils. *FASEB J* 10:792-798.

207. Sperelakis, N. 1994. Regulation of calcium slow channels of heart by cyclic nucleotides and effects of ischemia. *Adv Pharmacol* 31:1-24.

208. Hatakeyama, H., Kishimoto, T., Nemoto, T., Kasai, H., and Takahashi, N. 2006. Rapid glucose sensing by protein kinase A for insulin exocytosis in mouse pancreatic islets. *J Physiol* 570:271-282.

209. Yada, T., Itoh, K., and Nakata, M. 1993. Glucagon-like peptide-1-(7-36)amide and a rise in cyclic adenosine 3',5'-monophosphate increase cytosolic free Ca2+ in rat pancreatic beta-cells by enhancing Ca^{2+} channel activity. *Endocrinology* 133:1685-1692.

210. Grapengiesser, E., Gylfe, E., and Hellman, B. 1991. Cyclic AMP as a determinant for glucose induction of fast Ca^{2+} oscillations in isolated pancreatic beta-cells. *J Biol Chem* 266:12207-12210.

211. Holz, G.G. 2004. Epac: A new cAMP-binding protein in support of glucagon-like peptide-1 receptor-mediated signal transduction in the pancreatic beta-cell. *Diabetes* 53:5-13.

212. Islam, D., Zhang, N., Wang, P., Li, H., Brubaker, P.L., Gaisano, H.Y., Wang, Q., and Jin, T. 2009. Epac is involved in cAMP-stimulated proglucagon expression and hormone production but not hormone secretion in pancreatic alpha- and intestinal L-cell lines. *Am J Physiol Endocrinol Metab* 296:E174-181.

213. Zhao, J., Ma, L., Wu, Y.L., Wang, P., Hu, W., and Pei, G. 1998. Chemokine receptor CCR5 functionally couples to inhibitory G proteins and undergoes desensitization. *J Cell Biochem* 71:36-45.

214. Zhang, Y., Luo, Y., Zhai, Q., Ma, L., and Dorf, M.E. 2003. Negative role of cAMP-dependent protein kinase A in RANTES-mediated transcription of proinflammatory mediators through Raf. *FASEB J* 17:734-736.

215. Ismailov, II, and Benos, D.J. 1995. Effects of phosphorylation on ion channel function. *Kidney Int* 48:1167-1179.

216. Drucker, D.J., Jin, T., Asa, S.L., Young, T.A., and Brubaker, P.L. 1994. Activation of proglucagon gene transcription by protein kinase-A in a novel mouse enteroendocrine cell line. *Mol Endocrinol* 8:1646-1655.

217. Lotfi, S., Li, Z., Sun, J., Zuo, Y., Lam, P.P., Kang, Y., Rahimi, M., Islam, D., Wang, P., Gaisano, H.Y., *et al*. 2006. Role of the exchange protein directly activated by cyclic adenosine 5'-monophosphate (Epac) pathway in regulating proglucagon gene expression in intestinal endocrine L cells. *Endocrinology* 147:3727-3736.

218. Jin, T., and Drucker, D.J. 1996. Activation of proglucagon gene transcription through a novel promoter element by the caudal-related homeodomain protein cdx-2/3. *Mol Cell Biol* 16:19-28.

219. Hardin, J., Kroeker, K., Chung, B., and Gall, D.G. 2000. Effect of proinflammatory interleukins on jejunal nutrient transport. *Gut* 47:184-191.

220. Barrenetxe, J., Sainz, N., Barber, A., and Lostao, M.P. 2004. Involvement of PKC and PKA in the inhibitory effect of leptin on intestinal galactose absorption. *Biochem Biophys Res Commun* 317:717-721.

221. Barrenetxe, J., Barber, A., and Lostao, M.P. 2001. Leptin effect on galactose absorption in mice jejunum. *J Physiol Biochem* 57:345-346.

222. Ducroc, R., Guilmeau, S., Akasbi, K., Devaud, H., Buyse, M., and Bado, A. 2005. Luminal leptin induces rapid inhibition of active intestinal absorption of glucose mediated by sodium-glucose cotransporter 1. *Diabetes* 54:348-354.

223. Amador, P., Garcia-Herrera, J., Marca, M.C., de la Osada, J., Acin, S., Navarro, M.A., Salvador, M.T., Lostao, M.P., and Rodriguez-Yoldi, M.J. 2007. Inhibitory effect of TNF-alpha on the intestinal absorption of galactose. *J Cell Biochem* 101:99-111.

224. Hirsch, J.R., Loo, D.D., and Wright, E.M. 1996. Regulation of Na+/glucose cotransporter expression by protein kinases in Xenopus laevis oocytes. *J Biol Chem* 271:14740-14746.

225. Wright, E.M., Hirsch, J.R., Loo, D.D., and Zampighi, G.A. 1997. Regulation of Na^+/glucose cotransporters. *J Exp Biol* 200:287-293.

226. Au, A., Gupta, A., Schembri, P., and Cheeseman, C.I. 2002. Rapid insertion of GLUT2 into the rat jejunal brush-border membrane promoted by glucagon-like peptide 2. *Biochem J* 367:247-254.

227. Cheeseman, C.I. 1997. Upregulation of SGLT-1 transport activity in rat jejunum induced by GLP-2 infusion *in vivo*. *Am J Physiol* 273:R1965-1971.

228. Wong, T.P., Debnam, E.S., and Leung, P.S. 2007. Involvement of an enterocyte renin-angiotensin system in the local control of SGLT1-dependent glucose uptake across the rat small intestinal brush border membrane. *J Physiol* 584:613-623.

229. Levens, N.R. 1985. Control of intestinal absorption by the renin-angiotensin system. *Am J Physiol* 249:G3-15.

230. Cox, H.M., Cuthbert, A.W., and Munday, K.A. 1987. The effect of angiotensin II upon electrogenic ion transport in rat intestinal epithelia. *Br J Pharmacol* 90:393-401.

231. Kawano, K., Ikari, A., Nakano, M., and Suketa, Y. 2002. Phosphatidylinositol 3-kinase mediates inhibitory effect of angiotensin II on sodium/glucose cotransporter in renal epithelial cells. *Life Sci* 71:1-13.

232. Seki, T., Yokoshiki, H., Sunagawa, M., Nakamura, M., and Sperelakis, N. 1999. Angiotensin II stimulation of Ca^{2+}-channel current in vascular smooth muscle cells is inhibited by lavendustin-A and LY-294002. *Pflugers Arch* 437:317-323.

CURRICULUM VITAE

Ramona Pais
Untere Hauptstraße 36

85354 Freising

Tel : 017683191794

ramonapais2003@gmail.com

PERSÖNLICHE DATEN

Geburtsdatum	10.03.1984
Geburstort	Abu Dhabi, U.A.E
Staatsangehörigkeit	Indisch
Familienstand	verheiratet

AUSBILDUNG

07/2008-03/2012	**Promotion an der Technischen Universität München,** Lehrstuhl für Ernährungsphysiologie, Professor Dr. Hannelore Daniel; DFG grant, GRK1482 *"Role of adipokines in the regulation on intestinal GLP-1 secretion."*
07/2004-07/2007	**Masterstudium der Medizinische Biochemie** Université Manipal, Indien
05/2001-03/2004	**Bachelorstudium der Biotechnologie, Angewandte Botanik und Chemie** Université Bangalore, Indien

PRAKTIKA

08/2007-03/2008	**Manipal Institute of Regenerative Medicine**, Bangalore, Indien. *Thema: "Nanotechnology based approach to develop a defined culture microenvironment for human embryonic stem cells." und* *"Redefining the niche in human embryonic stem cell colonies: Role of Rho kinases in improving HUEs culture and directing differentiation towards early trophectoderm like nice cells (TNhC)*

01/2006-06/2007	**Kasturba Medical College,** Lehrstuhl für Biochemie und Gynäkologie, Manipal, Indien. *Thema: "Indicators of oxidative stress in Polycystic Ovarian Syndrome."*
01/2005-12/2005	**Kasturba Medical College,** Lehrstuhl für Biochemie, Manipal, Indien. *Thema: "A comparative study of protein carbonyls and thiol levels in normal males and females."*

SONSTIGES

Sprachen:	Englisch, Hindi, Deutsch
Hobbys:	Musik, Literatur, Schwimmen und Aerobic